European Society
ESGAR
Gastrointestinal and Abdominal Radiology

Insights into Imaging

Education and strategies in European radiology

ESGAR 2018 Book of Abstracts / Volume 9 / Supplement 2 / June 2018

ESGAR 2018 / June 12 – 15 / Dublin, Ireland
29th Annual Meeting and Postgraduate Course

ESR
European Society of Radiology

European Society
ESGAR
Gastrointestinal and Abdominal Radiology

JUNE 12 - 15

ESGAR 2018

DUBLIN
IRELAND

European Society of Gastrointestinal and Abdominal Radiology

29th ANNUAL MEETING
AND POSTGRADUATE COURSE

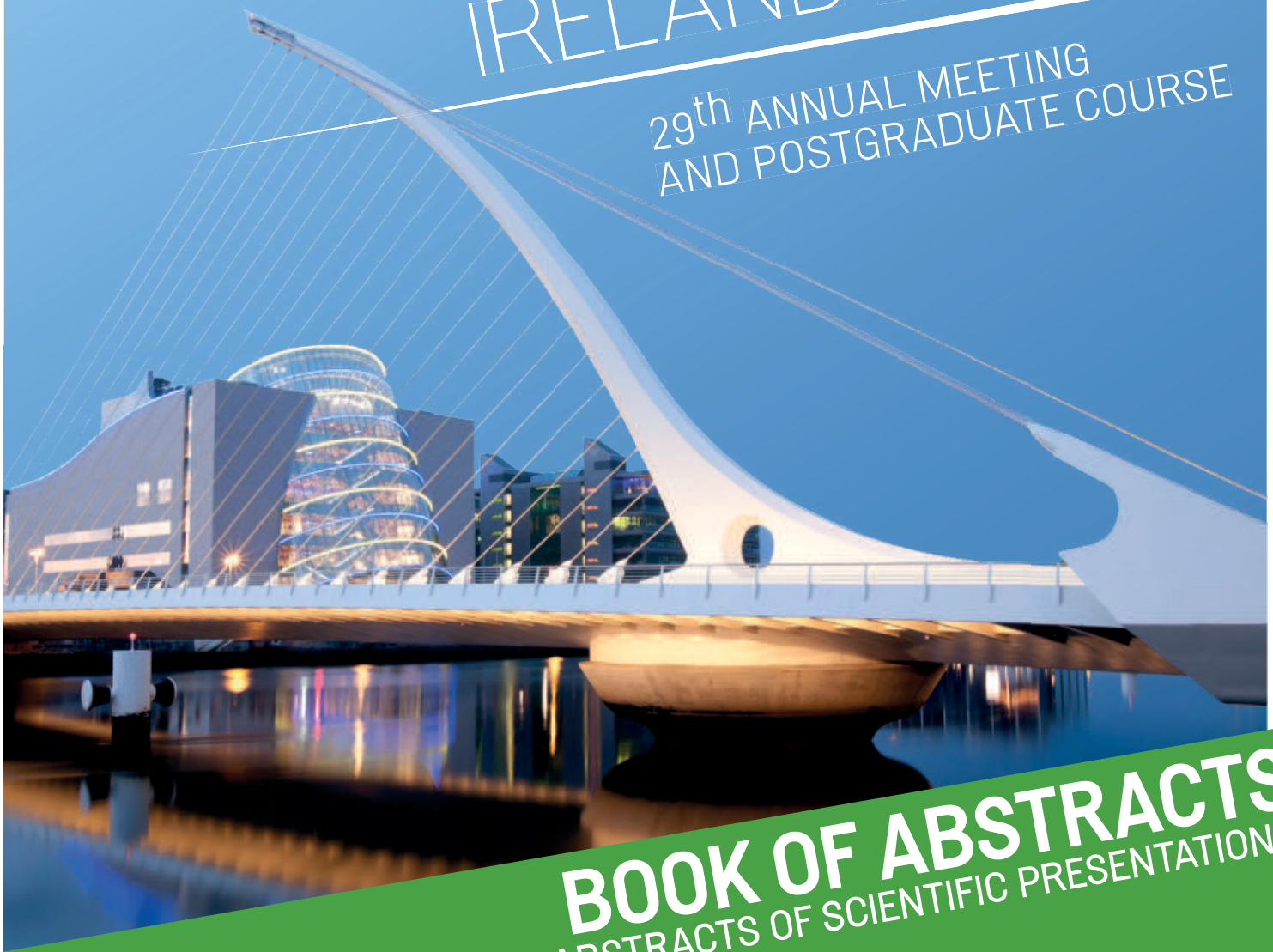

BOOK OF ABSTRACTS

INCLUDES ABSTRACTS OF SCIENTIFIC PRESENTATIONS

ORGANISING SECRETARIAT

Central ESGAR Office
Esslinggasse 2/3
AT – 1010 Vienna
Phone: +43 1 535 89 27
Fax: +43 1 535 89 27 -15
E-Mail: office@esgar.org

WEBSITE

www.esgar.org

CONFERENCE VENUE

The Convention Centre Dublin
Spencer Dock
North Wall Quay
IE - D01 T1W6 Dublin 1

CME CREDITS

The "ESGAR European Society of Gastrointestinal and Abdominal Radiology" (or) "ESGAR 2018 – 29th ANNUAL MEETING AND POSTGRADUATE COURSE" is accredited by the European Accreditation Council for Continuing Medical Education (EACCME) to provide the following CME activity for medical specialists. The EACCME is an institution of the European Union of Medical Specialists (UEMS), www.uems.net.

The "ESGAR 2018 29th Annual Meeting and Postgraduate Course, Dublin, Ireland, 12/06/2018-15/06/2018" has been accredited by the European Accreditation Council for Continuing Medical Education (EACCME®) with 25 European CME credits (ECMEC®s). Each medical specialist should claim only those hours of credit that he/she actually spent in the educational activity.

CONTRIBUTING SOCIETIES

ECCO European Crohn's and Colitis Organisation

ASAR Asian Society of Abdominal Radiology Since 2007

ESUR European Society of Urogenital Radiology

SAR Society of Abdominal Radiology

SPONSORS

ESGAR wishes to gratefully acknowledge the support of its Corporate Members:

BAYER

BRACCO LIFE FROM INSIDE

GE Healthcare

Guerbet Contrast for Life

PHILIPS

The Final Programme of ESGAR 2018 is available on the ESGAR Website www.esgar.org

Date of publishing: June 2018

DOI 10.1007/s13244-018-0634-1

TABLE OF CONTENTS

ESGAR EXECUTIVE COMMITTEE

PRESIDENT
S. Halligan, London/UK

PRESIDENT-ELECT
R.G.H. Beets-Tan, Amsterdam/NL

VICE PRESIDENT
A. Laghi, Rome/IT

SECRETARY/ TREASURER
M. Zins, Paris/FR

PAST PRESIDENT
C. Matos, Lisbon/PT

EDUCATION COMMITTEE
S. Jackson, Plymouth/UK

MEMBERSHIP COMMITTEE
M.A. Bali, London/UK

RESEARCH COMMITTEE
J. Stoker, Amsterdam/NL

WORKSHOP COMMITTEE
G. Brancatelli, Palermo/IT

MEETING PRESIDENT 2018
H. Fenlon, Dublin/IE

PRE-MEETING PRESIDENT 2019
A. Laghi, Rome/IT

MEMBERS AT LARGE
A. Ba-Ssalamah, Vienna/AT
V. Vilgrain, Clichy/FR
C.J. Zech, Basel/CH

ESGAR EXECUTIVE DIRECTOR
B. Lindlbauer, Vienna/AT

LANGUAGE ABSTRACT EDITOR

C. Clarke, Nottingham/UK

ESGAR 2018 MEETING PRESIDENT

Prof. Helen Fenlon
University College Dublin
Department of Radiology
Mater Misericordiae University Hospital and BreastCheck
36 Eccles Street
IE – Dublin 7

ESGAR 2018 PROGRAMME COMMITTEE

CHAIRMEN
M. Zins, Paris/FR
C. Matos, Lisbon/PT

MEMBERS
M.A. Bali, London/UK
A. Ba-Ssalamah, Vienna/AT
R.G.H. Beets-Tan, Amsterdam/NL
G. Brancatelli, Palermo/IT
H. Fenlon, Dublin/IE
S. Halligan, London/UK
S. Jackson, Plymouth/UK
A. Laghi, Rome/IT
J. Stoker, Amsterdam/NL
V. Vilgrain, Clichy/FR
C.J. Zech, Basel/CH

ESGAR 2018 LOCAL ORGANISING COMMITTEE

R. Browne, Dublin/IE
C. Cronin, Dublin/IE
T. Geoghegan, Dublin/IE
M. Keogan, Dublin/IE
M. Lee, Dublin/IE
M. Maher, Cork/IE
D.E. Malone, Dublin/IE
M. McNicholas, Dublin/IE
M. Morrin, Dublin/IE
J. Murphy, Galway/IE
A. Ryan, Waterford/IE
M. Ryan, Cork/IE
T. Scanlon, Limerick/IE
N. Sheehy, Dublin/IE
M. Shelly, Limerick/IE
S.J. Skehan, Dublin/IE
M. Staunton, Cork/IE

O. Akhan, Ankara/TR
C. Aubé, Angers/FR
M.A. Bali, London/UK
I. Bargellini, Pisa/IT
T.V. Bartolotta, Palermo/IT
A. Ba-Ssalamah, Vienna/AT
R.G.H. Beets-Tan, Amsterdam/NL
E. Biscaldi, Genova/IT
A. Blachar, Tel Aviv/IL
G. Brancatelli, Palermo/IT
D.J. Breen, Southampton/UK
F. Caseiro Alves, Coimbra/PT
N. Courcoutsakis, Alexandroupolis/GR
L. Crocetti, Pisa/IT
L. Curvo-Semedo, Coimbra/PT
R. Dondelinger, Liège/BE
M. D'Onofrio, Verona/IT
H. Fenlon, Dublin/IE
A. Furlan, Pittsburgh, PA/US
Y. Gandon, Rennes/FR
V. Goh, London/UK
S. Gourtsoyianni, London/UK
S. Gryspeerdt, Roeselare/BE
L. Guimaraes, North York, ON/CA
J.A. Guthrie, Leeds/UK
S. Halligan, London/UK
A. Hatzidakis, Heraklion/GR
T. Helmberger, Munich/DE
F. Iafrate, Rome/IT
M. Karcaaltincaba, Ankara/TR
N. Kartalis, Stockholm/SE
H.-U. Laasch, Manchester/UK
A. Laghi, Rome/IT
M. Laniado, Dresden/DE
J.M. Lee, Seoul/KR
M. Lewin, Paris/FR
O. Lucidarme, Paris/FR
M. Maas, Amsterdam/NL
A. Madureira, Porto/PT
M. Maher, Cork/IE
D.E. Malone, Dublin/IE
T. Mang, Vienna/AT
V. Maniatis, Aabenraa/DK
D. Marin, Durham, NC/US
L. Martí-Bonmatí, Valencia/ES
C. Matos, Lisbon/PT
Y. Menu, Paris/FR
G. Morana, Treviso/IT
G.H. Mostbeck, Vienna/AT
A. Palkó, Szeged/HU
P. Paolantonio, Rome/IT
N. Papanikolaou, Lisbon/PT
R. Pozzi Mucelli, Verona/IT
P. Prassopoulos, Alexandroupolis/GR
E. Quaia, Edinburgh/UK
G.A. Rollandi, Genova/IT
M. Ronot, Clichy/FR
W. Schima, Vienna/AT
S. Schmidt Kobbe, Lausanne/CH
A. Schreyer, Regensburg/DE
O. Seror, Bondy/FR
S.J. Skehan, Dublin/IE
M. Staunton, Cork/IE
S. Stojanovic, Novi Sad/RS
J. Stoker, Amsterdam/NL
J.P. Tasu, Poitiers/FR
S.A. Taylor, London/UK
S. Terraz, Geneva/CH
D.J.M. Tolan, Leeds/UK
C. Triantopoulou, Athens/GR
V. Valek, Brno/CZ
V. Vilgrain, Clichy/FR
M.-P. Vullierme, Clichy/FR
D. Weishaupt, Zurich/CH
G.A. Zamboni, Verona/IT
C.J. Zech, Basel/CH
M. Zins, Paris/FR


European Society
ESGAR
Gastrointestinal and Abdominal Radiology

11:00 - 12:30 **The Auditorium**

Scientific Session SS 1

Focal liver lesions: new trends in imaging of HCC

SS 1.1

Comparison of European association for the study of the liver, liver imaging and reporting data system criteria and radiological opinion for diagnosing HCC in cirrhotic livers

C.G.D. Clarke[1], R. Albazaz[2], C.R. Smith[2], I. Rowe[2], D. Treanor[2], J.I. Wyatt[2], M.B. Sheridan[2], J.A. Guthrie[2]; [1]Nottingham/UK, [2]Leeds/UK

Purpose: Imaging criteria for the non-invasive diagnosis of HCC have been established by many organisations. The reported diagnostic performance of MRI in the diagnosis of HCC is widely variable. Our aim was to determine the sensitivity and specificity of these criteria by correlating with a histological diagnosis from whole liver explants.

Material and methods: This is a single-centre, retrospective review. Participants were selected based on the following: consecutive adults (>=18yrs) listed for liver transplantation in 2014/2015, with cirrhosis at the time of MR scanning with hepatocyte-specific contrast agent, and at least one liver lesion >=1cm on MR with histology from subsequent liver explant for comparison. Patients were randomly allocated to two independent consultant radiologists for review. Each lesion was assessed against international criteria [European association for the study of the liver (EASL), liver imaging and reporting data system (LIRADS)], and given a ‚radiologist impression' score of 1-5 (1=definitely benign, 5=definitely HCC).

Results: Total of 268 patient records were reviewed, with 118 eligible lesions identified from 50 patients. Median lesion size was 15.5 (interquartile range 12-21) mm. Mean age 56 (+/-7.7) yrs with M:F ratio of 4:1. Sensitivity, specificity and PPV for EASL was 0.47, 0.82 and 0.83, for LIRADS LR5 was 0.39, 0.88 and 0.85, for LIRADS LR4+5+TIV was 0.73, 0.69, and 0.81, and for ‚radiologist impression' of probably or definitely HCC, available in 108 lesions, was 0.79, 0.79 and 0.88.

Conclusion: MR imaging has moderate sensitivity and good specificity in the diagnosis of HCC and there is considerable variation depending on the criteria used. 'Radiologist impression' has better sensitivity when compared to LIRADS and EASL.

SS 1.2

withdrawn by the authors

SS 1.3

Radiological-pathological correlation of pre-transplant imaging and explanted livers: what is the prevalence of HCC in patients with liver imaging reporting and data system 2017 category 5, 4/5 and 4 lesions?

A.C. O'Brien, R. Keane, B. Pierce, C. O'Brien, N. Nolan, P.A. McCormick, D.E. Malone, S.J. Skehan, R. Ryan, R. Gibney; Dublin/IE

Purpose: The Irish National Centre for Liver Transplantation (OLT) serves a population of 4.5 million. Liver imaging reporting and data system (LI-RADS) category designation is made at a multidisciplinary meeting by 1 or more of 4 abdominal radiologists. The aim of this study is to evaluate the prevalence of HCC in OLT patients whose pre-OLT imaging showed LI-RADS 4 or 5 lesion(s).

Material and methods: OLT patients with a pre-operative diagnosis of HCC and explants with HCC found at pathology from 01/01/2014 to 09/09/2017 were identified using the OLT database. Corresponding pre-OLT imaging reports (CT/MRI) were reviewed. In patients with LI-RADS 2017 class 5, 4/5 or 4 lesions, the histopathology coding of explanted livers was reviewed. Data were collated in an MSExcel spreadsheet and analysed on a per patient basis in 2 groups (LI-RADS 5 and LI-RADS 4/5 or 4).

Results: 53 OLT patients met selection criteria. Pre-operative imaging reported LI-RADS 5, 4/5 or 4 lesions in 41 of 53 explanted livers. LI-RADS 5: n = 36 patients (7 had pre-OLT TACE), 35 had HCC, 1 had macroregenerative cirrhosis without HCC; 1 also had a collision tumour (HCC/cholangiocarcinoma). HCC prevalence: 97%. LI-RADS 4/5: n =1 patient, HCC confirmed at OLT. LI-RADS 4: n = 4 patients, 3 had HCC and dysplastic nodules only were identified in the other patient. HCC prevalence 80%.

Conclusion: The prevalence of HCC in OLT patients with LI-RADS 2017 class 5 lesions is acceptably high. The small LI-RADS 4/5 or 4 group had a lower HCC prevalence. More data are needed for optimal management of these patients.

SS 1.4

Prospective intraindividual comparison of gadoxetic acid and gadoterate meglumine for the diagnosis of HCCs with liver imaging reporting and data system

Y.K. Kim[1], J.H. Min[2], W.K. Jeong[1]; [1]Seoul/KR, [2]Daejeon/KR

Purpose: This prospective study intraindividually compared the efficacy of gadoxetic acid (Gd-EOB-DTPA)-enhanced MRI and gadoterate meglumine (Gd-DOTA)-enhanced MRI for the diagnosis of HCC with the liver imaging reporting and data system (LI-RADS).

Material and methods: Between November 2016 and November 2017, we prospectively included 91 patients with chronic liver disease who underwent both Gd-EOB-DTPA-MRI and Gd-DOTA-MRI (interval range, 9 to 30 days) for first detected hepatic nodule on US: 107 lesions (95 HCCs, 2 cholangiocarcinomas, 7 hemangiomas, 2 dysplastic nodules, 1 neuroendocrine tumor; size range: 0.8-3.0 cm) were identified by surgical resection. Two observers reviewed two MRIs based on the LI-RADS v2017.

Results: We found a tendency toward higher sensitivity (observer 1, 76.8% vs 57.9% and observer 2, 81.1% vs. 61.3%) and accuracy (observer 1, 81.2% vs 65.8% and observer 2, 84.6% vs. 68.7%) with LR-5 category on Gd-DOTA-MRI than with that on Gd-EOB-DTPA-MRI ($P < 0.001$). When applying arterial hyperenhancement with either washout on 3-min Gd-EOB-DTPA MRI or isointensity with capsule on 3 min Gd-DOTA-MRI, 16 HCCs on Gd-EOB-DPTA-MRI and 10 HCCs on Gd-DOTA-MRI were upgraded to LR-5 category while achieving 100% specificity with both MRIs. One cholangiocarcinoma was correctly classified with Gd-EOB-DTPA MRI due to targetoid appearance.

Conclusion: In the diagnosis of HCC with LI-RADS, MRI using extracellular contrast agent showed better sensitivity and accuracy than Gd-EOB-DTPA-MRI although they showed 100% specificity. We could achieve better diagnostic performance with applying washout on 3 min Gd-EOB-DTPA-MRI or isointensity with capsule on 3-min Gd-DOTA MRI than conventional criteria, while maintaining 100% specificity.

SS 1.5

Prospective evaluation of dynamic MR with gadoxetic acid for the non-invasive diagnosis of HCC in newly detected nodules

C. Ayuso, A. Darnell, J. Rimola, A. García-Criado, R. Vilana, A. Forner, J. Bruix; Barcelona/ES

Purpose: To evaluate the diagnostic accuracy of gadoxetic acid-MR (EOB-MR) for non-invasive HCC diagnosis in liver nodules <2 cm detected by screening US.

Material and methods: Cirrhotic patients with newly detected solitary nodules <2 cm by US were included. After written informed consent, extracellular contrast-MR (EC-MR) and EOB-MR were performed in less than 1 month. Final diagnosis was based on the validated European Association for the Study of the Liver (EASL)/American Association for the Study of Liver Diseases (AASLD) guidelines criteria (specific vascular profile on EC-MR or biopsy). Blind, double reading was performed in EOB-MR studies. Criteria for HCC diagnosis using EOB-MR were arterial contrast uptake and either washout in the portal phase or hypointensity in the hepatobiliary phase (HBp).

Results: 62 consecutive cirrhotic patients Child-Pugh A (53) or B (9) were included. Final diagnosis was: 41 (66.1%) HCC, 2 intrahepatic cholangiocarcinoma (ICC), 1 colo-rectal cancer metastasis, and 18 benign conditions. Patients with benign lesions were followed during a median of 23 months to discard malignancy. EC-MR diagnosed 26 out of 41 HCC nodules (sensitivity 63.4%, CI95%: 46.9-77.9). The sensitivity and specificity for EOB-MR were 56.1% (CI95%: 39.7-71.5) and 90.5% (CI95%: 69.8-98.8), respectively, with a positive predictive value (PPV) of 92 (CI95%: 74-99) and negative predictive value (NPV) of 51.4 (CI95%: 34.4-68.1). False positives were observed in the two ICC. In EOB-MR, wash-in was present in 82.9% and portal wash-out in 42%. Low signal intensity in the 20-minute HBp was observed in 63.4% of HCC nodules, whereas the remaining 15 HCCs were iso- or hyperintense.

Conclusion: EOB-MR is not superior to EC-MR for non-invasive diagnosis of HCC in nodules <2 cm in cirrhotic patients.

SS 1.6

Proliferation status of HCC predicted by whole-lesion texture analysis on gadolinium ethoxybenzyl diethylenetriamine pentaacetic acid-enhanced MRI

Z. Ye; Chengdu/CN

Purpose: To explore the potential association between whole-lesion texture features on gadolinium ethoxybenzyl diethylenetriamine pentaacetic acid (Gd-EOB-DTPA)-enhanced MRI and the Ki67 labeling index (Ki67 LI) in HCC patients.

Material and methods: 61 consecutive surgically confirmed HCC patients were prospectively examined on a 3.0 T scanner. Texture features on individual sequence, including pre-contrast T1-weighted (T1-pre), T2-weighted (T2WI), arterial phase (AP), portal venous phase (PVP) and hepatobiliary phase (HBP) imaging were derived using an in-house software (Analysis Kit, GE Healthcare). The Ki67 LI was histopathologically determined and classified into low-proliferation (Ki-67 LI<15%) and high-proliferation group (Ki-67 LI>15%). Lasso model was adopted for feature selection. Differences in texture features between low- and high-proliferation groups were compared. Diagnostic performance of each selected texture parameter in differentiating high-proliferation from low-proliferation group was evaluated by receiver operation characteristic (ROC) analysis.

Results: The cluster prominence and high grey level run emphasis of T1-pre, the Haralick correlation and inverse difference moment (IDM) of T2WI, the IDM of AP, the cluster shade and high grey level run emphasis of PVP and the correlation of HBP showed significant differences between low- and high-proliferation groups (P<0.05). The largest areas under ROC curve (AUCs) of T1-pre (high grey level run emphasis), T2WI (Haralick correlation), AP (IDM), PVP (high grey level run emphasis) and HBP (correlation) were 0.76 (CI[0.63, 0.86]), 0.70 (CI[0.57, 0.81]), 0.69 (CI[0.56, 0.87]), 0.71 (CI[0.58, 0.82]) and 0.70 (CI[0.57, 0.81]), respectively, for identifying high-proliferation HCC. Correlation of HBP showed highest sensitivity (91.43%, CI[76.9%, 98.2%]) while IDM of AP showed highest specificity (96.15%, CI[80.4%, 99.9%]).

Conclusion: Whole-lesion texture features on Gd-EOB-DTPA-enhanced MRI are promising in predicting and characterizing proliferation status of HCC.

SS 1.7

Hypervascular tumors in patients with primary Budd-Chiari syndrome: is the washout sign specific for HCC? An MRI study

M. Van Wettere, O. Bruno, P.-E. Rautou, A. Plessier, V. Vilgrain, M. Ronot; Clichy/FR

Purpose: To reappraise the imaging characteristics of focal liver lesions (FLL) in patients with Budd-Chiari syndrome (BCS), with a focus on the diagnostic value of washout for the differentiation between benign and malignant tumors.

Material and methods: Between 2000 and 2016, patients with a diagnosis of BCS and FLL on MRI were included. MRI was retrospectively reviewed by two radiologists blinded to the nature of these lesions. Patients and tumor characteristics were recorded, with a focus on signal intensity on MRI sequences. HCC and benign tumors were compared using Fisher's test or a Chi-squared test and the Student's t test or Mann-Whitney test.

Results: 49 patients (34 female, 69%) with 241 benign lesions and 12 HCC were analyzed. Patients with HCC were significantly older (mean 44±16 vs. 33±9, p =.005), with higher baseline serum alpha-fetoprotein (AFP) level (median 16 [2-9000] vs. 3 [2-25] ng/mL, p =.007). HCC was significantly larger (mean 32±16 vs. 11±5mm, p<0.001), more frequently hypointense on T1-weighted (58% vs. 4%, p=.001) and hyperintense on T2-weighted images (58% vs. 18%, p=.003) than benign lesions. 28% of the benign lesions showed both hypervascularization and washout too. In lesions >10mm, the sensitivity/specificity of these features was 75%/67%. Adding signal hyperintensity on T1-w images raised the specificity to 82%.

Conclusion: Washout appearance was observed in close to one-third of benign lesions leading to an unacceptably low specificity of this feature for the diagnosis of HCC. Other imaging ancillary features and patients characteristics should be carefully looked at, especially pre-contrast signal intensity and serum AFP level.

SS 1.8

Liver imaging reporting and data system v2017 categorization of HCC using multiphasic MDCT: comparison between patients with and without moderate to severe fatty liver

S.S. Kim[1], J.A. Hwang[1], H.C. Shin[1], S.-Y. Choi[2]; [1]Cheonan-si, Chungcheongnam-do/KR, [2]Bucheon/KR

Purpose: To compare the sensitivity of the liver imaging reporting and data system (LI-RADS) v2017 for categorizing HCC using multiphasic MDCT between patients with and without moderate to severe fatty liver (MSFL).

Material and methods: This retrospective study was approved by the institutional review board, and the informed consent requirement was waived. A total of 106 high-risk patients with 112 pathologically proven HCCs who underwent multiphasic MDCT were included. Patients were classified into MSFL (n=26) and non-MSFL (n=80) group according to unenhanced CT liver and spleen parenchymal attenuation. Two independent radiologists assigned LI-RADS categories and accessed HCC features on MDCT. Sensitivities of LR-5/tumor in vein (TIV) and frequencies of major HCC features on MDCT were compared between two groups.

Results: Sensitivities of LR-5/TIV were not significantly different between MSFL and non-MSFL group (73.1% [19/26] vs. 83.7% [72/86], P = 0.255; 80.8% [21/26] vs. 87.2% [75/86], 0.522 in reviewers 1 and 2, respectively). No significant differences in frequencies of arterial hyperenhancement, washout, and capsule were observed between the two groups (96.2% [25/26] vs. 98.8% [85/86], P = 0.412; 80.8% [21/26] vs. 89.5% [77/86], P = 0.308; and 53.8% [14/26] vs. 57% [49/86], P = 0.778, respectively). Two HCCs (7.7% [2/26]) in MSFL group showed higher attenuation compared with background liver on unenhanced image.

Conclusion: LI-RADS using MDCT showed comparable sensitivity for the diagnosis of HCCs regardless of MSFL.

SS 1.9

Pre-treatment estimation of liver function using T1 mapping of gadolinium-ethoxybenzyl-diethylenetriamine pentaacetic acid-enhanced MRI and normal liver volume in patients with HCC

T. Duan, L. Cao, M. Wang, B. Song; Chengdu/CN

Purpose: This study aimed to prospectively evaluate liver function in patients with HCC using T1 mapping before and after 20 minutes of gadolinium-ethoxybenzyl-diethylenetriamine pentaacetic acid (Gd-EOB-DTPA) injection and normal liver volume, compared with indocyanine green (ICG) retention at 15 min (ICG R-15).

Material and methods: 101 consecutive patients with HCC were included in this study. T1 relaxation time of the livers before and 20 minutes after Gd-EOB-DTPA injection (pre-T1 and post-T1) was measured, and the reduction (Δ) and reduction rate of T1 relaxation time (Δ%) were calculated. Volumes of normal liver parenchyma were conducted and the products of T1 parameters and volume were calculated. ICG R-15 was also recorded. Liver function insufficiency was defined as ICG R-15 >10. T1 parameters, volumes and the products were correlated with both ICG R-15 using Spearman rank correlation analysis. Receiver operation characteristic (ROC) analysis of predicting the liver function insufficiency was performed for T1 parameters, volumes and the products.

Results: The post-T1 ($r=0.450$, $P<0.001$), Δ ($r=-0.287$, $P=0.011$), Δ% ($r=-0.419$, $P<0.001$) volume ($r=-0.374$, $P<0.001$), product of Δ and volume ($r=-0.442$, $P<0.001$) as well as product of Δ% and volume showed weak to moderate correlations with ICG R-15. In predicting the liver function insufficiency, the area under the ROC of post-T1, Δ, Δ%, volume, product of Δ and volume and product of Δ% and volume were 0.767, 0.619, 0.722, 0.745, 0.791 and 0.856, respectively.

Conclusion: A combination of T1 mapping and normal liver volume can help in evaluating liver function.

SS 1.10

Combining CT-liver perfusion and MRI with hepato-specific contrast agent to increase diagnostic accuracy in patients with suspected HCC: work in progress

A.A. Hatzidakis, G. Kalarakis, K. Perisinakis, E. Chryssou, A. Papadakis, A. Karantanas; Heraklion/GR

Purpose: Gadoxetic acid-enhanced MRI (GaE-MRI) is used for HCC surveillance. We sought to compare the diagnostic accuracy of CT-liver perfusion (CTLP) plus GaE-MRI versus GaE-MRI alone for detection and characterization of suspected HCC lesions.

Material and methods: Sixteen patients (all male, 12 cirrhotic) under HCC surveillance before or after percutaneous HCC treatment, underwent GaE-MRI and CTLP (with a maximum interval of 6 weeks). In total, 16 pairs of CTLP and GaE-MRI examinations were studied. GaE-MRI, was performed on a 1.5T-system (Siemens Vision-Hybrid). HCCs were characterized according to conventional MRI criteria. CTLP-maps of mean slope of increase were generated using a 128-CT-system (GE Revolution HD) and the lesions were depicted based on a previously determined cut-off value. Diagnoses based on GaE-MRI alone and GaE-MRI plus CTLP were compared with digital subtraction angiography (DSA).

Results: Of the total 44 lesions identified (median diameter 20mm, range 5-124mm), 19 were characterized as HCCs by DSA. GaE-MRI identified 16 true-positive, 19 true-negative lesions and misdiagnosed 6 false-positive and 3 false-negative lesions, providing 84.2% sensitivity and 76% specificity. The combination of GaE-MRI and CTLP identified 19 true-positive, 24 true-negative and 1 false-positive lesion increasing sensitivity and specificity to 100% and 96%, respectively ($p=0.0025$). Another 12-mm nodule, characterized as HCC by CTLP/GaE-MRI, was initially not detected by DSA, but was revealed in a subsequent one, 6 months later.

Conclusion: Combination of GaE-MRI and CTLP may increase small (<15mm diameter) hepatic nodule characterization accuracy, enabling more efficient patient selection for early and individualized loco-regional treatment.

11:00 - 12:30 **The Liffey A**

Scientific Session SS 2

Insights in imaging of rectal cancer

SS 2.1

The standard of MRI rectal cancer staging reporting in clinical practice: a case for standardization?

P.J. Brown, H. Rossington, D.J.M. Tolan; Leeds/UK

Purpose: Rectal cancer staging with magnetic resonance imaging (RCS-MRI) allows accurate assessment of tumours. Significant variability exists in the content of reports. Template-style reporting can improve reporting standards, but its use is not widespread. Given the implications for treatment we have evaluated standard practice amongst radiologists to measure the current quality of RCS-MRI reports.

Material and methods: 16 UK colorectal cancer multidisciplinary teams (MDTs) serving a population over 5 million in Yorkshire were invited to submit a maximum of 10 consecutive RCS-MRI reports from January 2016 for each radiologist participating in the colorectal MDT. All radiologists were subspecialists in GI imaging with training in RCS-MRI. Reports were compared to a reference standard based on key data points in The Union for International Cancer Control (UICC)-TNM 5 staging and other recognised factors influencing case management.

Results: 293 RCS-MRI reports were submitted from 32 of 42 (76%) eligible radiologists. 81 of 293 (28%) reports used a template. Template report usage significantly increased recording of key data points versus non-template reports for extra-mural vascular invasion (EMVI) status (98.8% v 53.3%, $p < 0.001$) and circumferential-resection margin (CRM) status (98.8% v 63.2%, $p < 0.001$). Local tumour stage (97.5% v 92.0%, NS) and nodal status (98.8% v 95.8%, NS) were usually reported with similar frequency.

Conclusion: Non-template reporting in RCS-MRI excludes critical variables that influence clinical decisions for rectal cancer. Standardised template reporting significantly improves collection of key data.

SS 2.2

Multi-exponential T2* mapping distinguishes benign from malignant lymph nodes in rectal cancer patients: an ex vivo and in vivo experiment

I. Santiago[1], J. Santinha[1], A. Ianus[2], N. Papanikolaou[1], C. Matos[1], N. Shemesh[1]; [1]Lisbon/PT, [2]London/UK

Purpose: To investigate multi-exponential decay in multi-gradient-echo (MGE) MRI for benign/malignant lymph node (LN) distinction in rectal cancer patients, both ex vivo at 16.4T and in vivo at 1.5T.

Material and methods: Ex vivo experiment: 33 benign and 32 malignant LNs were retrieved from 11N+ rectal cancer patient specimens, preserved in 4% formaldehyde, moved to 1% phosphate buffered saline (PBS) for 24h, immersed in Flourinert and acquired in a 16.4T Bruker scanner. A fat-suppressed MGE acquisition was acquired: 50 TEs (echo time) starting at 1.6ms; 1.4ms interval; repetition time (TR)=1500ms; flip angle (FA)=50º; slice thickness (ST)=0.3mm; in-plane resolution=0.1x0.1mm^2; bandwidth=125000Hz; 25 averages. In vivo experiment: 8 rectal cancer patients underwent MGE during staging on a 1.5T Philips scanner: 32 TEs starting at 2.37ms; 2.37ms interval; TR=1519ms; FA=55º; ST=4mm; in-plane resolution=0.42x0.42mm^2; bandwidth=431.3Hz; 2 averages. Six patients underwent total mesorectal excision without neoadjuvant therapy and of the LNs retrieved, 36 benign and 27 malignant were matched to MGE images. Data from ex vivo whole-node volume of interest (VOI) and in vivo single-slice whole-node region of interest (ROI) were used for analysis. Datasets were fitted using 1-, 2- and 3-compartment T2* models. Models were compared based on Bayesian information criterion. Histogram analysis was performed for ex vivo and receiver operating curves (ROC) were computed. Mann-Whitney U test was employed for parameter comparison.

Results: 2-compartment model ranked first in both datasets. For ex vivo, significant differences were found in metrics derived from T2*a, T2*b, f and ΔΩ, the most discriminative being P75 of f($p=0.002$). For in vivo, T2*a showed the highest specificity for malignancy (0.94) and T2*b showed the highest discriminative power (auROC=0.76). The specificity of T2*a, T2*b and their combination exceeded that of reported conventional imaging criteria.

Conclusion: Our results indicate multi-compartment T2* mapping may be of added value for LN staging in rectal cancer.

SS 2.3

Comparison of 8 diffusion MR models to distinguish benign/malignant mesorectal lymph nodes from rectal cancer patients performed ex vivo at ultrahigh field

A. Ianus[1], I. Santiago[2], D. Alexander[1], C. Matos[2], N. Shemesh[2]; [1]London/UK, [2]Lisbon/PT

Purpose: To assess how different compartment models capture the signal behaviour and differentiate benign from malignant lymph nodes (LNs) retrieved from rectal cancer patients' specimens, using a rich diffusion MRI protocol, at 16.4T.

Material and methods: Twenty-six benign and 32 malignant LNs originating from 11 consecutive N+ patients who underwent surgery without neoadjuvant therapy were preserved in 4% formaldehyde, moved to 1% phosphate-buffered saline (PBS) 24h before acquisition, immersed in Flourinert and imaged in a 16.4T Bruker scanner. Stimulated echo acquisition mode diffusion-weighted imaging was employed using 4 different b values, varying diffusion gradient times and 6 different gradient directions for each parameter combination. Data were normalized for each diffusion time and fitted to 8 different diffusion models. Averaged signal over whole-node and up to 10 individual LN regions of interest (ROIs), as delineated by a dedicated radiologist, were used. Models were compared based on goodness of fit. The benign vs malignant differentiation ability of each model was analysed using general linear model (GLM) with binomial distribution and receiver operating characteristic (ROC) curves were computed.

Results: ZeppelinSphere was the model that ranked first in most instances, whereas the Ball model (equivalent to ADC) ranked last in most instances. For whole-node analysis, Tensor and ZeppelinBall models best differentiated benign from malignant LNs (area under ROC=0.78 and 0.77, respectively). For individual ROIs, models with restriction (BallSphereSphere and ZeppelinSphere) yielded better results.

Conclusion: Accounting for restricted diffusion improved the data fit of diffusion MRI signal in LNs from rectal cancer specimens, which may provide more specificity towards tissue microstructure. It also impacted lymph node differentiation.

SS 2.4

T2-weighted signal intensity to predict complete and good response after neoadjuvant chemoradiation therapy in patients with rectal cancer

R.A.P. Dijkhoff[1], S.G. Drago[2], J. Van Griethuysen[1], D.M.J. Lambregts[1], F.C.H. Bakers[3], R.G.H. Beets-Tan[1], M. Maas[1]; [1]Amsterdam/NL, [2]Monza/IT, [3]Maastricht/NL

Purpose: To determine whether T2-weighted signal intensity (T2W-SI) before and after neoadjuvant chemoradiation therapy (CRT) can predict complete and good response in patients with rectal cancer.

Material and methods: 171 consecutive patients with rectal cancer treated with neoadjuvant CRT underwent MRI before and 8-10 weeks post-CRT. The primary tumour and remnant after CRT were manually delineated on T2W-MRI. Histogram analyses were performed on these volumes of interest with pyradiomics. Extracted parameters were mean, median, standard deviation (SD), range, minimum, maximum T2W-SI before and after CRT. Change between pre- and post-CRT T2W-SI parameters was calculated. Heterogeneity of T2W-SI was assessed by the coefficient of variance (CoV=SD/mean). T2W-SI parameters were compared between complete (CR; ypT0), good responders (GR; ypT0-1) and non-responders (NR; ypT2-4). Reference standard was either histology after surgery or a wait-and-see programme with at least 2 years of recurrence-free follow-up.

Results: 36/135 patients had a CR and 49/171 a GR. Pre-CRT maximum SI (941.62 vs. 1149.63, p=0.028), heterogeneity of the SI (0.265 vs. 0.291, p=0.017) and SI range (828.56 vs. 1074.52, p=0.009) were significantly lower in CR than in NR. Pre-CRT minimum SI was significantly higher in both CR (113.06 vs. 75.10, p=0.017) and GR (117.02 vs. 69.46, p=0.001) compared to NR. Mean difference in SI between primary and restaging was larger in both CR and GR compared to NR (CR: -14257 vs. NR: -105.44, p=0.114 and GR: 176.83 vs. NR: -87.72, p=0.001).

Conclusion: The pre-CRT T2W-SI is significantly higher in CR and GR with a larger decrease in mean SI after CRT. These parameters could be a potential non-invasive marker for predicting complete/good response in patients with rectal cancer before and after CRT.

SS 2.5

The tram track sign: a new, highly specific and reliable sign for the detection of complete response after neoadjuvant therapy in rectal cancer

I. Santiago, M.J. Barata, N. Figueiredo, O. Parés, C. Matos; Lisbon/PT

Purpose: To assess the diagnostic value of the tram track sign to predict pathologic/sustained clinical complete response (CR) after neoadjuvant therapy in rectal cancer.

Material and methods: We retreived from our prospectively organized rectal cancer database all patients who underwent neoadjuvant therapy followed by restaging MRI (+)10 weeks post-radiotherapy, between October 2013 and March 2017. Two dedicated radiologists blindly and independently reviewed T2 and diffusion-weighted images and graded response according to tumor regression grade (mrTRG) and diffusion weighted imaging (mrDWI) using an in-house ordinal scale from 1-5. They also assessed the presence/absence of the tram track sign (mrTTS) - a double, uninterrupted, markedly T2-hypointense line at previous tumour location. Endoscopic data at same timepoint, graded according to an ordinal scale from 0-4, was also retrieved. For statistical analysis, primary endpoints were to compare the accuracy of endoscopy, mrTRG, mrDWI and mrTTS for the identification of sustained complete responders (SCR), defined as patients with pathologic CR or clinical CR at 1 year.

Results: 47 patients considered eligible: 26 males, mean age 63.8y. 20 underwent surgery. No significant differences were found for endoscopy. For observer 1, significant differences were found between $mrTRG_{1-2}$/$mrTRG_{3-5}$(p=0.03) and $mrTTS_{+}$/$mrTTS_{-}$(p=0.02), and for observer 2, between $mrDWI_{1-2}$/$mrDWI_{3-5}$(p=0.03) and $mrTTS_{+}$/$mrTTS_{-}$(p<0.01). Inter-rater agreement was poor for mrTRG[0.15(p=0.14)], moderate for mrDWI[0.55 (p<0.01)] and very good for mrTTS[0.83(p<0.01)]. mrTTS provided a sensitivity of 0.56/0.61 for observers 1/2, respectively, and a specificity/PPV of 1 for both readers.

Conclusion: mrTTS has very high specificity, positive predictive value and interrater agreement for the identification of SCR in rectal cancer. Its sensitivity is, however, low; therefore, it should be combined with other post-neoadjuvant therapy assessment tools.

SS 2.6

Patterns of fibrosis on rectal MRI in clinical complete responders undergoing wait-and-see after chemoradiotherapy for rectal cancer: correlation with functional outcome

T.N. Boellaard[1], D.M.J. Lambregts[1], A. Delli Pizzi[2], M. Van Der Sande[1], B.J.P. Hupkens[3], J. Van Griethuysen[1], G.L. Beets[1], R.G.H. Beets-Tan[1], M. Maas[1]; [1]Amsterdam/NL, [2]Chieti/IT, [3]Maastricht/NL

Purpose: To study whether morphologic patterns of fibrosis on T2W-MRI in non-operated clinical complete responders after chemoradiotherapy (CRT) for rectal cancer are related to long-term functional outcome.

Material and methods: N=68 patients were retrospectively analysed. All had a sustained complete response and underwent MRI follow-up (FU) 3-6 monthly as part of wait-and-see program (median FU 34 months (range 16-62)). Morphology of the rectal wall was assessed (2-reader consensus) on the T2W FU-MRIs and classified according to 4 patterns: [1] no fibrosis (=normalised rectal wall), [2] minimal fibrosis, [3] full-thickness fibrosis or [4] irregular/spiculated fibrosis. Long-term functional outcome was assessed with the Vaizey score, a 0-24 point score on bowel function/incontinence, as the main outcome. Vaizey-scores were compared between the 4 patterns of fibrosis.

Results: 5 patients showed no fibrosis, 45 minimal, 15 full-thickness and 3 irregular/spiculated fibrosis. Mean Vaizey score was 1.6 for the patients with no fibrosis versus 4.5/3.9/4.0 for the patients with minimal/full-thickness/irregular fibrosis, respectively (P=0.557). For the patients (n=38) with a distal rectal tumour (≤3 cm from the anorectal junction), mean Vaizey score was 1.3 in the no fibrosis group versus 4.7 for the minimal fibrosis and 6.5 for the full-thickness fibrosis group (no patients had irregular fibrosis; P=0.198).

Conclusion: Patients with a clinical complete response after CRT who show a normalised rectal wall without fibrosis appear to have a better functional outcome in terms of incontinence and bowel function compared to patients with fibrosis.

SS 2.7

18F-fluorodeoxyglucose positron emission tomography ([18F]-FDG PET)/MRI in locally advanced rectal cancer after preoperative chemo-radiotherapy: a comparison with conventional imaging

F. Crimì, C. Lacognata, I. Maretto, A. Perin, D. Cecchin, P. Zucchetta, F. Pomerri; Padua/IT

Purpose: To assess the accuracy of restaging after preoperative chemoradiotherapy (pCRT) with whole-body PET/MRI, pelvic T2-weighted (T2W) plus diffusion-weighted imaging (DWI) MRI (pelvic-MRI), pelvic T2W MRI (standard-MRI) and thoracoabdominal CT when predicting histopathologic TNM stage in locally advanced rectal cancer (LARC).

Material and methods: 26 patients with LARC underwent PET/MRI and CT before and after pCRT for TNM staging. 21 were treated with total mesorectal excision and 5 with transanal local excision. Histopathologic findings or a follow-up of at least 1-year were the reference standards. One radiologist evaluated pelvic MRI and CT. A second radiologist evaluated standard MRI. A third radiologist and a nuclear medicine physician assessed PET/MRI. T staging results were grouped in T0 and residual disease (T≥1). N stage was classified on a per-patient basis as positive or negative using MRI dimensional criteria (≥5mm per node), MRI lymph node global size reduction rate criteria (reduction<70%) and PET/MRI dimensional criteria and/or nodal FDG uptake.

Results: Sensitivity and specificity for ypT0 were 100%-85.7% for PET/MRI, 94.7%-85.7% for pelvic-MRI and 94.7%-57.1% for standard-MRI. For ypN+ with dimensional criteria, sensitivity and specificity were 100%-88.9% for PET/MRI and 75%-88.89% for pelvic-MRI. The values for pelvic-MRI changed to 87.5% and 72.2% using lymph node global size reduction rate criteria. PET/MRI correctly diagnosed two liver and one distant nodal metastases while missed a lung metastasis.

Conclusion: PET/MRI improves the accuracy of ycTN staging compared to MRI, but performs worse than CT in ycM staging. Initial results are promising; however, a larger cohort of patients should be examined introducing sequences for lung and gadolinium for liver metastases.

SS 2.8

Ulcerated scars post neoadjuvant therapy in rectal cancer: can morphologic changes and diffusion-weighted imaging restriction patterns predict a complete response?

M.J. Barata, I. Santiago, N. Figueiredo, O. Parés, C. Matos; Lisbon/PT

Purpose: Are changes in angle, thickness and pattern of restriction to diffusion of the tumour scar predictive of complete response in patients with rectal cancer presenting with an ulcer at tumour site on endoscopy after neoadjuvant therapy (NAT)?

Material and methods: All patients with rectal cancer who underwent NAT and presented with an ulcerated scar on restaging endoscopy were retrieved from our database. MRIs were reviewed independently and blindly by 2 radiologists, which recorded, in 4 different timepoints post-radiotherapy: 1st (mean: 8,6 weeks), 2nd (mean: 20,7 weeks), 3rd (mean: 33,4 weeks) and last (mean: 81,2 weeks): the angle between deepest point and inner borders of ulcerated scar (ANG); the scar thickness (STh); and the distribution pattern of high-signal intensity on diffusion-weighted imgaing (DIST). Primary outcome was presence/absence of signs of viable tumour at pathology or ≥1-year follow-up (including regular digital rectal examination, endoscopy and MRI), patients considered non-complete responders (NCR) and complete responders (CR), respectively. Mann-Whitney-U and Fisher´s exact test were used for statistical analysis. Interobserver agreement was assessed using intraclass correlation coefficient (ICC).

Results: 15 patients considered eligible (mean age= 66y; 8 men), 7 underwent surgery, 6 had persistent disease at pathology. Significant differences were found for both readers in percentage change of ANG and STh (median values): ANG1st_ANG3rd: Reader1:NCR=+9,2%; CR=-24,7%, p=0.02; Reader2: NCR=+44%; CR=-18,2%, p<0.01; ICC:0,44; ANG2nd_ANG3rd: Reader1: NCR=+3,1%; CR=-16,2%, p=0.01; Reader2: NCR=+11,5%; CR=-13,8%, p=0.04; ICC:0.34; ANG1st_ANGlast: Reader1: NCR=+15,8%; CR=-24%, p=0.03; Reader2: NCR=+45,3%; CR=-30%, p=0.04; ICC:0.70; STh1st_STh2nd: Reader1: NCR=0%;CR =-14,9%; p<0.01; Reader2: NCR=0%; CR=-18,3%; p=0.04; ICC:0,80; STh2nd_STh3rd: Reader1: NCR=5,1%; CR=-9,8%; p<0.01; Reader2: NCR=+40%; CR=-6,3%; p=0.04; ICC:0,48; STh1st_STh3rd: Reader1: NCR=0%; CR=-29,6%; p=0.02; Reader2: NCR=22,2%; CR=-26,8%; p<0.01; ICC:0,96; DIST was significantly different for both readers at last timepoint (absent/endoluminal linear vs intramural/irregular; p=0.01, ICC: 0.88).

Conclusion: Patients with an ulcerated scar on endoscopy after NAT were more likely to be CRs when progressive contraction and thinning of the scar was observed on follow-up MRIs, and when an absent/endoluminal linear pattern of restriction to diffusion was observed at last follow-up.

SS 2.9

Endorectal ultrasound is accurate for the assessment of anterior resection margin in low rectal cancer

J. Shur[1], D. Burling[2], A. Corr[1], J.T. Jenkins[1]; [1]London/UK, [2]Harrow/UK

Purpose: Accurate assessment of anterior resection margin (ARM) in low rectal cancer (LRC) helps ensure an R0 excision and appropriate triage to neoadjuvant treatment (naCRT), and with MRI can be difficult due to paucity of mesorectal fat and presence of vessels posterior to Fascia of Denonvilliers. The purpose of this study is to compare endorectal ultrasound (ERUS) with MRI for prediction of involved ARM in LRC.

Material and methods: We identified rectal cancer patients who underwent ERUS over a 5-year period. We reviewed imaging reports and case notes of those with a LRC (within 5cm of anorectal junction) and threatened ARM reported on MRI in whom ERUS was undertaken for further evaluation. Histopathology was used as a reference standard for the involvement of ARM and sensitivity, specificity, positive predictive value (PPV) and negative predictive value (NPV) were calculated for ERUS and MRI.

Results: 24 patients had LRC with threatened ARM reported on MRI. Complete data including MRI, ERUS and subsequent histopathology report in 9 patients were available, 5 who had naCRT. ERUS agreed with MRI for ARM involvement in 3 cases. 6 patients were appropriately triaged to more extensive resection (removal of posterior capsule of prostate or posterior vaginal wall) following confirmation of involved margin by ERUS, and 3 had less extensive surgery following confirmation of a clear margin seen at ERUS. Sensitivity, specificity, PPV and NPV was 80%, 75%, 80% and 75% respectively for ERUS compared to 40%, 20%, 33% and 25% for MRI.

Conclusion: ERUS is an accurate technique for complementary assessment of ARM in low rectal cancer.

SS 2.10

The diagnostic performance of diffusion-weighted MRI and computed tomography in the detection of extramural venous invasion in rectal cancer

A. Gursoy Coruh, E. Peker, A. Erden; Ankara/TR

Purpose: To evaluate the diagnostic utility of diffusion-weighted magnetic resonance imaging (DWI-MR) and CT in the detection of extramural venous invasion (EMVI) in rectal cancer.

Material and methods: Out of 358 patients with rectal cancer, totally 58 patients (30 patients with mrEMVI score: 3-4 and ctEMVI score: 2-3 and 28 control patients without EMVI) were enrolled in the study. Apparent diffusion coefficient (ADC) values of the tumor and EMVI(+) vein were measured. Diameter of superior rectal vein (SRV) and inferior mesenteric vein (IMV), distant metastatic spread were evaluated on CT. Pathology was accepted as the gold standard.

Results: Mean diameters of SRV (4.8±0.9mm vs. 3.6±0.8mm) and IMV (6.9±0.8mm vs. 5.4±0.9mm) were significantly larger ($p<0.001$) and ADC values of the tumor and the vein were significantly lower (926.4±281.8 s/mm^2 vs. 1026.6±246.8 s/mm^2, $p=0.032$) in EMVI (+) patients compared to the control group. A diameter of 3.95mm for the SRV (sensitivity: 93%, specificity: 66%, accuracy: 80%); 5.95 mm for the IMV (sensitivity: 93%, specificity: 71%, accuracy: 82%) and 0.929 s/mm^2 for ADC value was found as cut-off value by ROC analysis, for discrimination of EMVI (+) and EMVI (-) patients. When at least two of these 3 criteria are present, sensitivity, specificity values and accuracy increase (sensitivity: 100%, specificity: 75%, accuracy: 87%). The presence of distant metastases at presentation was significantly more prevalant in EMVI (+) patients ($p=0.002$).

Conclusion: Measurement of ADC values and SRV-IMV diameters seems to be a reliable method in the detection of EMVI in rectal cancer. EMVI (+) patients appear to have a higher risk for distant metastes at diagnosis.

11:00 - 12:30 **Liffey Hall 2**

Scientific Session SS 3

Imaging of acute abdominal conditions

SS 3.1

Can volumes of extrapancreatic inflammation and pancreas on abdominal computed tomography predict severity of acute pancreatitis?

E. Guler, T. Kose, M. Harman, O. Ozutemiz, N.Z. Elmas; Izmir/TR

Purpose: To evaluate the volumes of extrapancreatic inflammation and pancreas in predicting severity of acute pancreatitis compared with current scoring systems and laboratory markers.

Material and methods: This retrospective study included 30 patients (17 women, 13 men; median age 66.5 years) with acute pancreatitis who were examined with computed tomography (CT) in early disease onset. Extrapancreatic inflammation volume (EPIV), pancreatic volume (PV), ratio of EPIV to PV, Balthazar score, CT severity index (CTSI), and modified CTSI were calculated. Amylase, lipase, C-reactive protein (CRP), and white blood cell (WBC) levels at the time of obtained CT scans were reviewed. Outcome parameters included the length of hospital stay and development of complications. Spearman's rank correlation and Mann-Whitney U tests were used in the analysis of correlations.

Results: Significant positive correlations were found between EPIV and Balthazar score, CTSI, and mCTSI (r:0.709, r:0.741, r:0.799, respectively and $p<0.001$ for all). There were no significant correlations between pancreatic volume and scoring systems. Positive correlations between EPIV/PV and 3 scoring systems were depicted ($p<0.001$). Duration of hospitalization correlated with CTSI and mCTSI (r:0.47 and r:0.546, $p<0.05$). Significant correlations between the presence of complications and EPIV, EPIV/PV, CTSI, and mCTSI were observed ($p<0.05$). There were no significant correlations between amylase, lipase, CRP, WBC levels and 3 scoring systems.

Conclusion: EPIV and EPIV/PV can predict severity of acute pancreatitis. CTSI and mCTSI calculated in early onset of disease correlate with length of hospital stay and complications.

SS 3.2

Changes in radiology workflow in the setting of antibiotic treatment for uncomplicated appendicitis

D.J. Bowden, M. Sheehan, A. Lee, R. Dunne, A. Hill, M. Lee, M. Morrin; Dublin/IE

Purpose: At a university teaching hospital, a single centre, prospective trial of the management of acute uncomplicated appendicitis (AUA), randomising patients into conservative treatment with antibiotics versus treatment with surgery was undertaken (COMMA trial NCT#02916134). We analysed the pattern of imaging requested in this group, and compared it with the pattern of imaging in patients who had undergone appendicectomy for clinically suspected appendicitis during the year preceding the trial. The aim is to estimate the impact on radiology workflow in a busy academic centre on transitioning from standard surgical treatment of AUA to antibiotic treatment.

Material and methods: Patients who underwent appendicectomy before the COMMA trial and all patients enrolled in the COMMA trial were studied (pre-COMMA Nov 2014–Sept 2015, COMMA Sept 2015 – Dec 2017). The frequency of positive imaging and histology was recorded in both groups.

Results: In pre-trial period, 282 appendicectomies were performed. This group underwent 63 ultrasound scans (22%), 57 (20%) CTs and 1 MRI (0.3%). Negative histology at appendicectomy during the pre-trial period was 23% (n=64). During the trial period, 259 patients with clinically suspected appendicitis were assessed. This group underwent 149 ultrasounds (56%), 78 CTs (30%) and 70 MRIs (27%). Of this group, 202 were randomized to antibiotic treatment and 198 to surgery. Negative histology at appendicectomy was 2.5% (n=5).

Conclusion: Pre-operative imaging substantially reduces the number of negative appendicectomies. There was a substantial increase in radiology tests ordered in the transition from surgical treatment of AUA to antibiotic treatment which will have considerable implications for radiology workflow and will require significantly increased resources to be diverted to radiology in order to be implemented.

SS 3.3

Can CT accurately predict the presence of a single adhesive band in adhesive small bowel obstruction?

J. Sammon, J. Byrne, A. Okrainec, A. Hanbidge; Toronto, ON/CA

Purpose: Small bowel obstruction (SBO) is a common surgical emergency, with adhesions being the most frequent etiology (65-80%). Laparoscopic management has become an established technique, with successful outcomes higher in cases of single adhesive band (SB-SBO). Most patients have CT prior to surgery, however, the presence of a single adhesive band is usually not commented on in reports.

Material and methods: Patients undergoing laparoscopic surgery for adhesive SBO 2006–2014 were eligible. 110 patients were identified. 14 patients were excluded: 12 CT >3 days pre-surgery and 2 no CT features of SBO. Two abdominal radiologists independently reviewed the CTs. A single band was recorded for patients who had a single transition point or had two closely related transition points. Other factors including the degree, presence of a closed loop, free fluid, decreased perfusion, mesenteric oedema, bowel wall thickening and pneumatosis.

Results: 58 patients successfully underwent laparoscopic surgery, with 38 patients requiring conversion to laparotomy. 33/58 laparoscopic patients had SB-SBO and 9/38 converted patients had SB-SBO. Inter-observer variability between the two readers for SB-SBO on CT was very good with κ=0.739 (95% CI: 0.579-0.899) and κ=0.807 (95% CI: 0.687-0.927) with the surgical result. Reader 1 accurately assessed the presence of a SB-SBO in 40/42 cases (95% sensitivity {95% CI: 0.888-1.017}) and Reader 2 in 37/42 cases (88% sensitivity {95% CI: 0.783-0.979}).

Conclusion: CT can predict the presence of a single adhesive band and predict more complex cases, helping the surgical team triage patients appropriately to a laparoscopic approach, improving patient morbidity and length of hospital stay.

SS 3.4

Increased unenhanced bowel-wall attenuation: a specific sign of bowel necrosis in closed-loop small-bowel obstruction

C. Rondenet[1], I. Millet[2], L. Corno[1], I. Boulay-Coletta[1], P. Taourel[2], M. Zins[1]; [1]Paris/FR, [2]Montpellier/FR

Purpose: To identify computed tomography (CT) findings associated with bowel necrosis in patients with surgically confirmed strangulating closed-loop small-bowel obstruction (CL-SBO) due to adhesions or internal hernia.

Material and methods: This retrospective study was approved by our institutional review board, and informed consent was waived. To identify CT signs of bowel necrosis, two gastrointestinal radiologists performed blinded, independent, retrospective reviews of 41 CT studies from consecutive patients who had CL-SBO due to adhesions or internal hernias and who underwent surgery within 48h. Based on surgical and pathological findings, patients were classified as having reversible ischemia or histologically documented necrosis. Univariate statistical analyses were performed to assess associations between CT signs and bowel necrosis. K statistics were computed to assess interobserver agreement.

Results: We included 25 (61%) women and 16 (39%) men with a median age of 79 years. Bowel necrosis was found in 25/41 (61%) patients and ischemic but viable bowel in 16/41 (39%) patients. Increased unenhanced bowel-wall attenuation was the only CT finding significantly associated with bowel necrosis (P=0.0002). This sign had 58% (95%CI, 37-78) sensitivity and 100% (95% CI, 79-100) specificity for necrosis. Interobserver agreement was fair (0.59; 95%CI, 0.37-0.82).

Conclusion: Increased unenhanced bowel-wall attenuation is specific for bowel necrosis and should lead to prompt surgery for bowel resection.

SS 3.5

Is unenhanced CT-scan enough for the diagnosis and the management of elderly patients with acute abdominal pain in emergency department?

M. Barat, A. Kiani, P. Calame, M. Lagadec, M. Zappa, V. Vilgrain, M. Ronot; Clichy/FR

Purpose: To compare the accuracy and reproducibility of unenhanced and contrast-enhanced CT-scan for the diagnosis of patients over 75 years old admitted in emergency department (ED) for acute abdominal pain (AAP).

Material and methods: 208 consecutive patients over 75 years old consulting the ED for AAP with a CT-scan with and without enhancement were retrospectively included. Three readers read both exams in two different readings: 1) unenhanced images only, 2) full exam. Sensitivity and specificity for diagnoses were compared to the gold standard, defined as the diagnosis obtained after a complete clinico-biological and radiological evaluation. Intra and inter-reader agreement were calculated for each reader using the kappa test and the interclass correlation. Sub-group analyses were performed for patients with an organic disease as final diagnosis and for patients requiring an interventional treatment.

Results: Diagnostic accuracy ranged from 64% to 68% without enhancement, and from 68% to 71% after contrast enhancement. Contrast-enhanced images did not significantly improve the diagnosis accuracy (P = 0.973 – 0.979). CT scan corrected the diagnosis proposed by the ED physician in 59.1% (range 58.1-60.0%) and 61.2% (range 57.6-65.5%) of the patients before and after contrast injection (p>0.05). Intra-observer agreement between readings was moderate to substantial (K=0.513-0.711). Inter-reader agreement was substantial for both unenhanced (k=0.745-0.789) and full exam readings (k=0.745-0.799). These results were similar in sub-group analysis.

Conclusion: Unenhanced CT-scan alone is accurate and reproducible enough for the diagnosis of patients >75 years old presenting with an AAP.

SS 3.6

Clinical utility of functional MRCP in the diagnosis of acute cholecystitis

S. Ramanathan, D. Kumar, M. Heidous, A.A. Faki; Doha/QA

Purpose: To assess the feasibility and diagnostic accuracy of functional MRCP (fMRCP) with hepatobiliary contrast in the diagnosis of acute cholecystitis.

Material and methods: 150 patients who underwent gadolinium ethoxybenzyl diethylenetriamine pentaacetic acid (Gd-EOB-DTPA) enhanced MR imaging for various clinical indications were included. Study group comprised 60 patients who presented with acute right upper quadrant pain and equivocal physical examination and/or ultrasound findings for acute cholecystitis. 90 patients who came for other indications were considered as control group. Gallbladder was assessed for morphological features of acute cholecystitis. Functional MRCP was evaluated for timing of contrast appearance in the biliary confluence, common bile duct (CBD), contrast reflux in to gall bladder (GB)/cystic duct and excretion into duodenum.

Results: In the control group, contrast reflux into GB/cystic duct occurred in 85/90 patients (94.4%) at 15 ± 4 minutes (range: 5-30 min). 5/90 patients who did not show reflux demonstrated no extrahepatic biliary excretion due to poor hepatocellular uptake for other reasons. In the study group, 35/60 (58%) patients demonstrated reflux within 30 min. All these patients improved on clinical and US follow up without acute cholecystitis. 25/60 patients did not demonstrate contrast reflux till 1 hour delayed image. Acute cholecystitis was proven in 21/25 patients (84%) by cholecystectomy and development of convincing morphological features of acute cholecystitis. 4/25 (16%) patients did not demonstrate contrast reflux.

Conclusion: fMRCP is highly sensitive (96%) and specific (94%) in the diagnosis of acute cholecystitis, provided there is optimal extrahepatic biliary excretion. It is particularly helpful in cases of acute cholecystitis where the clinical and sonographic features are inconclusive.

SS 3.7

Role of imaging in the diagnosis of acute uncomplicated appendicitis in an adult population in a large prospective clinical trial

A. Lee, M. Sheehan, D. Bowden, P. O'Leary, A. Hill, M. Lee, R. Dunne, M. Morrin; Dublin/IE

Purpose: Acute appendicitis is the most common cause of an acute abdomen in adults. The purpose of this study is to assess the use of imaging in the diagnosis of acute uncomplicated appendicitis (AUA).

Material and methods: Over an 18-month period, a prospective trial of patients who met inclusion criteria for AUA were randomised into two treatment limbs based on radiological findings on ultrasound+/-CT or MRI: conservative management with antibiotic therapy or surgical appendicectomy. CT or MRI were performed if US was inconclusive.

Results: 117 patients that were suspected of having AUA, met the inclusion criteria and were randomised. 38.5% (N=45/117) had ultrasound alone prior to randomisation. 19.6% (N=23/117) had MRI and 11.11% (N=13/117) had CT following a negative or inconclusive US. 38.5% were randomised after US alone, of which 53.33% (N=24/45) were randomised to the surgical arm. 79.16% (N= 19/24) had an appendicectomy with a pathologically proven AUA. Of note, negative histology rate was very low at appendicectomy 2.5% (N=5). Discordant cases included 3 pathologically normal appendices, 1 of which had a faecolith at surgery; 1 gangrenous appendix (complicated appendicitis); and 1 granulomatous appendix (thickened but not inflamed). 46.6% (N=21/45) of whom had US alone were randomised to the conservative arm. Of these, 90.47% (N=19/21) were successfully managed conservatively. 2 patients returned for an appendicectomy. 1 patient had pathologically proven AUA and 1 had a histologically normal appendix.

Conclusion: Traditionally, patients suspected of having AUA have been treated with surgical resection. However, pre-operative imaging substantially reduces the number of unnecessary negative appendicectomies, in addition to identifying those patients who will respond to a conservative treatment with antibiotics.

SS 3.8

Acute jejunoileal diverticulitis: multicenter descriptive study of 33 patients

P. Lebert[1], I. Millet[2], O. Ernst[1], I. Boulay-Coletta[3], L. Corno[3], P. Taourel[2], M. Zins[3]; [1]Lille/FR, [2]Montpellier/FR, [3]Paris/FR

Purpose: Acute jejunoileal diverticulitis is a very rare and potentially serious disease involving mostly the elderly. The diagnosis is based on imagery but remains unrecognized. The purpose of this study is to describe the clinical and computed tomography (CT) features and the outcomes of acute jejunoileal diverticulitis.

Material and methods: Cases of acute jejunoileal diverticulitis managed at three French hospitals were identified retrospectively from 2005 through 2015. The final diagnosis relied either on a clinical and radiological data review by a panel of experts, or on the surgical findings. Demographic, clinical, laboratory, and 18-month outcome data were collected. CT scans were reviewed by having two radiologists reach a consensus about the inflammatory diverticulum, evidence of complications, and presence of other bowel diverticula.

Results: We identified 33 cases in 33 patients with a median age of 78 years, including 30 (86%) in whom an inflammatory diverticulum was identified, at the jejunum (n=26, 87%) or ileum (n=4, 13%). Extra-intestinal gas was seen in 10 (30%) and fluid in 11 (33%) patients. Other small-bowel diverticula were visible in all 33 patients. The diverticulitis was mild and resolved with non-operative treatment in 22 (67%) patients and severe in the remaining 11 (33%) patients, of whom 8 required emergency surgery.

Conclusion: Acute jejunoileal diverticulitis is a rare and usually non-serious condition that chiefly involves the jejunum. A detailed CT assessment may allow non-operative treatment.

SS 3.9

Emergency CT evaluation of pancreatic surgery complications in relationship to preoperative rectal/pharyngeal swabs status

A. Fighera, G. Cardano, A.J. Cybulski, L. Bertuzzo, G. Marchegiani, G.A. Zamboni, G. Mansueto; Verona/IT

Purpose: Multiresistant bacteria are becoming more and more common, and represent a cause of significant increase in morbidity and mortality in surgical patients. Our purpose was to analyze a series of patients who underwent emergency CT for suspected abdominal complications after pancreatic surgery, correlating the findings with the preoperative rectal/pharyngeal swabs.

Material and methods: We searched our picture archiving and communication system (PACS) system for the first emergency postoperative CT scan for suspected abdominal complications after pancreatic surgery performed in our institution in 1 year, thus obtaining 89 CT scans. Twenty-one patients had positive preoperative rectal or pharyngeal swabs, and 68 negative swabs. We reviewed the scans to assess for the presence and type of complications.

Results: Among the 89 patients who underwent emergency CT, 21 (23.6%) had positive swabs and 68 (66.4%) negative swabs. Patients with positive swabs underwent CT on average 6.6 days after surgery, compared to 8.9 days for patients with negative swabs (p= 0.0021). The prevalence of patients with positive swabs was higher among the 28 patients with CT signs of bleeding: 28.6% patients with bleeding had positive swabs. For fistulas and collections, the proportion of patients with positive or negative swabs was similar to that of the population who underwent these emergency CT scans.

Conclusion: Patients who undergo pancreatic surgery with preoperative positive swabs, undergo abdominal CT for suspected complications on average 2.3 days earlier than patients with negative swabs. The prevalence of patients with positive swabs is increased in patients with a CT positive for bleeding.

SS 3.10

Computed tomography for acute abdominal haemorrhage: impact upon emergency embolisation

A.C. O'Brien, G.M. Healy, N. Rutledge, A. Patil, J.W. McCann, C.P. Cantwell; Dublin/IE

Purpose: To assess the utility of computed tomography (CT) prior to attempted embolisation of acute abdominal haemorrhage.

Material and methods: All patients who underwent attempted emergency embolisation for acute abdominal haemorrhage at our institution between 01/01/2010 and 31/12/2016 were included. Obstetric, variceal bleeds and haemodynamically stable patients were excluded. 138 patients underwent 154 procedures, of which 131 were preceded by CT. Of the 154 procedures, successful treatment was performed for active bleeding (74 cases), pseudoaneurysm (26), AV shunt (6), irregular/truncated artery (10) and tumour (3). Empiric treatment was performed in 20 cases.

Results: Performing a CT before attempted emergency embolisation was associated with a significantly higher chance of successful treatment compared to those with no CT (81% vs 59% respectively, p=0.023). For those who underwent CT, an acute vascular finding (active bleed, pseudoaneurysm, AV shunt, irregular/truncated artery) was associated with a higher chance of successful treatment compared to those with no acute vascular finding (85% vs 52%, p=0.002). Patients with no acute vascular findings on CT (n=18), demonstrated active bleeding (5), pseudoaneurysm (2) and irregular/truncated artery (3) on formal angiography.

Conclusion: Performing CT prior to emergency embolisation for acute abdominal haemorrhage increases the probability of successful treatment. An acute vascular finding on CT further increases the probability of success. However, the absence of acute vascular findings should not exclude consideration for embolisation in the acute patient.

11:00 - 12:30 **Wicklow Hall 2A**

Scientific Session SS 4
Abdominal oncology

SS 4.1
Diagnostic value of dynamic perfusion MRI imaging in patients with local advanced rectal cancer in the assessment of chemo-radiation treatment: relation to tumor regression grade at histology
S.G. Drago, A. Pecorelli, C. Talei Franzesi, M. Cressoni, S. Sironi, D. Ippolito; Monza/IT

Purpose: To investigate the value of dynamic contrast-enhanced perfusion-MRI parameters in the evaluation of the response to chemo-radiation therapy in patients with local advanced rectal cancer in comparison with histology.
Material and methods: Fourteen patients with biopsy proven rectal adenocarcinoma who underwent dynamic contrast-enhanced MR performed on 1.5T MRI system (Achieva, Philips), before (MR1) and after chemo-radiation therapy (MR2), were enrolled in this study. The protocol included T1 gadolinium-enhanced THRIVE sequences acquired on axial planes. A dedicated workstation was used to generate color permeability maps; region of Interest (ROI) was manually drawn on tumor tissue and normal rectal wall, hence the following parameters were calculated and statistically analyzed: Relative venous enhancement (RVE), maximum enhancement (ME) and time to peak (TTP). Perfusion parameters were related to pathologic tumor regression grade (Mandard's criteria; TRG1=complete regression, TRG5=no regression).
Results: Five tumors (36%) showed complete or subtotal regression (TRG1-2) at histology and classified as responders; 9 tumors (64%) were classified as non-responders (TRG3-5). Perfusion MRI parameters were significantly higher in the tumor tissue than healthy tissue in MR1 and MR2 ($p<0,05$). At baseline (MR1), no significant difference in perfusion parameters was found between responders and non-responders. After chemo-radiation therapy, at MR2, responders showed significantly ($p< 0.05$) lower perfusion values (RVE(%)76±25; ME(%):96±41;TTP(sec):13±26) compared to non-responders (RVE(%):153±50; ME(%):169±42;TTP(sec):38±68). Moreover, in responders, perfusion values decreased significantly at MR2 (RVE(%)76±25; ME(%):96±41;TTP(sec):13±26) compared to MR1 (RVE(%):118±15;ME(%):120±18;TTP(sec): 14±24) ($p<0,05$). Furthermore, in non-responders, there was no significant difference between perfusion values at MR1 and MR2.
Conclusion: Dynamic contrast perfusion-MRI analysis represents a complementary diagnostic tool for identifying vascularity characteristics of tumor tissue in local advanced rectal cancer, useful in the assessment of treatment response.

SS 4.2
Diagnostic accuracy of standardised uptake value (SUVmax) in predicting malignancy of supraclavicular lymph nodes from primary oesophageal cancer
C. O'Rourke, I. Welaratne, S. Cournane, L. McLoughlin, J.V. Reynolds, C. Johnston, N. Sheehy; Dublin/IE

Purpose: The purpose of this study was to determine the diagnostic accuracy and optimum cut-off value of SUVmax on positron emission tomography (PET) to predict malignancy of supraclavicular lymph nodes (SCLNs) in patients with oesophageal carcinoma.
Material and methods: All diagnosed cases of oesophageal cancer were retrospectively reviewed (2012-2016). Patients that had a confirmed diagnosis of oesophageal cancer with avid SCLNs on staging PET were included in the study. 33 SCLNs that subsequently underwent ultrasound guided biopsy for staging were analysed. The maximum uptake values (SUVmax) of the SCLNs and primary tumours were measured. A receiver operating characteristic (ROC) analysis was performed to determine the optimum cut off of SUVmax in predicting malignancy.
Results: 24/33 PET-detected SCLNs were malignant. ROC analysis identified the best nodal SUVmax cut-off to be 3.0. The diagnostic accuracy of PET was 76.0% (sensitivity = 78.9%, specificity = 66.6%). For SCLNs with SUVmax > 3.0, PET showed a positive predictor value (PPV) of 88.2%; for SCLNs < 3.0, PET showed a negative predictor value of 50%. The median SUVmax of pathologically negative and positive nodes were 2.8 (range 1.8 - 6.0) and 5.3 (range 1.9 -13.4). The median primary tumour SUVmax was 13.8 (range 3.7 - 30.0). The SUVmax of metastatic lymph nodes were significantly higher than those of benign lesions ($p < 0.05$).
Conclusion: Our study revealed an accuracy rate of 76% for PET detected SCLNs in patients with oesophageal carcinoma. For SCLNs with SUVmax > 3.0, PET had a high PPV (88%), which can minimize the need for further diagnostic tests.

SS 4.3
Dedicated DW-MR imaging as a selection tool for hyperthermic intraperitoneal chemotherapy in patients with peritoneal carcinomatosis from colorectal origin
I. Van't Sant, M. Engbersen, H. Van Eden, D.M.J. Lambregts, N.F.M. Kok, A.G.J. Aalbers, R.G.H. Beets-Tan, M.J. Lahaye; Amsterdam/NL

Purpose: Combined cytoreductive surgery (CRS)/hyperthermic intraperitoneal chemotherapy (HIPEC) treatment gives a subset of patients with peritoneal carcinomatosis (PC) from colorectal origin (CRPC) with a limited and resectable peritoneal tumor load and prospect of long-term survival or even cure. A non-invasive imaging method to accurately select potential CRS/HIPEC candidates preoperatively is highly demanded. We compared the peritoneal cancer index (PCI) estimated preoperatively by diffusion-weighted MR imaging (DW-MRI) with PCI found at surgery to assess whether DW-MRI can be used to select CRS/HIPEC candidates.
Material and methods: Forty-nine consecutive patients (M/F=23/29) with confirmed or suspected PC from histologically proven colorectal origin were included. All patients underwent preoperative dedicated whole-body DW-MRI before exploratory laparoscopy or CRS/HIPEC. PCI was prospectively assessed by two independent radiologists on MR-imaging and was compared to PCI found at surgery (reference standard). Based on PCI patients were categorized as operable (PCI 0-20) or inoperable (PCI 21-39).
Results: Mean PCI at surgery was 12.2 (range 0-34). Mean radiological PCI for reader 1 was 10.9 (range 2-33) and 9.2 (range 0-32) for reader 2. Radiologist 1 and 2 staged respectively 46/49 and 44/49 patients correctly (accuracy 94%/90%). Both radiologists detected all operable patients with a PCI<21 at surgery (sens=100%). Respectively 3 and 5 patients were understaged by DW-MRI. No patients were overstaged. The intraclass correlation between the radiologists was excellent (ICC=0.91, 95% CI: 0.758-0.959).
Conclusion: In a large cohort, DW-MRI seems to be an accurate and robust selection tool to noninvasively select CRPC patients in which CRS/HIPEC is feasible. Further multicenter studies must be performed to see whether DW-MRI may replace surgical PCI staging.

SS 4.4

Radiological considerations in multiple site cytoreductive surgery for metastatic colorectal cancer: a cohort study

A.D. Stirling, A.N. Murphy, C.S. McQuade, J. Mulsow, C. Shields, H. Fenlon, C.G. Cronin; Dublin/IE

Purpose: Cytoreductive surgery (CRS) can improve survival in selected patients with metastatic colorectal cancer. These are complex, major surgeries that should be undertaken in specialist centres. The aim of this study is to evaluate outcomes relevant to radiological practice and resource management in patients undergoing multiple site CRS for metastatic colorectal cancer.

Material and methods: Patients who underwent multiple site CRS were identified from a prospectively maintained database of all patients with metastatic colorectal cancer referred to a national centre for the management of colorectal cancer and peritoneal malignancy. The number and anatomical location of the operative sites, peritoneal carcinomatosis index (PCI) and completeness of cytoreduction were recorded from electronic medical records. The number of multidisciplinary discussions, the extent of follow-up imaging and the number of image-guided interventions were recorded from a national picture archiving and communication system (NIMIS PACS).

Results: 72 patients were included over a 3-year period from May 2014-2017. The mean number of operative sites was 3 (range 2-7). The most common sites of CRS were: peritoneum and omentum (43%), liver (38%), and female reproductive organs (22%). This cohort had extensive imaging requirements averaging 10.5 investigations (either CT, MRI or positron emission tomography/CT, excluding initial staging) and 4.4 multidisciplinary discussions. The mean number of image-guided interventions was 2.4 (range 0-16).

Conclusion: The radiology input to the treatment paradigm of those undergoing CRS for metastatic colon cancer is substantial. Awareness of this will help guide resource management in this complex patient cohort.

SS 4.5

Role of gadolinium ethoxybenzyl diethylenetriamine pentaacetic acid MRI in characterizing nodules with atypical enhancement on CT: results of a prospective monocentric study

R. Faletti, M. Gatti, E. Caramia, A.M. Bozzato, A. Ferraris, S. Fiore, L. Bergamasco, P. Fonio; Turin/IT

Purpose: To assess the use of gadolinium ethoxybenzyl diethylenetriamine pentaacetic acid (Gd-EOB-DTPA) MRI in patients with "atypical" HCC diagnosed at multiphase CT.

Material and methods: 51 cirrhotic patients with at least one "naïve" lesion showing atypical dynamics enhancement on multiphase CT underwent Gd-EOB-DTPA MRI were prospectively enrolled. Images were reviewed by two radiologists in consensus. The atypical lesions were re-categorized by MRI into: group A) typical HCC; group B) hypervascular without washout and hypointense in the hepatobiliary phase (HBP) and group C) hypovascular nodules, hypointense in the HBP, hyperintense on diffusion-weighted imgaing (DWI). Patients were classified according to the Barcelona Clinic Liver Cancer (BCLC) guidelines prior and after the MRI. Data were analysed using non-parametric tests.

Results: 15 typical and 75 atypical lesions were found at CT. Twenty-six (66%) atypical lesions were re-classified into in group A, 8 (21%) in group B and 5 (13%) in group C; among the atypical lesion 17 were not confirmed, 12 were not detected and the diagnosis remained uncertain in 7 at MRI. Typical lesions resulted bigger than atypical lesions (22.3±16.9 vs. 12.3±7.3 mm; p=0.0004) and in particular, a lesion >15mm had a positive likelihood ratio (LR+) of 2.25 to be typical. BCLC stage was changed after MRI in 61% (31/51) patients. Based on MRI a biopsy was indicated for 7 nodules compared to 43 based on CT and 75% of group C lesions were confirmed histologically as HCC.

Conclusion: Gd-EOB-DTPA could correctly classify the majority of small and "atypical" HCC found on CT with high clinical impact on BCLC staging and management decision.

SS 4.6

CT-liver-perfusion dose reduction protocols for detection of hepatocellular carcinomas: is it achievable?

A.A. Hatzidakis, G. Kalarakis, K. Perisinakis, N. Kosidekakis, N. Kokkinos, A. Karantanas; Heraklion/GR

Purpose: To compare the diagnostic efficiency of standard "35-passes" CT-liver-perfusion (CTLP) acquisition protocol versus two "18-passes" CTLP-protocols for hepatocellular carcinoma (HCC) detection.

Material and methods: Fourteen patients (13 male, age 57-87) with 32 confirmed HCCs (median diameter 25mm, 11-125mm) underwent CTLP using a high temporal resolution acquisition protocol with 35 passes, pass-duration 1.7 sec, and total duration 59 sec. Eleven different perfusion maps were generated. Regions of interest (ROIs) were positioned on non-tumorous parenchyma and on HCCs. Maps were also retrospectively generated using the 18 first passes (total acquisition time 31 sec) and the 18 odd numbered passes (total acquisition time 59 sec). Receiver operating characteristic (ROC) analysis was employed to evaluate the ability of each map to discriminate HCCs from non-tumorous liver parenchyma. Comparison of ROC curves was performed to evaluate statistical significance of differences in the discriminating efficiency of the derived perfusion maps between different acquisition protocols.

Results: Hepatic arterial blood flow, mean slope of increase, time to peak, positive enhancement integral, and hepatic arterial fraction were found to be the prevailing parameters regarding HCC discrimination when the "35-passes" protocol was used, with estimated area under ROC curve of 1.000, 0.995, 0.993, 0.990, 0.983 respectively, without significant differences in their discriminating power (p>0.05), followed by Tmax, mean transit time (MTT), permeability–surface area product (PS), blood flow (BF), blood volume (BV), IRFT0. Comparison of ROC curves between "35-passes" and "18-passes" protocols yielded no significant differences (p>0.05) for any of the studied maps.

Conclusion: Dose reduction in CTLP for HCC detection can be safely achieved by reducing the number of passes to 18, since the diagnostic accuracy of the produced perfusion maps is not downgraded.

SS 4.7

Peri-hilar cholangiocarcinoma preoperative CT and MRI: accuracy and inter-observer agreement

A. Sarno[1], A. Contro[1], A. Ruzzenente[1], S. Conci[1], G. Tedesco[1], V. Ciaravino[1], R. De Robertis[2], N. Cardobi[2], M. D'Onofrio[1]; [1]Verona/IT, [2]Peschiera del Garda/IT

Purpose: To evaluate the accuracy of CT and MRI in the preoperative staging of peri-hilar cholangiocarcinoma.

Material and methods: CT and MRI study of 60 patients (45 males and 15 females, mean age 67 years) with peri-hilar cholangiocarcinoma were retrospectively reviewed by two radiologists. All patients underwent surgical evaluation. The review of imaging data was performed blinded to surgical and pathological results and separately. Involvement of biliary systems and vessels was judged. Sensitivity, specificity and accuracy were calculated with respect to surgical and pathological results. Inter-observer agreement was calculated with K agreement test.

Results: 50 patients were resected with curative intent (R0/R1) and 10 patients underwent explorative/palliative surgical treatment. The right bile ducts were involved in 31 patients, the left in 42 and both were involved in 26. Portal vein and hepatic artery involvement were present respectively in 36,2% and 23,2% of patients. Lymph-node involvement was observed in 25 patients. The sensibility, specificity and accuracy of MR and CT were similar. Accuracy for CT was 76.4%, 79.1% and 55.1% for biliary, vascular and lymph-node involvement. For MR accuracy was 74.0%, 82.2% and 51.6%, respectively. Inter-observer agreement (K value) was higher for MR compared to CT in biliary involvement (0.57 and 0.41), lower for arterial involvement (0.41 and 0.44) and lymph-node involvement (0.18 and 0.22). The agreement of the two readers showed statistically significant differences (p<0.001) for the right lobe.

Conclusion: CT and MRI are accurate in peri-hilar cholangiocarcinoma staging. MRI is superior to judge biliary systems involvement. Inter-observer agreement was inferior for the right lobe.

SS 4.8

Improved delineation of hepatic metastases from colorectal cancer using noise-optimized virtual monoenergetic reconstructions from dual-energy computed tomography

J.L. Wichmann[1], M.H. Albrecht[1], S.S. Martin[1], L. Lenga[2], D. Leithner[1], B. Bodelle[1], T.J. Vogl[1], R. Hammerstingl[1]; [1]Frankfurt am Main/DE, [2]Essen/DE

Purpose: To assess the impact of noise-optimized virtual monoenergetic imaging (VMI+) reconstructions on quantitative and qualitative image parameters in patients with hepatic metastases from colorectal cancer at abdominal dual-energy computed tomography (DECT).

Material and methods: Forty-two patients (29 men; 67.1±12.3 years) with histopathologically-confirmed hepatic metastases from colorectal cancer underwent triphasic contrast-enhanced abdominal DECT. Images from the portal-venous phase were post-processed with the standard linear blending technique (M_0.6) as well as with the traditional virtual monoenergetic (VMI) and novel VMI+ algorithms in 10-keV intervals from 40 to 100 keV. Attenuation measurements were performed in hepatic lesions, unaffected liver tissue, rectus abdominis muscle, and adjacent visceral fat to calculate objective signal-to-noise (SNR) and contrast-to-noise (CNR) ratios. Five-point scales were used to evaluate overall image quality and lesion delineation by three blinded radiologists with varying levels of experience.

Results: SNR and CNR (negative values indicating best contrast of hypoattenuating lesions) of liver metastases were best in 50-keV VMI+ series (3.5±2.1 and -3.6±2.0), significantly superior to all other reconstructions (all $P<0.001$; SNR M_0.6: 2.4±1.5; CNR M_0.6: -2.6±1.8). Qualitative image parameters showed highest values for 50-keV VMI+ reconstructions (median 5, respectively; $P\leq0.023$) regarding overall image quality. Qualitative assessment of lesion delineation peaked in 40-keV VMI+ (median 5) and 50-keV VMI+ (median 4; $P=0.067$), significantly superior to all other reconstructions (all $P<0.001$; M_0.6: median 3).

Conclusion: Novel VMI+ reconstructions at 50 keV can substantially increase quantitative image quality and improve subjective assessment of image quality and lesion delineation of hepatic metastases from colorectal cancer compared to standard image reconstruction and traditional VMI.

SS 4.9

How are we doing? Radiologist and multi-disciplinary team clinician opinions on the quality of MRI rectal cancer staging reports

P.J. Brown, H. Rossington, D.J.M. Tolan; Leeds/UK

Purpose: Rectal cancer staging with magnetic resonance imaging (RCS-MRI) allows accurate assessment of tumours. Significant variability exists in the content of reports. Colorectal multi-disciplinary teams (CRC-MDTs) make treatment decisions based on these reports. We evaluated the satisfaction of CRC-MDT members with current standards of radiology reporting to identify areas for improvement.

Material and methods: 16 UK CRC-MDTs serving a population over 5 million in Yorkshire, were invited to complete an online questionnaire assessing opinions on RCS-MRI report content and clarity. This included questionnaires for RCS-MRI radiologist 'reporters' and other CRC-MDT 'users' who use the reports to plan care (including colorectal surgeons, oncologists, pathologists and nurse specialists). 21 of 42 (50%) 'reporters' and 48 'users' completed the survey. All RCS-MRI reporting radiologists were subspecialists in GI imaging.

Results: Questionnaires indicated items which were 'always' contained in reports, with tumour stage, nodal status and CRM status included in more than 80% of cases. However there was lower than expected reporting for tumour distance from the anal verge (81% 'reporters' v 65% 'users'), relationship to peritoneal reflection (29% 'reporters' v 46% 'users'), extramural vascular invasion (57% 'reporters' v 67% 'users') and inter-reporter consistency (76% 'reporters' v 75% 'users'). There was no statistically significant difference between the opinions of reporters and users. Despite this 92% of 'users' were satisfied or very satisfied (on a five-point scale) with RCS-MRI.

Conclusion: CRC-MDT users were satisfied with RCS-MRI reports despite inconsistencies for reporting critical variables. CRC-MDT user satisfaction of reports may not act as a sufficient stimulus to improve standards of RCS-MRI reporting.

SS 4.10

Comparison of gadobutrol and gadofosveset trisodium in MRI for rectal cancer

R.A.P. Dijkhoff[1], J. Santinha[2], S.G. Drago[3], D.M.J. Lambregts[1], J. Van Griethuysen[1], F.C.H. Bakers[4], R.G.H. Beets-Tan[1], N. Papanikolaou[2], M. Maas[1]; [1]Amsterdam/NL, [2]Lisbon/PT, [3]Monza/IT, [4]Maastricht/NL

Purpose: To compare the pharmacokinetics of gadobutrol (GDB; micromolecular contrast-agent) with the albumin-binding contrast-agent gadofosveset trisodium (GDF) in MRI for staging or rectal cancer using semiquantitative analyses.

Material and methods: 12 patients with primary rectal cancer were included. 6 patients underwent dynamic contrast-enhanced-MRI (DCE-MRI) with GDF and were matched with 6 patients who had DCE-MRI with GDB. DCE-MRI protocol was the same in all patients. Regions of interests were manually placed in the tumour and DCE-MRI was processed with OncoAnalysis Horos Plugin (Computational Clinical Imaging Group, Champalimaud). Semiquantitative parameters (wash-in-slope, wash-out-slope, area-under-the-curve (AUC), maximum enhancement (MaxEnh) and time-to-peak (TTP)) based on signal intensity time curves were extracted and compared between GDB and GDF. Using the coefficient of variance (standard deviation/mean) heterogeneity was calculated for all semiquantitative parameters.

Results: Contrast-uptake parameters such as mean wash-in-slope (19.86 vs. 22.16, respectively, $p=0.690$) and mean maximum enhancement (283.72 vs. 286.86, respectively $p=0.615$) were comparable between patients with GDB and GDF, with only slight differences between both contrast agents. Also, maximum wash-in-slope (58.71 vs. 57.88, $p=0.974$) was comparable for both contrast agents. The differences between GDB and GDF for maximum/minimum/mean washout-slope were remarkably small, given the difference in size of the agents. GDF led to a more homogeneous maximum enhancement than GDB (0.55 vs. 0.33, respectively, $p=0.079$).

Conclusion: The albumin-binding contrast agent GDF shows similar contrast-uptake parameters compared to micromolecular GDB in this small sample of rectal tumours. It seems that GDF behaves similarly to a micromolecular agent shortly after injection, which might be explained by the absence of binding to albumin immediately after injection. Possibly, results of DCE-MRI with GDF might be extrapolated to micromolecular agents, regarding wash-in phase.

11:00 - 12:30 **Wicklow Hall 2B**

Scientific Session SS 5

Updates in upper and lower GI tract disorders

SS 5.1

Post chemoradiotherapy assessment of anal carcinoma using MRI: comparison with positron emission tomography in biopsy proven patients

R. Faletti, M. Gatti, V. Carrozzo, L. Bergamasco, P. Fonio; Turin/IT

Purpose: To assess the use of MRI in local response assessment and detection of early local relapse after chemoradiotherapy (CRT) in patients with anal squamous cell carcinoma (AC).

Material and methods: Eight patients with histologically proven AC who completed pre-(t0), post-CRT 4-week(t1) and 20-week(t2) MRIs and pre-(t0) and post-CRT 20-week(t2) positron emission tomography (PET) scan were prospectively included. Images were reviewed by two radiologists in consensus, blinded to clinical outcome: tumor size (D-mm), apparent diffusion coefficient (ADC-mm^2/s), time to peak (TTP-sec) and standard uptake value (SUV) were recorded. Lesion biopsy performed at 6-month was the gold standard test for evaluation of response to treatments. Data were analyzed using chi-squared test, Wilcoxon signed-rank test and Pearson's correlation coefficient.

Results: All patients were classified as responders. ADC, TTP and D were significantly different from t0 to t1 (0.8±0.2vs.1.2±0.2; p=0.002; 95±55vs.191±59;p=0.03 and 31±14.5vs.18±17;p=0.002) and from t0 to t2 (0.8±0.2vs.1.4±0.2;p=0.001, 95±55vs.214±67;p=0.006 and 31±14.5vs.10.5±10;p=0.001). From t1 to t2 ADC and TTP were not different (p=0.12 and p=0.50) unlike D (p=0.04). A difference from t0 to t1 of 20% in ADC (increase), TTP (reduction) and D (reduction) was identified as forecast of responder. SUV was significantly different from t0 to t2 (9.9±4vs.1.2±2.1;p=0.02). ADC was strongly inversely correlated with SUV values (r= -0.74).

Conclusion: D, ADC and TTP summarized in "the-rule-of-20%" seemed to be a good marker of early (4-week) response to treatment. The correlation ADC/SUV suggested an association between tumor cellularity and metabolic activity. ADC had a stronger relationship with outcome and may be more useful for predicting the prognosis of AC than SUV.

SS 5.2

MRI for response assessment after neoadjuvant chemoradiotherapy in oesophageal cancer: added value of diffusion-weighted imaging

S.E. Vollenbrock, F.E.M. Voncken, D.M.J. Lambregts, M. Maas, J.M. Van Dieren, L.C. Ter Beek, B.M.P. Aleman, R.G.H. Beets-Tan, A. Bartels-Rutten; Amsterdam/NL

Purpose: High accuracy is needed to select oesophageal cancer patients with a complete response (CR) after neoadjuvant chemoradiation (nCRT) for organ-preserving treatment instead of oesophagectomy. Performance of T2-weighted MRI (T2W-MRI) and additional diffusion-weighted MRI (T2W+DW-MRI) was determined.

Material and methods: Thirty-seven patients with locally advanced oesophageal cancer underwent MRI (1.5 Tesla; T2W-MRI and DW-MRI, b-values=0,200,800 s/mm^2) before and after nCRT with a maximum of 21 days between MRI and surgery. Three radiologists initially scored T2W-MRI only. Thereafter they rescored T2W with DW-MRI. A 5-point score was used (1=definite CR, 3=inconclusive, 5=definite residual tumour). Histopathology after oesophagectomy represented the reference standard (Mandard tumour regression grade 1=CR, 2-5=residual tumour). Area under the receiver operating characteristic (AUROC), sensitivity and specificity were calculated considering MRI scores 3-5 as tumour-positive.

Results: Three out of 37 patients were excluded due to poor image quality. Seven (21%) of the remaining 34 patients achieved a CR. AUROCs were 0.57, 0.66 and 0.66 for T2W-MRI only and 0.75, 0.70 and 0.71 for T2W+DW-MRI (p=0.09, 0.32, 0.70). Sensitivity for detecting residual tumour was 100%, 89% and 89% for T2W-MRI only and 93%, 96% and 85% for T2W+DW-MRI. Specificity improved from 14%, 43% and 43% on T2W-MRI to 57%, 43% and 57% for T2W+DW-MRI.

Conclusion: T2W+DW-MRI is promising for response assessment after nCRT in oesophageal cancer patients. Sensitivity is high, indicating that the risk of missing residual tumour is minimal. Specificity is lacking, indicating that the degree of residual tumour is overestimated. A multimodality approach with endoscopy, endosonography and positron emission tomography (PET)-CT may further improve response assessment.

SS 5.3

Prognostic value of positron emission tomography (PET)-CT in oesophageal cancer patients undergoing oesophagectomy

E. O'Malley, C. Waters, C. Collins, J. Bruzzi; Galway/IE

Purpose: Above the age of 50 oesophageal cancer incidence is 30-40/100,000 in the Irish Health Service Executive Western area. Stage I disease has 60% overall survival at 5 years, stage II 30%, stage III 20% and stage IV less than 5%. Accurate staging is important when selecting surgical candidates and multiple modalities are used including CT, endoscopic ultrasound and PET CT. PET CT may provide extra prognostic value which is not used in clinical practice. Conflicting data exist about the usefulness of maximum standardised uptake value (SUV_{max}) and other measurements such as metabolic tumour volume (MTV) and total lesion glycolysis (TLG). This study analyses PET CT findings and compares tumour measurements including MTV and TLG with the post-surgical mandard response score, 5-year survival and histological staging.

Material and methods: This retrospective analysis looked at PET CT studies from 2010 to 2016. Patient demographics, survival time, histopathology staging and PET CT measurements were collected. PET CT measurements included SUV_{max}, SUV_{peak}, SUV_{mean} MTV and TLG.

Results: We identified 64 patients who underwent oesophagectomy. Median age at surgery was 64 (39-78). Histopathology was adenocarcinoma 72% and squamous cell carcinoma 28%. Mean MTV was 47.9 ml, mean SUV_{max} 9.9, mean SUV_{peak} 7.95, mean SUV_{mean} 6.23 and mean TLG 207.79. Mean 5-year survival was 1.5 years. There was no significant correlation between PET CT measurements and survival, mandard score or histological staging.

Conclusion: FDG avid measurements alone are not a useful prognostic factor in oesophageal cancer patients undergoing surgery.

SS 5.4

Restaging of resectable esophageal cancer using positron emission tomography (PET)/CT after neoadjuvant treatment: combining the best of both worlds

D. Tamandl, B. Füger, A. Haug, A. Ba-Ssalamah; Vienna/AT

Purpose: To assess the feasibility and diagnostic performance of PET/CT in the restaging of esophageal cancer after neoadjuvant therapy.

Material and methods: We included 88 esophageal cancer patients without distant metastases, who were resected after neoadjuvant treatment. PET/CT with a diagnostic, contrast-enhanced CT (CE-CT) scan, was performed before resection and the radiological staging was compared to postoperative histopathology as the reference standard. Locoregional stage (T, N-stage) was retrieved from the CT scan, whereas PET analysis consisted of measurement of standardized uptake value (SUV) mean, SUV max, Tumor diameter, metabolic tumor volume (MTV) and total lesion glycolysis (TLG). Sensitivity, specificity and accuracy of the CT staging in reference to pathology were calculated. PET parameters were compared using analysis of variance (ANOVA).

Results: Of the 88 patients amenable for analysis, eleven patients (13%) had received combination radiochemotherapy, whereas 75 patients (85%) had neoadjuvant chemotherapy either in combination or monotherapy with various agents. For overall T-staging, true positive, false positive and false negative rates for CT vs. PET/CT (qualitatively) were: 59.1% vs. 68.1%, 25% vs 15.9% and 15.9% vs. 15.9%, leading to an accuracy of 57.6% vs. 68.2%. For T3+4 stages alone, CT had a better diagnostic performance (sensitivity 85.7, specificity 81.8%). Volumetric PET parameters, but neither SUVmax nor SUVmean correlated with T- stage: MTV (p=.011), TLG (p=0.35), PET-Diameter (p=0.001). Likewise, there was an association to American joint committee on cancer (AJCC) stage: MTV (p=.015), TLG (p=0.37), PET-Diameter (p=0.002).

Conclusion: In restaging of esophageal cancer after neoadjuvant therapy, both CE-CT and PET provide independent information on the post-therapeutic locoregional tumor stage.

SS 5.5

More frequent follow-up CT examinations after surgical resection than endoscopic resection of early gastric cancers: are they really useful?

S.E. Jung, M.H. Choi; Seoul/KR

Purpose: A recommended interval to follow-up CT or endoscopy after treatment is not provided in the national comprehensive cancer network (NCCN) guidelines. No study has analyzed the role and interval of CT after both surgical and endoscopic resection for gastric cancer. To evaluate the utility and timing of CT in the detection of recurrent tumor after surgical and endoscopic resection (endoscopic submucosal dissection) for early gastric cancer (EGC).

Material and methods: A total of 670 patients after surgical (n = 535) and endoscopic resection (n = 135) for EGC between 2007 and 2009 were enrolled. Mean numbers of CT and endoscopy between both treatment groups were compared. The mean and cumulative dose length product (DLP) of CTs were calculated. Recurrence-free survival and overall survival were evaluated using a Kaplan-Meier method.

Results: The mean interval of CT was significantly shorter and the mean number of CTs was significantly larger in the surgical resection group than in the endoscopic resection group. All 34 gastric recurrences were diagnosed by endoscopy. Six extragastric recurrences were detected by CT out of total 5417 CT examinations. The average cumulative DLP was significantly higher in the surgical than in the endoscopic resection group (P = 0.004).

Conclusion: Follow-up CT was more frequently performed in patients after surgical resection than in those after endoscopic resection of EGCs even though CT showed limited usefulness for detecting recurrent tumors after either treatment methods. Since there was no extragastric recurrence in patients with mucosal cancer after resection, routine use of CT should be avoided after treatment of mucosal cancer.

SS 5.6

An investigation of the association between sarcopenia and post-operative morbidity and mortality in patients with gastric cancer using CT

S. O'Brien, M. Twomey, F. Moloney, R.G. Kavanagh, M. Maher, O.J. O'Connor, C. O'Suilleabhain; Cork/IE

Purpose: Surgical resection for gastric adenocarcinoma is associated with significant post-operative morbidity and mortality. The aim of this study was to assess the prognostic significance of sarcopenia in patients undergoing curative resection for gastric adenocarcinoma with respect to post-operative morbidity, disease-free and overall survival.

Material and methods: A retrospective analysis of a cohort of consecutive patients who underwent surgical resection for gastric adenocarcinoma between 2008 and 2014 was conducted. Patient demographics, radiological parameters and pathological data were collected. Osirix was used to measure skeletal muscle area at a set level, which was normalized for height to calculate skeletal muscle index. Sarcopenia entailed a skeletal muscle index of less than 52.4cm^2/m^2 for men and 38.5cm^2/m^2 for women. Statistical analysis was performed using the statistical package for the social sciences (SPSS). Regression analysis was used to identify predictors of outcomes.

Results: Fifty-six patients (41 male, 15 female, mean age 68.4±11.9 years) met the inclusion criteria. Thirty-six percent (20/56) of patients were sarcopenic pre-operatively. Both sarcopenic and non-sarcopenic patient groups were equally matched with the exception of weight and body mass index (p=0.036 and p=0.001). Sarcopenia was associated with a decreased overall survival (Log Rank=0.003) and was an adverse prognostic predictor of overall survival on multivariable analysis (hazard ratio=10.915, p=0.001). Sarcopenia was a predictor of in-hospital serious complications on multivariate analysis (odds ratio=3.508, p=0.042).

Conclusion: In patients undergoing curative resection for gastric cancer, there is a statistically significant association between sarcopenia and both decreased overall survival and serious post-operative complications. The measurement and reporting of skeletal muscle index on pre-operative CT should be considered for patient preparation purposes.

SS 5.7

Prediction of tumor response to chemotherapy using perfusion CT in patients with unresectable advanced gastric cancer

D.H. Lee[1], S.H. Kim[1], S.M. Lee[2]; [1]Seoul/KR, [2]AnYang/KR

Purpose: To evaluate whether parameters obtained from perfusion CT (PCT) can predict treatment response after palliative chemotherapy in patients with unresectable advanced gastric cancer (AGC).

Material and methods: This prospective study was approved by the institutional review board and informed consents were obtained. Twenty-one patients with unresectable AGC (M:F=13:8; mean age, 53.7 years old) were included. We performed PCT and palliative chemotherapy in all 21 patients. After palliative chemotherapy, treatment response was assessed for each patient using RECIST ver. 1.1 and patients who achieved complete or partial response were classified into responder group. Relationship between tumor response to palliative chemotherapy and PCT parameters was evaluated using the Mann-Whitney test and receiver operating characteristic analysis.

Results: After chemotherapy, 6 patients showing partial response were classified into the responder group and the remaining 15 patients into the non-responder group. Permeability surface value was significantly different between two groups (51.0 ml/100g/min in responder group versus 23.4 ml/100g/min in non-responder group, P=0.002). Other PCT parameters were not significantly different between two groups. The area under the curve to predict responders was 0.911 (95% confidence interval, 0.787-0.990; P=0.004) for permeability surface value and the sensitivity of 100% (6/6) and specificity of 80% (12/15) were achieved when a cut-off permeability surface value was set at 29.7 ml/100g/min.

Conclusion: Obtaining perfusion parameters from PCT was feasible for patients with unresectable AGC and can aid the prediction of treatment response after palliative chemotherapy as the permeability surface value in patients within the responder group was significantly higher than within the non-responder group.

SS 5.8

MRI of the gastric antrum for the quantification of gastric motility: comparison between obese and normal weight patients

S. Picchia[1], M. Rengo[1], M.A. Bali[2], D. Bellini[3], S. Badia[3], A. Laghi[1]; [1]Rome/IT, [2]London/UK, [3]Latina/IT

Purpose: To compare gastric motility in obese patients and normal weight volunteers with magnetic resonance (MR).

Material and methods: This is a non-randomized single-centre study. The motility analysis was performed on 1.5T MRI using 2DtrueFISP sequences on coronal and axial plane. Images were acquired before, immediately after a liquid meal (Nutridrink plus 2 yolks, 1 albumen and 150 ml of water) and every 20 minutes for a total of 5 different acquisition times (T0-T5) and a total exam time of 100 minutes. This 525-kcal meal was composed of 25% fat, 25% protein and 50% carbohydrate. Each gastric motility scan lasted 60 seconds, with 100 images acquired in free breathing. Antral length (AL), maximal contraction amplitude (MCA) and contraction frequency (CF) were evaluated on a dedicated software. Results obtained in obese patients and normal weight volunteers were compared.

Results: Our final population consisted of twenty patients (10 obese and 10 normal weight). MR showed that during fasting and postprandial period, in obese patients all the evaluated parameters (AL, MCA and CF) were significantly lower than normal weight volunteers (mean basal AL obese patients=6.75±0.8cm/normal weight patients=8.12±0.43cm, p value<0.05; mean postprandial AL obese patients=7.56±1.03cm/normal weight patients=9.4±0.12mm, p value<0.05; mean basal MCA obese patients=7.1±0.72mm/normal weight patients=8.97±0.43, p value<0.05; mean postprandial MCA obese patients=8.3±1.5mm/normal weight patients=9.76±0.76mm, p value<0.05; mean basal CF obese patients=8.7±0.98cpm/normal weight patients=10.3±0.9, p value<0.05; mean postprandial CF in obese patients=9.8±1.4cpm/in normal weight patients=11.2±1.2cpm, p value<0.05).

Conclusion: MRI identified differences in antral motility between obese patients and normal weight volunteers. The obesity-related cause could become a potential new therapeutic target.

SS 5.9

Utility of diffusion-weighted MRI with different b values in the evaluation of perianal fistulas

M.H. Turkcanoglu, A.H. Yardımcı, C.T. Bektas, B. Kocak, O. Kilickesmez; Istanbul/TR

Purpose: To determine the optimal b-value for diffusion-weighted imaging (DWI) in the diagnosis of perianal fistula and to demonstrate the diagnostic efficacy of this b-values and fistula tract thickness on DWI.

Material and methods: Magnetic resonance (MR) images of 200 patients with the suspicion of perianal fistula referred to our Radiology Clinic were evaluated retrospectively. In our study, primary fistula tracts, internal orifices, abscess formations, horseshoe components and secondary tracts were evaluated. Axial fat-suppressed T2-weighted spin-echo (SE) images, DWI1 and DWI2 (b values, 400 and 1000s/mm^2) contrast-enhanced T1-weighted images were analyzed for each patient by using a four-point scale. The combination of contrast-enhanced T1-weighted images with T2-weighted images was used as reference standard.

Results: 216 fistulas were detected in 200 patients (39 female,161 male). The sensitivity of DWI obtained at low b-value is higher in the evaluation of primary tract, internal orifice, secondary tract and horseshoe components in perianal fistulas. For the evaluation of abscess formations, it is seen that both low and high b-value DWI are equally sensitive. It has been shown that primary tract thickness is significant in detection of fistulas on DWI. The cut-off value for fistula thickness is 3.0 mm. Area under the curve 0.876 (0.831-0.922). Optimal cut-off value was obtained with 75.3% sensitivity, 100% positive predictive value, 100% specificity, 39.5% negative predictive value.

Conclusion: The choice of optimal b values significantly affects the detection of perianal fistulas in DWI. Low b values (b=400s/mm(2)) had the best specificity and sensitivity. It has been shown that primary tract thickness is significant in detection of fistulas on DWI.

SS 5.10

Deep infiltrating endometriosis: can magnetic resonance imaging predict the need for a colorectal surgeon?

A. Brusic, S. Esler, L. Churilov, P. Chowdry, M. Sleeman, P. Maher, N. Yang; Heidelberg, VIC/AU

Purpose: To identify Magnetic Resonance (MR) features that predict the need for colorectal (CR) surgeon intervention during gynaecologist-led laparoscopic surgery for deep infiltrating endometriosis (DIE).

Material and methods: Retrospective cohort multivariate analysis. The cohort consisted of women with laparoscopically-proven DIE, preoperative pelvic MR at Austin Health and subsequent surgery and histopathological confirmation at Mercy Hospital (2006-2015, n=122). MRIs were reviewed independently by two radiologists blinded to outcomes. MR characteristics of pelvic endometriosis were correlated to outcomes, to identify features associated with CR-surgeon intervention.

Results: The readers demonstrated concordant findings for: presence of bowel lesions (kappa=0.68, 95%CI:0.55-0.81), bowel lesion length (Lin's concordance coefficient 0.73, 95%CI:0.66-0.81); and bowel lesion depth (kappa=0.82, 95%CI:0.74-0.88). MR detected bowel lesions appeared more strongly associated with the need for CR-surgeon intervention than current practice (defined as the presence of a CR-surgeon in theatre), but this was not statistically significant (area under receiver operating characteristic curve (ROC-AUC) 0.79 vs 0.74, p=0.23). MR bowel lesions measuring ≥20mm or bowel lesions invading the muscularis or submucosa, however, did demonstrate a statistically significant correlation with CR-surgeon intervention and performed better than current practice (ROC-AUC 0.84, p=0.014 and 0.90, p<0.0001, respectively).

Conclusion: The current decision-making process to identify those patients with DIE that require a CR-surgeon to aid bowel resection is poorly defined and variable, resulting in sub-optimal resource allocation. This study identifies reproducible, objective MR features that better predict the need for CR-surgical intervention than the current practice. This provides a basis for a prospective study for validation and development of a predictive scoring system to aid surgical planning and resource allocation.

11:00 - 12:30 **The Auditorium**

Scientific Session SS 6
Small Bowel: imaging Crohn's disease

SS 6.1
Diagnostic accuracy of layered pattern of enhancement during MRI exams in predicting active inflammation in Crohn's disease: systematic review and meta-analysis
F. Rivosecchi[1], D. Bellini[1], D. Caruso[1], D. De Santis[1], M. Zerunian[1], A. Laghi[2]; [1]Latina/IT, [2]Rome/IT

Purpose: To assess diagnostic accuracy of layered pattern (LP) on contrast-enhanced magnetic resonance imaging (MRI) in detecting active inflammation in patients with Crohn's disease.
Material and methods: Methods for analysis were based on preferred reporting items for systematic reviews and meta-analyses (PRISMA). We searched MEDLINE, Cochrane library, Embase and Web of Science databases. Pooled estimates for sensitivity, specificity, pooled positive likelihood ratios (LR) and pooled negative LR were calculated using random effect model. I^2 was used to evaluate heterogeneity. Quality assessment of diagnostic accuracy studies (QUADAS) II was used to assess the quality of studies included.
Results: Of the 638 articles initially identified thorough databases searching, 7 were included for quantitative synthesis. Cumulative data for diagnostic accuracy on per patients basis were sensitivity 51% (95% CI: 44–59%; I^2: 78.5%), specificity 80% (95% CI: 74–85%; I^2: 91.4%), pooled positive LR 2.5 (1.32 to 4.73; I^2: 63.2%), pooled negative LR 0.67 (0.58 to 0.77; I^2: 0.0%). Heterogeneity was high among studies.
Conclusion: In conclusion, diagnostic accuracy of layered pattern on MRI has a low sensitivity and a high specificity in detecting active inflammation in Crohn's disease. Our results are limited due to the high heterogeneity among studies included.

SS 6.2
Intra- and inter-observer variability in visually graded small bowel motility features from dynamic MRI of Crohn's disease patients
R. Gollifer[1], A. Menys[1], A. Plumb[1], F. Vos[2], J. Stoker[3], D. Atkinson[1], S.A. Taylor[1]; [1]London/UK, [2]Delft/NL, [3]Amsterdam/NL

Purpose: Automated measurement of small bowel motility metrics is highly reproducible and is giving insights into the aetiology of abdominal symptoms in Crohn's disease. It is unknown if a simple qualitative assessment of motility by abdominal radiologists is sufficiently robust, and in particular is reproducible between observers.
Material and methods: 105 Crohn's disease subjects underwent a 20-second breath hold cine motility sequence, after mannitol ingestion, as part of magnetic resonance enterography. Five global small bowel motility metrics were visually graded by two experienced radiologists using a 10-point scale to assess 1) mean, 2) spatial variability, 3) temporal variability, 4) area of motile bowel and 5) distension quality. 26 datasets were analysed twice with a minimum gap of 2 weeks. Inter-and intra-reader variability was assessed using Bland-Altman plots.
Results: Inter-reader variability was generally poor for all motility features graded e.g. the Bland-Altman mean difference in the spatial variability metric was -0.76 au and the Bland-Altman 95% limits of agreement were -5.8 to +4.3 across a range of values from 0.35 to 8.45. For radiologist 2, the worst agreement was for the spatial variability metric with a mean difference between the original grading and the repeat grading of -0.11 au and the Bland-Altman 95% adjusted limits of agreement were -4.1 to 3.9 across a range of values from 0.7 to 7.4.
Conclusion: Simple visual assessment of small bowel has poor inter and intra-observer agreement for most motility metrics and cannot replace automated software measurement.

SS 6.3
Development and validation of a simplified magnetic resonance index of activity for Crohn's disease
J. Rimola, I. Ordas, S. Rodriguez, E. Ricart, J. Panés; Barcelona/ES

Purpose: To develop and validate a simplified and accurate magnetic resonance index of activity (sMaRIA) for assessing activity and therapeutic response on patients with luminal Crohn's disease (CD).
Material and methods: Magnetic resonance enterography (MRE) data from 98 patients, including active and inactive segments (colon and terminal ileum), from two prospective studies were re-analysed to develop the sMaRIA using endoscopy (Crohn's disease endoscopic index of severity (CDEIS)) as the gold standard. Further analysis of responsiveness in a cohort of 37 patients who underwent MRE and endoscopy before and after 12 weeks of therapeutic intervention was performed. Comparison between MaRIA and sMARIA for detecting active/severe lesions and therapeutic response was performed.
Results: Logistic regression analysis showed that wall thickness >3mm, presence of edema, ulcers and fat stranding were independent predictors of disease activity and were used therefore as descriptors of sMaRIA. The sensitivity and specificity of sMaRIA at segment level for detecting active disease using a cutoff ≥5 were 90% and 81% (area under curve (AUC)=0.91, 95%CI 0.88-0.94), and for detecting severe lesions (ulcers) using a cutoff ≥10 were 85% and 92% (AUC=0.94, 95%CI 0.91-0.96). Correlation between sMaRIA and CDEIS/MaRIA was excellent (r=0.84 and r=0.97, respectively; p<0.001). The sMaRIA accurately detected changes in lesion severity in response to a therapeutic intervention and was as reliable as endoscopy for the assessment of mucosal healing.
Conclusion: Simplified MaRIA index allows a faster and easier assessment of inflammation in CD by keeping high accuracy for both diagnosis and therapeutic response. Main advantages over MaRIA includes, a less time consuming calculation and is not confounded by missing segments.

SS 6.4
Evaluation of image findings on CT enterography for endoscopic complete remission after anti-tumor necrosis factor-alpha therapy in patients with Crohn's disease
S.H. Kim, J.E. Kim, T.O. Kim, J.-H. Yoon; Busan/KR

Purpose: To evaluate the image findings of CT enterography (CTE) obtained in patients with endoscopic complete remission (CR) after anti-tumor necrosis factor (TNF)-alpha therapy for Crohn's disease.
Material and methods: Between August 2010 and October 2017, 36 consecutive patients with Crohn's disease who received anti-TNF-alpha therapy and underwent pre-and post-therapy CTE as well as ileocolonoscopy were initially enrolled. CTE was performed with standard-dose enteric phase scan. Eleven patients were excluded due to a mismatch of follow-up intervals or a long interval (over 2 weeks) between CTE and ileocolonoscopy. Therefore, 25 patients (16 men, 9 women, mean age 26 years; range 18-43 years) were finally analyzed. Two blinded readers reviewed pre-and post-therapy CTE image findings in consensus as for active inflammation, i.e., mural hyperenhancement, mural thickening (thickness>3mm), mural stratification, and increased pericolonic fat attenuation in the rectum, colon, and terminal ileum, respectively. The endoscopic CR indicated mucosal healing identified by ileocolonoscopy and served as the reference standard.
Results: Eleven patients had endoscopic CR. Six patients of them (6/11, 55%) had residual mild mural thickening and mild mural hyperenhancement on post-therapy CTE compared to pre-therapy CTE. The other 5 patients did not have any post-therapy CTE abnormalities. Non-endoscopic CR group (4 partial remissions and 10 poor remissions) showed a higher concordance rate of 86% (12/14) with post-therapy CTE than endoscopic CR group did (45%, P=0.0358).
Conclusion: Residual mild mural thickening and mild mural hyperenhancement were seen on post-therapy CTE over half of the patients having endoscopic CR after anti-TNF-alpha therapy for Crohn's disease.

SS 6.5

Established damage detected at MRE in patients with Crohn's disease in complete endoscopic remission

J. Rimola, I. Alfaro, D. Vas, J. Castro, E. Ricart, J. Panés; Barcelona/ES

Purpose: To identify the Magnetic Resonance Enterography (MRE) lesions that persist in patients with Crohn's disease (CD) in endoscopic remission as indicators of established damage, and to determine its relationship with pre-treatment MRE lesions.

Material and methods: Patients with CD that had been included in prospective studies on autologous heamatopoyetic stem-cell transplant and/or anti-tumor necrosis factor (TNF) drugs were evaluated for this study. Inclusion criteria were: presence of at least one segment with severe inflammatory lesions detected at MRE and achievement of endoscopic remission after 1 year of treatment.

Results: 73 intestinal segments (28 patients) with severe inflammatory lesions at baseline achieved endoscopic remission after 1 year of treatment. The prevalence of creeping fat and bowel mural fat deposition did not change in association with the achievement of endoscopic remission (p=0.34 and p=0.35 respectively). Furthermore, luminal strictures persisted in 50% of segments with initial strictures, and wall thickness remained >3mm in 29% of segments with severe inflammatory lesions at baseline. Regression analysis showed that predictive lesions on pre-treatment MRE for established residual mural lesions after achieving endoscopic remission were the presence of bowel fat deposition (OR=48.3, p=0.001) and strictures at baseline (OR=15.96, p=0.004), whereas creeping fat was the only predictive factor for persistent extramural lesions (OR=35.8, p<0.001) and for either mural or extramural lesions (OR=16.25, p<0.001).

Conclusion: Up to 41% of bowel segments with initial severe inflammation in long-standing endoscopic remission after treatment had residual lesions at MRE. Presence of bowel fat deposition, strictures and creeping fat at pre-treatment MRE may predict the development of established damage.

SS 6.6

Preoperative evaluation of small bowel complications in Crohn's disease: comparison of diffusion-weighted and contrast-enhanced MR imaging

M. Barat[1], C. Hoeffel[2], M. Bouquot[1], R. Dautry[1], M. Boudiaf[3], K. Pautrat[1], R. Kaci[1], C. Eveno[1], M. Pocard[1], P. Soyer[1], A. Dohan[1]; [1]Paris/FR, [2]Reims/FR, [3]Meudon la Foret/FR

Purpose: To compare diffusion weighted-imaging (DW) magnetic resonance imaging (MRI) to contrast-enhanced (CE) MRI in the preoperative assessment of small bowel complications of Crohn's disease (CD) with MR enterography (MRE).

Material and methods: Thirty-eight patients who underwent surgery for CD complications and preoperative MRE were included. MRE examinations were blindly analyzed independently by one junior and one senior abdominal radiologist for the presence of fistula, stenosis and abscesses. During a first reading session T2-weighted images (T2-WI), steady-state sequences (True-FISP) and DW-MRI were reviewed (set-1) and during a separate distant session, T2-WI, True-FISP and CE-MRI were reviewed (set-2). Performances of each reader for the two sets were evaluated using imaging, intraoperative and pathological findings as the standard of reference.

Results: Forty-eight fistulas, 43 stenosis and 11 abscesses were deemed present using the standard of reference. For the senior radiologist, sensitivities for the detection of fistulas, stenosis and abscesses ranged from 80% to 100% for set 1 and from 88% to 100% for set 2 and specificity ranged from 56% to 70% for set 1 and from 53% to 93% for set 2, with no significant differences between the different sets (P-values, 0.342-0.429). For the junior radiologist, higher performances were obtained with set 2 (P-values, 0.001 - 0.007).

Conclusion: For a senior radiologist, DW-MRE has similar sensitivities than CE-MRE for the diagnostic of CD complications. For a junior radiologist, CE-MRE yields better results than DW-MRE.

SS 6.7

Mural diffusion restriction pattern of small bowel: a possible tool for grading inflammation in Crohn's disease

N. Faluhelyi, O. Farkas, P. Bogner; Pécs/HU

Purpose: To identify different diffusion restriction (DR) patterns in the small bowel wall and determine their diagnostic use in magnetic resonance enterography (MRE) examination of patients with Crohn's disease (CD).

Material and methods: MRE (1.5 T GE Optima 450w MR) examinations were performed after oral administration of mannitol (2.5%) solution. Diffusion-weighted images (axial DWI with b0, b400 and b800) and T2 images of 30 consecutive patients with small bowel CD activity were retrospectively analysed. In 8 patients, intravenous contrast agent (Gadovist) was also administered and pre- and postcontrast T1 images were added to the analysis. Descriptive statistics, analysis of variance (ANOVA), Kruskal-Wallis and Mann-Whitney tests were performed.

Results: In 14 cases, DR was homogenously present in the inflamed bowel wall. Only mucosal DR was seen in 6 patients and DR showed a layered pattern (both mucosal and serosal restriction with a central band of relatively lower restriction) in 10 cases. Restriction patterns were corresponding to the contrast enhancement pattern of all additional contrast-enhanced cases. Patients with layered pattern had a significantly higher Clermont score (median: 31.68, range: 3.87) than the rest of the patients (median: 21.12 range: 18.94, p=0. 04746). The three groups proved to have a different mural thickness with the thickest wall in the "layered" group (mean: 8.7 mm, SD: 0.82, p<0.00001).

Conclusion: The well-known contrast enhancement patterns of bowels in active CD (homogenous, mucosal and layered) are also identifiable as DR patterns on DWI-MRE. Layered restriction pattern can be a marker of more severe activity of small bowel inflammation in Crohn's patients.

SS 6.8

The utility of diffusion-weighted imaging in the characterisation and assessment of activity of small bowel and colonic Crohn's disease on MR enterography

J.P. Walsh, D. Byrne, H. Fenlon, C. Cronin; Dublin/IE

Purpose: To demonstrate the utility of diffusion-weighted imaging (DWI) in characterisation and assessment of activity of small bowel and colonic Crohn's disease on MR enterography (MRE).

Material and methods: Of 145 patients who underwent MRE over an 18 month period (July 2016 – December 2017), we retrospectively analysed imaging performed for 63 consecutive patients (39 female, 24 male) with biopsy-proven Crohn's disease. Appearances on T2 weighted, T1 contrast-enhanced sequences and DWI, where available, were assessed. Using a semi-quantitative technique, MRE activity scores were calculated for involved segments. Results were compared with endoscopy and histologic findings, where available.

Results: Of 71 segments analysed, 58 demonstrated abnormality on contrast-enhanced or DWI imaging (50 small bowel, 8 colon). Abnormal contrast enhancement was identified in 48 of 50 abnormal small bowel segments and 8 of 8 colonic segments. Abnormal DWI signal was identified in 25 of 31 small bowel segments and 8 of 8 colonic segments. DWI was unavailable for 26 segments. Calculated sensitivity of contrast-enhanced MRE for active small bowel inflammation was 96.0% [86.3-99.5%], while that of DWI was 80.7% [62.5-92.6%]. Analysis of colonic activity was confounded by small sample size.

Conclusion: While there was a trend towards greater sensitivity for contrast-enhanced MRE over DWI for detection of acute small bowel inflammation, this did not reach the level of statistical significance. While an ideal MRE protocol would likely include both sequences, this study suggests that DWI may provide an alternative to contrast-enhanced sequences, especially for longitudinal assessment of disease activity.

SS 6.9

Magnetic resonance enterography (MRE) and enteric ultrasound (US) in newly diagnosed or relapsing Crohn's disease: patient acceptability, perceived burden and preferences

S.A. Taylor, A. Miles, T. Metric Investigators; London/UK

Purpose: Magnetic resonance enterography (MRE) and ultrasound (US) are widely used to image Crohn's disease. The aim was to compare patient acceptability and burden of MRE and US to each other, and to other enteric investigations, and identify drivers of preferences.

Material and methods: 159 patients (mean age 38, 94 female) prospectively recruited to a multicentre diagnostic accuracy study comparing MRE and US completed a detailed experience questionnaire pertaining to the burden and acceptability of small bowel investigations, including MRE and US. Data was compared t-tests, chi-square tests and McNemar tests as appropriate. Predictors of burden and patient preference were tested using linear and logistic regression.

Results: US, MRE and colonoscopy were rated as very/fairly acceptable by 98.6%, 88.3% and 60.0% of patients respectively ($p<0.001$). MRE recovery time was significantly longer than US ($p<0.001$), but shorter than colonoscopy ($p<0.001$). Patients were less willing to undergo MRE again than US (90.7% vs. 98.5%, $p=0.012$, but more willing than for colonoscopy (74.7%, $p=0.017$). MRE resulted in greater burden than US ($t=13.56$, $df=144$, $p<0.001$), although overall burden scores were low. Younger age and significant levels of emotional distress were associated with MRE burden. A majority (80.0%) preferred US to MRE. Higher MRE discomfort predicted a preference for US but patients rated test accuracy as more important than scan discomfort.

Conclusion: MRE and US are well tolerated, although MRE generates greater patient burden, longer recovery times, and is less preferred than US. Patients, however, place greater emphasis on diagnostic accuracy than scan burden when determining preferences.

SS 6.10

Accuracy of emergency CT examination without bowel preparation in the assessment of disease activity and complications in ileocolonic Crohn's disease patients compared to standard magnetic resonance enterography

S.G. Drago, S. Lombardi, A. Casiraghi, C. Talei Franzesi, S. Sironi, D. Ippolito; Monza/IT

Purpose: To compare the agreement between abdomino-pelvic CT performed with intravenous contrast material without oral contrast administration, in an urgent setting at the Emergency Department, in comparison to MR-enterography (MRE) in detecting inflammatory bowel disease findings and its complications in Crohn's disease (CD) patients.

Material and methods: Forty-eight patients with known or suspicion of CD underwent abdomino-pelvic contrast-enhanced CT study on a 256-row MDCT (iCT, Philips Medical Systems), without any previous bowel distention. Afterward, the same group of patients underwent MR-Enterography on a 1.5 T (Philips, Achieva MR system) using oral administration of 1.5Lt of contrast agent and intravenous contrast. Two readers independently reviewed all the images of both techniques and analyzed the following cross-sectional findings: bowel wall thickness and enhancement, mesenteric lymph-nodes, vascular engorgement, fibro-fatty proliferation, fistulas and abscesses.

Results: Two readers assessed 56 diseased bowel segments with both modalities: small bowel, colon-sigmoid and rectum. Inter-observer agreement was higher for bowel obstruction (k=0.650 CT, k=0.671 MRE), its complications (k=0.810 CT, k=1 MRE) and lymphoadenopathy (k=0.810 CT, k=0.690 MRE). Higher inter-reader agreement was achieved for CT in comparison with MRE for wall thickening (k=0.750 CT, k=0.610 MRE), fibro-fatty proliferation (k=0.780 CT, k=0.523 MRE) and vascular comb sign (k=0.610 CT, k=0.360 MRE).

Conclusion: Abdominal contrast-enhanced CT without bowel distention offers high diagnostic value in the assessment of bowel wall involvement and its complications in CD and, in selected cases, immediate MR-Enterography examination could be postponed and reserved for follow-up.

11:00 - 12:30 **The Liffey A**

Scientific Session SS 7

Diffuse and chronic liver diseases: current assessment of liver fibrosis and steatosis

SS 7.1

Doppler ultrasonography devices, including elastography, allows accurate screening for severe fibrosis

P. Bazeries, J. Delahaye, V. Cartier, J. Lebigot, J. Boursier, C. Aubé; Angers/FR

Purpose: To evaluate the contribution of the elastography following a Mode B ultrasonography examination in the screening of severe hepatic fibrosis (METAVIR ≥ F3).

Material and methods: Five hundred and fourteen patients were prospectively included in a monocentric six years study. All patients underwent a liver biopsy to establish the fibrosis stage (METAVIR scoring). The signs of hepatic dysmorphism and portal hypertension were studied in ultrasonography examination with Doppler. Liver stiffness evaluation was performed using both the acoustic radiation force impulse (ARFI) (Siemens) and 2D shear-wave elastrography (SWE - Supersonic Imagine) techniques.

Results: Three ultrasound parameters were independent predictors of severe fibrosis: liver surface irregularity, spleen length (≥110 mm) and demodulation of the hepatic veins waveform. The presence of at least one of these 3 parameters had 85.6% sensitivity and 36.1% specificity for the diagnosis of severe fibrosis. The use of ARFI (diagnostic cut off ≥1.59m/s) after the detection of one of this three signs dramatically increased the specificity at 80.8%, at a price of a slight decrease in sensitivity (73.7%). Same results were obtained with SWE (diagnostic cut-off ≥9.5kPa) with 73.3% specificity and 81.5% sensitivity. Addition of an elastographic measurement allows obtaining a positive predictive value of approximately 50% for the diagnosis of severe fibrosis, which is an acceptable rate to refer patients to a hepatologist for a complete assessment of chronic liver disease.

Conclusion: The screening of severe hepatic fibrosis using 3 simple ultrasound signs with addition of elastographic measurement in case of positivity of one of them is a feasible and accurate procedure.

SS 7.2

Diagnostic performance of texture analysis for the assessment of hepatic fibrosis in patients with nonalcoholic fatty liver disease (NAFLD): preliminary results and comparison with MR elastography (MRE)

R. Cannella[1], M. Tublin[2], A. Borhani[2], J. Behari[2], A. Furlan[2]; [1]Palermo/IT, [2]Pittsburgh, PA/US

Purpose: To investigate the performance of texture analysis (TA) in the quantification of fibrosis in NAFLD and to compare it with MR elastography (MRE).

Material and methods: 54 adult patients (33 females, 21 males) with biopsy-proven NAFLD were prospectively enrolled and underwent MRI on a 1.5T system using a combination of T1-weighted gradient-recalled-echo (T1W 3D-GRE) sequence (slice thickness =4.6 mm) and 2D-MRE. Texture analysis was performed using a commercially available research software (TexRAD) on axial T1W images. A circular region of interest (ROI) (3 cm^2) was traced on an image at the level of the porta hepatis. Receiver operating curves (ROC), areas under the ROC (AUROC) and 95% confidence intervals were calculated to assess the accuracy of each textural parameter and of liver stiffness for the diagnosis of significant fibrosis (SF: F≥2) and advanced fibrosis (AF: F≥3). AUROCs were compared using the DeLong test.

Results: Thirty-seven subjects had SF and 20 had AF. The textural parameters with the best performance were SD and entropy with AUROC 0.755 (0.619-0.862, p≤0.0002) and 0.769 (0.634-0.873, p<0.0001) for SF and AUROC 0.746 (0.609-0.854, p≤0.0004) and 0.754 (0.618-0.861, p≤0.0002) for AF. The AUROC of MRE for SF was 0.785 (0.652–0.885, p≤0.0001) and for AF was 0.923 (0.817-0.978, p≤0.0001). While the AUROC of MRE for AF was significantly higher than that of SD and entropy (p=0.03 and p=0.04), there was no significant difference among AUROCs for SF (p=0.85 and p=0.74).

Conclusion: Texture analysis has fair accuracy for the quantification of hepatic fibrosis in NAFLD, although the performance is inferior to MRE for the assessment of AF.

SS 7.3

Supersonic B-ratio mode and shear-wave elastography performances in detection and graduation of steatosis and liver fibrosis in patients with liver transplantation

M. Dubois, V. Brun, M. Rayar, M. Auger, L. Beuzit, E. Quehen, Y. Gandon, B. Turlin, P. Houssel-Debry, A. Paisant; Rennes/FR

Purpose: To evaluate the diagnostic performance of Supersonic B-ratio mode and shear-wave elastography (SWE) for the assessment of steatosis and liver fibrosis in patients with liver transplantation.

Material and methods: After institutional review board approval and written informed consent, patients hospitalized from June 2017 to December 2017 for a systematic check-up after liver transplantation were prospectively included. Each patient underwent the same day SWE, liver biopsy (LB) and biological exams. Steatosis was measured using B-Ratio mode between the liver and kidney and liver stiffness with 3 SWE consecutive measures. LB was used as gold standard, grading steatosis S0 (0%), S1 (1-10%), S2 (11-30%) or S3 (>30%), and grading liver fibrosis from F0 to F4 according to the Metavir score.

Results: Fifty patients were included. Mean B-ratio value was significantly higher in patients with steatosis (0.94±0.13 vs 1.34±0.44, p<0.001). Sensitivity and specificity were, respectively, 77.3% (0.56-0.90) and 80% (0.58-0.92) (area under the receiver operating characteristic (AUROC)=0.82) for S≥1 with a B-ratio cut-off value of 1.02; 84.6% (0.56-0.97) and 85.7% (0.68-0.95) (AUROC=0.92) for S≥2 with a B-ratio cut-off value of 1.13; and 85.7% (0.46-0.99) and 76.5% (0.60-0.88) (AUROC=0.80) for S≥3 with a B-ratio cut-off value of 1.20. Mean SWE value for patients without significant fibrosis (≤F1) was 14.1±9.4 vs 27.4±0.31 for patient with fibrosis.

Conclusion: Supersonic B-ratio mode is a non-invasive and accurate method to detect and graduate steatosis in patients with liver transplantation. Fibrosis cut-off values seem to be higher in transplanted liver than in normal liver.

SS 7.4

A comparative evaluation of modified DIXON, CT (LAI) and US elastography, in quantification of liver fat, with MR spectroscopy as reference

R. Jain, S. Kale, N. Panchal, N. Kundaragi, B. M, R. Talwade, N. Reddy; Bangalore/IN

Purpose: Early diagnosis and treatment of fatty liver disease, along with modifications to lifestyle, helps reduce the rate of progression to end stage liver disease and hepatocellular cancer. Additionally, liver fat is a risk for post-operative complications of a transplant. Non-invasive MRI can be used to monitor liver fat. This study was conducted to compare the accuracy of modified DIXON, CT(liver attenuation index (LAI)) and US Elastography, with MR Spectroscopy (MRS) as a reference benchmark in quantification of liver fat.

Material and methods: Tests were performed on 80 patients (35 females and 45 males) which were grouped into hepatosteatosis-alcoholic (n=15), non-alcoholic non-obese (n=8), obese (n=23), liver donors (n=25) and post-chemotherapy (n=9). MRI images were obtained on 3T Philips Ingenia, CT indices calculated on Philips 128 Slice Ingenuity Core Scanner, US Elastography performed on Philips Affinity70. Results were independently interpreted by two radiologists. All data and interpretations were compiled and compared for patient groups, CT- LAI, elastography score (F0-F4), percentage of liver fat through mDIXON and MRS.

Results: Sensitivity values are 97% for MR Spectroscopy, 96.5% for mDIXON, 71% for CT (LAI) and 64% for US elastography. The study showed excellent correlation between MR spectroscopy and mDIXON (r^2 value of 0.93), moderate correlation with CT-LAI (r^2 value of 0.89) and poor correlation with US elastograpy (r^2 value of 0.003). 15 out of 80 patients underwent biopsy, the histopathology results for these were included in the study.

Conclusion: Modified DIXON is as accurate as MR spectroscopy as a noninvasive method for quantification of hepatosteatosis, compared to the widely used CT (LAI) and US elastography which have their inherent drawbacks of radiation and operator dependence.

SS 7.5

Clinical value of ultrasonic adaptive sound speed estimation for the diagnosis and quantification of hepatic steatosis

M. Dioguardi Burgio[1], M. Imbault[2], M. Ronot[1], A. Faccinetto[1], B. Van Beers[1], P.-E. Rautou[1], L. Castera[1], J.-L. Gennisson[2], M. Tanter[2], V. Vilgrain[1]; [1]Clichy/FR, [2]Paris/FR

Purpose: To evaluate the ability of a new ultrasound (US) method based on Sound Speed Estimation (SSE) in detection, quantification, and grading of hepatic steatosis using magnetic resonance (MR) proton density fat fraction (PDFF) as a reference standard and to calculate one US fat index based on the patient's SSE.

Material and methods: We consecutively included N=50 patients as study cohort and further N=50 as validation cohort who underwent both SSE and abdominal MR. Hepatic steatosis was classified according to MR-PDFF cut-offs as S0 ≤6.5%, S1 from 6.5 to 16.5%, S2 from 16.5 to 22% and S3≥ 22%. Receiver operating curve analysis was performed to evaluate the diagnostic performance of SSE in diagnosis of steatosis. Based on the optimal data fit derived from our study, we proposed a correspondence between the MR-PDFF and an US fat index. Coefficient of determination R^2 was used to evaluate fit quality and was considered as robust when R^2 >0.6.

Results: Study and validation cohort presented mean SSE value of 1.570±0.026 and 1.568±0.023 mm/µs for S0 and 1.521±0.031 and 1.514±0.019 mm/µs for S1-S3 (p<0.01) patients, respectively. SSE threshold of ≤1.537 mm/µs had 80% sensitivity and 85.7% specificity in diagnosis of steatosis in the study cohort. Robust correspondence between MR-PDFF and the US fat index was found both for the study cohort (R^2= 0.73) and the validation cohort (R^2= 0.76).

Conclusion: SSE can be used to detect, quantify and grade liver steatosis and to calculate an US fat index.

SS 7.6

Transducer-free hepatic magnetic resonance elastography using cardiac wave induction at 0.3 ms temporal resolution

M.A. Troelstra[1], J.H. Runge[2], A. Polcaro[1], O. Darwish[1], J. De Arcos[1], T. Schneider[3], A.J. Nederveen[2], R. Sinkus[1]; [1]London/UK, [2]Amsterdam/NL, [3]Guildford/UK

Purpose: This study aims to develop a transducer-free hepatic magnetic resonance elastography (MRE) method to facilitate clinical MRE implementation. We propose a cardiac-triggered motion-sensitised pencil-beam, for capturing cardiac-induced hepatic shear-waves at a high temporal resolution (>0.3 ms).

Material and methods: Six healthy volunteers were scanned on a Philips 3T-scanner. The pencil-beam navigator was positioned below the heart in liver segments 2-4. ECG-triggered sequences obtained 35-40 pencil-beam images (d=30mm, L=80mm, t=20ms) acquired in one R-R interval and repeated for 60 successive R-R intervals, divided over four breath-holds, attaining temporal resolutions >0.3 ms. Phase-images yielded space-time images of hepatic transient shear-wave propagation. Straight lines were fitted along phase perturbations at 1st and 2nd heart sound, to determine shear wave speed and shear stiffness $\mu=\rho c^2$ (assuming no loss-effects).

Results: Analysis showed two shear-wave propagations from the heart into the liver, at 1st (atrioventricular-valve closure) and 2nd heart sounds (aortic-/pulmonary-valve closure). 2nd heart sound waves showed an average wave speed of 1.49+/-0.07 m/s and stiffness of 2.24+/-0.21 kPa, 2x higher shear stiffness compared to classical-MRE at 40Hz. The 2nd heart sound shows a frequency emission spectra peak at 85Hz. Liver-tissue properties are approximately linear with frequency, resulting in stiffnesses of ~1kPa measured at 40Hz increasing to ~2kPa at 85Hz.

Conclusion: This approach allows transducer-free visualisation of hepatic cardiac-induced shear-waves at high temporal resolution (>0.3ms), using waves created by cardiac-valve closure. Results show fast wave propagation, caused by high-frequency content of waves generated from cardiac-valve closure. This transducer-free technique could facilitate clinical MRE implementation, once it is validated in a larger population.

SS 7.7

Reliability criteria for liver stiffness measurement with acoustic radiation force impulse

J. Boursier[1], C. Cassinotto[2], V. Cartier[1], A. Lannes[1], S. Shili[2], J. Lebigot[1], B. Lapuyade[2], P. Cales[1], J.-B. Hiriart[2], S. Michalak[1], B. Le Bail[3], A. Mouries[2], F. Oberti[1], I. Fouchard[1], F. Chermak[2], V. De Ledinghen[2], C. Aubé[1]; [1]Angers/FR, [2]Pessac/FR, [3]Bordeaux/FR

Purpose: To determine the reliability criteria of liver stiffness measurement (LSM) using acoustic radiation force impulse (ARFI) in chronic liver diseases.

Material and methods: 1094 patients with chronic liver diseases had liver biopsy and LSM with ARFI in two centers. Advanced fibrosis was defined as non-alcoholic steatohepatitis clinical research network (NASH CRN) histological scoring system F≥3 or Metavir F≥2.

Results: LSM failure rate was 0.9% (10/1094). Among the remaining 1084 patients (male: 61.9%; age: 54.3±13.3 years), 48.5% had advanced fibrosis and 16.8% cirrhosis. Etiologies of chronic liver disease were non-alcoholic fatty liver disease (NAFLD) (48.5%), viral hepatitis (26.3%), alcohol (12.2%), and other (13.0%). ARFI accuracy decreased with increasing interquartile range (IQR) of liver stiffness to the median (IQR/M) ratio, especially for intermediate/high levels of liver stiffness. Three reliability categories were thus defined: "very reliable" (IQR/M <0.15), "reliable" (0.15≤ IQR/M <0.35 or IQR/M ≥0.35 with ARFI median <1.37 m/s), and "poorly reliable" (IQR/M ≥0.35 with ARFI median ≥1.37 m/s). Using these criteria, the rates of patients correctly classified were, respectively: 80.9%, 73.7%, and 57.8% for advanced fibrosis (p=0.029 between very reliable and reliable; p <0.001 for other paired comparisons); and 92.6%, 83.4%, and 50.0% for cirrhosis (p<0.001 for all comparisons). 23.6% of the ARFI examinations were very reliable, 55.0% reliable, and 21.4% poorly reliable. The skin-liver capsula distance was an independent predictor of poorly reliable LSM, which occurred in 52.7% of patients having a distance ≥30mm.

Conclusion: Based on IQR/M ratio and ARFI median, we defined three reliability categories for LSM using ARFI, associated with different diagnostic accuracies. These new reliability criteria will increase confidence in ARFI results and diffusion of this technique.

SS 7.8

Non-invasive monitoring of hepatic steatosis via acoustic structure quantification of US with MR spectroscopy as a reference standard

D.H. Lee, J.Y. Lee; Seoul/KR

Purpose: To prospectively evaluate whether monitoring hepatic steatosis by ultrasonography with an acoustic structure quantification (ASQ) technique is feasible when using magnetic resonance spectroscopy (MRS) as a reference standard.

Material and methods: Thirty-six patients with suspected fatty liver disease underwent both ultrasonography with ASQ and MRS on the same day. After a mean follow-up period of 11.4±2.5 months, follow-up ultrasonography with ASQ and MRS were performed on 27 patients to evaluate whether hepatic steatosis improved. The focal disturbance (FD) ratio, as calculated using ASQ, and the hepatic fat fraction (HFF), estimated by MRS, were obtained at both initial and follow-up examinations. Pearson's correlation coefficient was calculated to assess correlations between ordinal values.

Results: The FD ratio showed a strong, negative linear correlation with the HFF after logarithmic transformation of both variables from the initial examinations of 36 patients (ρ=-0.888; P<0.001) and the follow-up examinations of 27 patients (ρ=-0.920; P<0.001). There was also a significant, negative linear correlation between the change in the logarithm of the FD ratio and the change in the logarithm of the HFF by MRS over the follow-up period (ρ=-0.645; P<0.001). In 16 patients with increased FD ratio on follow-up, HFF on follow-up MRS significantly decreased, and HDL level significantly increased whereas LDL tended to decrease.

Conclusion: The FD ratio was significantly correlated with the HFF at both the initial and follow-up examinations, and there was also a significant correlation between the changes in the FD ratio and the changes in the HFF over the follow-up period.

SS 7.9

Molecular features, histological parameters and enhancement measurements in nonalcoholic steatohepatitis patients using gadoxetic acid-enhanced MR Imaging (preliminary results)

N. Bastati-Huber[1], D.S. Feier[2], A. Beer[1], S. Pötter-Lang[1], H. Einspieler[1], A. Ba-Ssalamah[1]; [1]Vienna/AT, [2]Cluj-Napoca/RO

Purpose: To assess the relationship of organic anion transporting polypeptide (OATP1B1/3) expression with histological parameters and relative enhancement ratio in patients with nonalcoholic fatty liver disease (NAFLD), defined according to the steatosis activity and fibrosis (SAF) scoring system, which is based on the semiquantitative scoring of steatosis activity and liver fibrosis.

Material and methods: The local institutional review committee approved this study and waived written informed consent. This was a retrospective study of gadoxetic acid-enhanced 3T MR imaging performed in 52 consecutive patients with NAFLD (mean age (SD), 50.46 (16.52) years. The MR images were analyzed by using the relative enhancement (RLE) (the ratio of signal intensities of the liver parenchyma before and 20 minutes after intravenous administration of gadoxetic acid). Univariate and multiple regression analyses were applied to identify variables associated with OATP1B1/3 expression.

Results: OATP1B1/3 expression correlated with RLE (r=0.49, p=0.0002), the degree of liver fibrosis (r=-0.27, p=0.04) but not with steatosis (r=-0.16, p=0.23), ballooning (r=-0.22, p=0.1) or inflammation (r=-0.07, p=0.57). According to multivariate analysis both RLE and liver fibrosis are independent predictors of OATP1B1/3 expression (coefficient of determination R2=0.32, p=0.01).

Conclusion: The degree of OATP1B1/3 expression correlated statistically with gadoxetic acid relative enhancement and the degree of liver fibrosis in patients with NASH.

SS 7.10

The positive effects of bariatric surgery on non-alcoholic fatty liver disease: evaluating the changes in the liver fat fraction and liver dimensions by using ideal IQ sequences

Y. Metin, N. Orhan Metin, O. Özdemir, M.E. Kadıoğlu, E. Beykoz Çetin, S. Kalcan, M.K. Çolakoğlu; Rize/TR

Purpose: To evaluate the early and intermediate effects of bariatric surgery on liver fat fraction, liver length and liver volume using ideal IQ sequences at 3T MRI.

Material and methods: Body mass index (BMI), body weight, liver fat fraction (L-FF), liver volume and craniocaudal length were measured preoperatively (1 week before surgery) and postoperatively (1 and 6 months after surgery) in 46 patients (31 female, 15 male; age range, 21–60 years) who underwent bariatric surgery between May 2016 and August 2017. Liver volumes, L-FF were calculated from Ideal IQ sequences.

Results: BMI decreased from 46.3 ± 5.5 to 40.7 ± 5.3 (at first month), and to 32.6 ± 5.5 kg/m^2 at the end of sixth month. Mean liver volume decreased from 2641.2 ± 543.6 to 1954.1 ± 384.2 cm^3 (at first month) and to 1776.3 ± 361.1 cm^3 at the end of sixth month. L-FF decreased from 16.4 ± 10.2 to 7.2 ± 4.9% (at first month) and to 4.0 ±2.7% at the end of sixth month. At the first month, 60.9% of patients and at the sixth month 82.6% of patients had resolution of steatosis.

Conclusion: A significant decrease in liver volume, liver length and FF was achieved at first and sixth months after bariatric surgery. The reduction in L-FF is most prominent after the first month and continues at sixth month. The positive effects of bariatric surgery on liver dimensions and FF can be monitorized by using ideal IQ sequences.

11:00 - 12:30 **Liffey Hall 2**

Scientific Session SS 8

Malignant pancreatic tumours: new trends

SS 8.1

Lower energy levels and iodine density images increase pancreatic tumor conspicuity on rapid kV-switching dual energy CT

S. Aslan, M.S. Nural, İ. Camlidag; Samsun/TR

Purpose: To evaluate the efficacy of rapid kV-switching dual energy CT (rs-DECT) energy level optimization and iodine density (ID) images on pancreatic cancer detection and conspicuity.

Material and methods: 56 patients with pancreatic adenocancer were prospectively enrolled and underwent rsDECT in pancreatic protocol. Largest lesion diameters (LLDs) were measured on 45 keV, optimal CNR, 70 keV and ID images. Attenuation differences between the lesion and normal parenchyma (HU), image noise for each energy level, contrast gain and lesion contrast-to-noise ratio (CNR) were calculated. Iodine content of the lesions and the parenchyma were measured on ID images. Isodense lesions were treated as a subgroup and all measurements were also applied to them. All analyses were performed by two radiologists at different times and inter-reader agreement was evaluated.

Results: Optimal CNR was 52 ± 8,5 kEv. LLDs were measured on ID images (p< 0.001). Attenuation measurements on 45 keV and optimal keV were significantly higher than 70 keV images. Attenuation difference between the lesion and parenchyma was significantly different between 70 keV images and other energy levels but not different between 45 keV and optimal CNR. Highest image noise was calculated in 45 keV. Highest contrast gain was between 70 keV and optimal CNR and highest CNR was measured in optimal CNR. Iodine content of tumors were significantly lower than the parenchyma (1,83 mg/cc vs 3,05 mg/cc, p < 0.05). Isodense tumors also showed similar results. Inter-reader agreement was high (ICC 0,78 - 0,93).

Conclusion: rsDECT is a reliable method for pancreatic cancer detection and delineation, particularly isodense tumors.

SS 8.2

Prediction of residual tumor classification and overall survival in pancreatic cancer by preoperative CT

J.S. Bae[1], J.H. Kim[1], I. Joo[1], W. Chang[2], J.K. Han[1]; [1]Seoul/KR, [2]Seongnam/KR

Purpose: To predict resection (R) stage classification and overall survival on preoperative CT in patients who underwent surgery for pancreatic cancer.

Material and methods: In this retrospective study, 216 patients with pancreatic cancer who underwent CT and surgery were included. Preoperative CT findings were assessed by two radiologists and R classification was categorized into no residual tumor (R0) and residual tumor (R1 or R2). We assessed the correlation between CT findings and R classification. In addition, we used Kaplan-Meier estimation for survival analysis and Cox proportional hazard model to find prognostic factors for overall survival.

Results: There were 153 patients in R0 group and 63 patients in R1 or R2 group. Tumor size (odds ratio (OR) 1.045, 95% confidence interval [CI]: 1.005-1.086), definite peritumoral fat stranding (OR 3.826, 95% CI: 1.765-8.293), portal vein involvement (OR 2.795, 95% CI: 1.216-6.423), and suspicious distant metastasis (OR 2.916, 95% CI: 1.296-6.561) were independent predictors for residual tumor (P<0.05). On survival analysis, median survival period was 29.2 months in R0 group and 12.2 months in R1 or R2 group. T4 stage (hazard ratio (HR) 4.330, 95% CI: 1.208-2.555), N1 stage (HR 1.757, 95% CI: 1.208-2.555), common hepatic artery involvement (HR 4.821, 95% CI: 2.125-10.934) and R stage (HR 2.499, 95% CI: 1.649-3.789) were predictors of poor survival (P<0.05).

Conclusion: Preoperative CT is useful to predict R classification using tumor size, definite peritumoral fat stranding, portal vein involvement, and suspicious distant metastasis, as well as to anticipate poor survival using T stage, N stage, common hepatic artery involvement and R classification.

SS 8.3

Radiological assessment of local resectability status in patients with pancreatic cancer: interreader agreement and reader performance at two different classification systems

N. Kartalis[1], C. Valls[1], E. Axelsson[1], M. Andersson[2], I. Keussen[3], J. Strinnholm[4], W. Bartholomä[5], M. Del Chiaro[1], R. Segersvärd[1], L. Lundell[1], L. Loizou[1]; [1]Stockholm/SE, [2]Gothenburg/SE, [3]Lund/SE, [4]Umeå/SE, [5]Linköping/SE

Purpose: To assess the interreader agreement and reader performance in the evaluation of patients with pancreatic cancer (PC) at two classification systems of local resectability status, namely the national comprehensive cancer network (NCCN) and Karolinska Institutet's classification system (KICS).

Material and methods: In this institutional review board-approved retrospective study, six radiologists evaluated independently pancreatic CT-examinations of 30 patients randomly selected from a tertiary referral centre's multidisciplinary tumour board database. Based on well-defined criteria of tumour-vessel relationship, each patient was assigned into one of three NCCN and six KICS categories. We assessed the intraclass correlation coefficient (ICC; a score of 0–0.2 indicates poor agreement, 0.3–0.4 fair agreement, 0.5–0.6 moderate agreement, 0.7–0.8 strong agreement, and >0.8 a very strong agreement) and compared the percentages of correct tumour classification of the six readers at both systems (Chi-square test; a P-value <0.05 was considered significant). Standard of reference was a consensus evaluation of CT from three readers not involved in the analysis.

Results: The ICC for NCCN and KICS was 0.82 and 0.84, respectively (very strong agreement). The percentages of correct tumour classification at NCCN and KICS were 53-83% and 27-57%, respectively, with no statistically significant differences in the overall reader comparison per classification system.

Conclusion: Interreader agreement at both PC classification systems is very strong. NCCN may be advantageous in terms of reader performance compared to KICS.

SS 8.4

Intravoxel incoherent motion diffusion-weighted MR imaging: reproducibility and diagnostic value for characterization of solid pancreatic lesions

R. De Robertis[1], N. Cardobi[2], P. Tinazzi Martini[1], M. Zanirato[3], A. Stemmer[4], R. Grimm[4], M. D'Onofrio[1]; [1]Verona/IT, [2]Peschiera del Garda/IT, [3]Milan/IT, [4]Erlangen/DE

Purpose: To evaluate the reproducibility and the diagnostic potential of intravoxel incoherent motion (IVIM)-derived parameters for differentiation of solid pancreatic lesions and normal pancreas.

Material and methods: Forty-seven patients with solid pancreatic tumors (30 ductal adenocarcinomas (PDACs), and 17 neuroendocrine neoplasms (panNENs)), 5 patients with mass-forming pancreatitis (MFP), and 30 subjects with normal pancreas (NP) were included. All subjects underwent 1.5 T MR imaging including IVIM diffusion-weighted imaging with 11 b values (from 0 to 800 sec/mm^2). Apparent diffusion coefficient (ADC), true diffusion (D), pseudodiffusion (D*), and perfusion fraction (f) were calculated by two independent readers. Interobserver reliability of the measurements was assessed by using the intraclass correlation coefficient (ICC). A Kruskal-Wallis H test was used for comparison. The diagnostic performance of each parameter was evaluated using receiver operating characteristic (ROC) analysis.

Results: Interobserver agreement was excellent for pancreatic lesions (ICC = .981, .985, .963, and .989 for ADC, D, D* and f, respectively). ADC was not significantly different between lesions. F was significantly higher in NP and panNENs compared with PDACs (both p<.001). D was significantly higher in PDACs compared with NP and panNENs (p<.001 and .001). D* was significantly lower in MFP compared with panNENs, in PDACs compared with NP, and in PDACs compared with panNENs (p=.047, .047, and <.001, respectively). For the differentiation between PDACs and panNENs, f had the highest area under the curve (.976) in ROC analysis.

Conclusion: The measurement of IVIM-derived parameters in pancreatic lesions has excellent reproducibility. IVIM-related parameters could be helpful in distinguishing PDACs from panNENs.

SS 8.5

Perfusion measurements in pancreatic cancer by means of intravoxel incoherent motion MRI and CT perfusion: correlation with each other and with histological microvessel density

P.F.J. Mayer, F. Fritz, S. Skornitzke, W. Stiller, M. Klauss, H.U. Kauczor; Heidelberg/DE

Purpose: The aim of this study was to compare intravoxel incoherent motion (IVIM) diffusion-weighted (DW) MRI and CT perfusion to assess tumor perfusion of pancreatic ductal adenocarcinoma (PDAC).

Material and methods: In 19 patients with PDAC, DW MRI and CT perfusion were conducted on the day before surgery. IVIM analysis of DW MRI was performed and the parameters perfusion fraction f, pseudodiffusion coefficient D*, and diffusion coefficient D were extracted. The CT perfusion parameters blood volume (BV) and blood flow (BF) were estimated with a deconvolution-based analysis. In 10 patients, intratumoral microvessel density (MVD) and microvessel area (MVA) were analyzed from representative immunostained tissue slides, using an anti-CD34 antibody as endothelial marker. Pearson correlation coefficients between these parameters were calculated.

Results: There were significant positive correlations between MVD/ MVA and f/ BF ($r \geq 0.666$, $p \leq 0.036$). f significantly positively correlated with BF and BV ($r \geq 0.691$, $p \leq 0.001$). Correlation coefficients between BF and MVD/MVA were not significantly different from correlation coefficients between f and MVD/MVA ($p \geq 0.796$).

Conclusion: The study shows that, in PDAC, CT perfusion derived BF and IVIM derived f similarly reflect microvascularity and could possibly serve as imaging biomarkers for tumor characterization.

SS 8.6

Relationship between pathologic treatment response after neoadjuvant therapy and metabolic response on integrated time-of-flight fludeoxyglucose (FDG) positron-emission tomography/MRI in patients with FDG-avid borderline resectable pancreas cancer: a feasibility study

N. Samreen, I. Garg, J.G. Fletcher, M. Truty, G.B. Johnson, J.L. Fidler, K. Bradley, A. Goenka; Rochester, MN/US

Purpose: To determine if fludeoxyglucose (FDG) positron-emission tomography (PET)/MRI can be used to predict pathologic treatment response after neoadjuvant therapy in FDG-avid borderline resectable pancreatic ductal adenocarcinoma (PDAC).

Material and methods: Patients with FDG-avid PDAC on baseline integrated time-of-flight PET/MRI who also underwent a post-neoadjuvant therapy PET/MRI prior to surgical resection were included. Primary tumor SUVmax, SUVmean and volumetric PET parameters on pre- and post-neoadjuvant therapy scans were measured using anatomic guidance from simultaneously acquired contrast-enhanced MRI. Metabolic response on PET/MRI was correlated to histologic treatment response using College of American Pathologists grading system (path grade). Complete metabolic response was defined as FDG uptake indistinguishable from surrounding background and normalization of post-therapy CA 19-9 were evaluated as surrogates of path grade 1/0.

Results: 12 patients (range 55-79years; 50% males) underwent required PET/MRI, neoadjuvant therapy, and surgical resection. Treatment response grades were none (grade 3, n=2), moderate (grade 2, n=6), marked (grade 1, n=2) and complete pathologic response (pCR) (grade 0, n=2). There was no significant difference (p>0.05) in baseline PET parameters between group 1 (grade 3/2) and group 2 (grade 1/0). Complete metabolic response on post-therapy PET/MRI was observed in 5 patients – one with grade 2, and two each with grades 1 and 0. Positive and negative predictive values of complete metabolic response for path grade 1/0 were 80% and 100% whereas for normalization of post-therapy CA 19-9 were 20% and 33%, respectively.

Conclusion: FDG PET/MRI shows promise for response evaluation following neoadjuvant therapy with complete metabolic response by PET/MRI correlating with marked or complete pathologic response.

SS 8.7

MRI imaging of IPMN: evaluation of agreement between observers with different degrees of experience

L. Bertuzzo[1], G.A. Zamboni[2], G. Cardano[2], R. Pozzi Mucelli[2], G. Mansueto[2]; [1]Santorso-VI/IT, [2]Verona/IT

Purpose: The Sendai and Fukuoka consensus criteria were established to assess the risk of malignancy in pancreatic mucinous cystic lesions. The purpose of this study was to assess the agreement between readers with different experience in recognizing malignancy features in a series of IPMN.

Material and methods: Institutional review board (IRB) approval was waived for this retrospective study. We included 118 patients (45 M, 73 F, average age 68 years) with a diagnosis of IPMN who underwent MRI/MRCP in our center. Two readers, respectively with 10 and 4 years of experience in abdominal imaging, reviewed independently the scans assessing for wall/internal septa thickening, mural nodules, dilation of the main pancreatic duct (MPD) and contrast enhancement. The readers were blinded to clinical and laboratory information. Kappa statistics was calculated.

Results: 10 patients had mixed-type IPMN and 108 branch-duct IPMN. Patients had a median of 2 cysts >5 mm each (range 1-20; mean 2.6). A total of 307 cystic lesions were reviewed, with a mean size of 11.8 mm (5-50 mm). The two readers showed very good agreement regarding MPD dilation (k=0.908), wall thickening (k=0.893), and presence of mural nodules (k=0.856). The agreement was good for presence of filling defects (k=0.721), wall enhancement (k=0.725) and presence of mural nodules (k=0.663).

Conclusion: Readers with different levels of experience in abdominal imaging, when assessing IPMN at MRI-MRCP, show an interobserver agreement ranging between substantial (0.663) and almost perfect (0.908) when applying the Fukuoka criteria, confirming their usefulness for lesion evaluation standardization.

SS 8.8

Functional imaging of pancreatic adenocarcinoma using perfusion CT and diffusion-weighted imaging: correlation with clinicopathological features

J. Kovac, A. Đurić-Stefanović, L. Lazić, T. Nikolić, S. Jevtić, D.V. Vasin, D. Masulovic; Belgrade/RS

Purpose: To determine the value of perfusion CT and diffusion-weighted imaging (DWI) in the evaluation of patients with pancreatic adenocarcinoma, and to assess the correlation of perfusion CT parameters, and apparent diffusion coefficient (ADC) with clinicopathological features.

Material and methods: Forty-four patients with histologically proven pancreatic adenocarcinoma who underwent CT perfusion and DWI were prospectively included in the study. Tumor blood flow (BF) and blood volume (BV) were automatically calculated by commercial maximum slope based software. ADC was calculated for b 0, and 800 s/mm^2. BV, BF, and ADC values were compared using Mann-Whitney test between patients with pancreatic carcinoma and control group. Moreover, patients with pancreatic adenocarcinoma were classified into two groups according to the tumor grade (30 high-grade, and 14 low-grade lesions) and the difference of perfusion CT parameters and ADC was assessed. Correlation was tested using Spearman's test.

Results: The mean values of BV (ml/100g), BF (ml/min/100g), and ADC (x10^{-3} mm^2/s) were significantly lower in pancreatic carcinoma (BV=4.41±1.84, BF=24.03±12.81, ADC=1.028±0.19) than corresponding values of healthy pancreatic tissue (BV=16.92±6.88, BF=68.71±11.13, ADC=2.312±0.532). A statistically significant difference was found for BV, BF, and ADC between high and low-grade tumors (all p<0.05). Significant correlation was found among tumor diameter and BV (ρ=-0.445, p=0.029), M-stage and BV (ρ=-0.286, p=0.049), M-stage and ADC (ρ=0.274, p=0.038), ADC and BV (ρ=0.551, p=0.012), ADC and BF (ρ=0.665, p=0.023).

Conclusion: Perfusion CT and DWI provide an assessment of tumor vascularity and cellularity and can be used for preoperative prediction of high-grade pancreatic adenocarcinoma.

SS 8.9

Percutaneous radiofrequency ablation of pancreatic adenocarcinoma

A. Sarno[1], G. Tedesco[1], R. De Robertis[2], S. Paiella[1], R. Salvia[1], I. Frigerio[2], R. Girelli[2], D. Melisi[1], C. Bassi[1], M. D'Onofrio[1]; [1]Verona/IT, [2]Peschiera del Garda/IT

Purpose: The objective of this study is to evaluate the feasibility and safety of percutaneous radiofrequency ablation (RFA) of locally advanced pancreatic cancer located in the pancreatic body.

Material and methods: Patients with biopsy-proven locally advanced pancreatic adenocarcinoma were considered for percutaneous radiofrequency ablation. Postprocedural CT studies and CA 19.9 tumor marker evaluation were performed at 24 hours and 1 month. At CT, the treatment effect was evaluated by excluding the presence of complications. The technical success of the procedure is defined at CT as the achievement of tumoral ablated area.

Results: Thirty-five patients have been included in the study. Five of the 35 patients were excluded. At CT, the mean size of the intralesional postablation necrotic area was 32 mm (range: 15-65 mm). None of the patients developed postprocedural complications. Mean CA 19.9 serum levels 1 day before, 1 day after, and 1 month after the procedure were 285.8 U/mL (range: 16.6-942.0 U/mL), 635.2 U/mL (range: 17.9-3368.0 U/mL), and 336.0 U/mL (range: 7.0-1400.0 U/mL), respectively. The mean survival after RFA procedure of the patients, calculated on the data collected for 26 subjects, is 312 days (range: 65-718 days).

Conclusion: Percutaneous radiofrequency ablation of locally advanced adenocarcinoma has a high technical success rate and is effective in cytoreduction.

SS 8.10

Application of Fukuoka radiological criteria in pathologically confirmed IPMNs of the pancreas: is it possible to differentiate between invasive/high-moderate grade dysplasia IPMNs and noninvasive/low-grade dysplasia IPMNs?

C. Fabris, G.A. Zamboni, R. Negrelli, L. Bertuzzo, G. Marchegiani, G. Mansueto; Verona/IT

Purpose: IPMNs are intraductal cystic neoplasms with malignant potential. The Fukuoka criteria are commonly used to assess the risk of malignancy. Our purpose was to try to differentiate between high-moderate grade dysplasia IPMNs and low-grade dysplasia IPMNs using the mentioned criteria.

Material and methods: We reviewed the preoperative MRIs from 46 patients (27 males, 19 females; mean age 63,7 years) with a confirmed pathologic diagnosis of IPMN. Two readers analyzed in consensus the MRIs for tumor size (>/< 3 cm), diameter of the main pancreatic duct (MPD) (>/< 10 mm), presence of enhancing solid components, radiologic signs of pancreatitis, enhancing or non-enhancing nodules, thickened/enhancing walls, abrupt change in MPD caliber with distal atrophy, lymphadenopathy. The data were compared using Fisher's test dividing the patients into two groups: high-moderate grade dysplasia IPMNs (32) vs low-grade dysplasia IPMNs (14).

Results: MPD >10 mm (p=0.04), change in MPD caliber and distal atrophy (p=0.037) and radiological signs of pancreatitis (p=0.008) were significantly more common in patients with high-moderate grade dysplasia IPMNs than in patients with low-grade dysplasia. Enhancing solid components were present in 12/32 high-moderate-grade IPMNs and 1/14 low-grade IPMN (p=0.07). No significant differences were observed between the two groups for the other parameters evaluated.

Conclusion: Fukuoka criteria appear to be helpful in differentiating between invasive/high-moderate grade IPMNs and low-grade IPMNs. The most useful criteria are MPD >10 mm, change in MPD caliber and distal atrophy and radiological signs of pancreatitis.

11:00 - 12:30 **Liffey Hall 1**

Scientific Session SS 9

Radiomics and artificial intelligence in abdominal imaging

SS 9.1

Putting things in perspective: advanced image processing with Radiomics versus the radiologist's "gut feeling" to predict treatment response in rectal cancer

J.J.M. Van Griethuysen[1], M.J. Lahaye[1], M. Maas[1], H.J.W.L. Aerts[2], F.C.H. Bakers[3], R.F.A. Vliegen[4], R.G.H. Beets-Tan[1], D.M.J. Lambregts[1]; [1]Amsterdam/NL, [2]Boston, MA/US, [3]Maastricht/NL, [4]Heerlen/NL

Purpose: To compare the predictive performance of advanced image processing (Radiomics) and visual morphologic evaluation by expert-radiologists to predict response to neoadjuvant chemoradiotherapy (nCRT) on pre-treatment MRI of rectal cancer.

Material and methods: The pre-treatment MRIs (T2W + b1000/1100-DWI) of 130 patients were analyzed to predict the likelihood of a good (Mandard tumour regression grade (TRG) 1-2) or complete (TRG1/pCR) response, respectively, according to two methods. First, two expert-radiologists estimated the likelihood of a good or complete response, respectively, using a 5-point confidence score based on an overall visual morphologic assessment (size/shape/border/signal, TN-stage, fascia invasion, extramural vascular invasion (EMVI)). Second, 3421 Radiomics-features were extracted using PyRadiomics. Data were analyzed using bootstrap with 100 iterations, for each iteration, patients were randomly split 70:30 (training:testing). In the training set, top 25 features were selected using minimum-Redundancy Maximum-Relevance (mRMR). Selected features and the radiologists' scores were then fitted into separate logistic regression models, which were evaluated on the testing set.

Results: 63 patients had a good response and 29 a complete response. To predict a good response, average area under the ROC-curve (AUC) for the two expert-radiologists was 0.69 and 0.63, versus a maximum AUC 0.66 for the best-performing Radiomics-feature (ADC LoG-5mm-GLCM-IDN; a measure of heterogeneity). To predict a complete response AUC was 0.79 and 0.69 for the expert-radiologists versus AUC 0.72 for the best Radiomics-feature (ADC LoG-5mm-GLCM-IDN).

Conclusion: Visual morphologic assessment of pre-treatment MRI by expert-radiologists results in comparable performance as (individual) Radiomics-features to predict response to neoadjuvant treatment in rectal cancer.

SS 9.2

Neurons vs neural networks: comparison of machine learning/computational neural networks to radiologists in characterization of subcentimeter liver nodules in colorectal carcinoma found on staging CT scans

K. Khalili, R. Lawlor, M. Pourafkari, T.K. Kim, H.-J. Jang, M. Atri, S. Johnson, A. Martel; Toronto, ON/CA

Purpose: To determine if machine learning could improve assessment of "too small to characterize" hepatic nodules in patients presenting with colorectal carcinoma (CRC).

Material and methods: Imaging of patients with CRC was assessed for the following inclusion criteria: local CT scan in portovenous phase, <1cm hepatic nodule(s) & >2-year follow-up CT/MRI. 199 patients with 547 nodules were included. Malignancy was confirmed by ≥30% change, benignity by stability of >2 years. Machine learning (ML): predictive features from a pool of 100 extracted texture features were used in a random forest classifier (200 trees, 5-fold cross-validation) to develop diagnostic models from a training set of 150 patients (400 nodules). In addition, five convolutional neural networks (CNN) were trained using a fivefold cross-validation technique. Results were averaged across folds for both ML & CNN. The remaining 147 nodules were used as the test set to compare the performance of 3 abdominal radiologists to the better of ML versus CNN techniques, measured through receiver operating characteristic (ROC) analysis.

Results: Prevalence of disease were 25.5% and 40.5% in the learning and testing sets. In the ROC analysis of training set, CNN (mean AUC 0.89, range 0.84-0.94) outperformed ML (mean AUC 0.78, range 0.69-0.83) and thus was selected for comparison to radiologists. ROC analysis of the test set demonstrated a significantly better performance for radiologists (mean AUC 0.94, range 0.91-0.95) than CNN (0.85, p=0.008). Using a threshold of 0.5, CNN obtained a sensitivity/specificity of 80.0%/78.4%.

Conclusion: CNN shows promise in the characterization of subcentimeter hepatic nodules in CRC though not matching expert radiologists. Future work with larger training set is needed.

SS 9.3

Decreased expression of OATP8 in hepatocellular carcinoma evaluated by whole-lesion radiomics on Gd-EOB-DTPA enhanced MRI

L. Cao, J. Chen, H. Jiang, B. Song; Chengdu/CN

Purpose: To investigate the value of whole-tumor radiomic features on multiphasic gadolinium-ethoxybenzyl-diethylenetriaminepentaacetic acid (Gd-EOB-DTPA) enhanced MRI in evaluating organic anion transporting polypeptide 8 (OATP8) expression in HCC patients.

Material and methods: 67 consecutive surgically confirmed HCC patients were prospectively enrolled and underwent Gd-EOB-DTPA enhanced MR examination. Radiomic features on each sequence were derived using in-house software (Analysis Kit, GE Healthcare). The expression intensities of OATP8 were histopathologically determined and scored as: 0, no expression; 1, weak expression; 2, moderate expression; and 3, high expression. Lasso logistic regression was used for feature selection. Correlation analysis and nonparametric test were conducted accordingly. Receiver operating characteristic (ROC) analysis was applied to determine diagnostic performances of selected features in evaluating the decreased OATP8 expression.

Results: The CorrelationAllDirection_offset1_SD, IDMAllDirection_offset4_SD and LongRunEmphasis_angle45_offset1 at T1-pre imaging, the IDMAllDirection_offset1_S at portal venous phase (PVP), and the IDMAllDirection_offset1_SD and IDMAllDirection_offset4_SD at hepatobiliary phase (HBP) of HCC showed significant correlation with OATP8 expression ($p<0.05$). All features differed significantly between decreased expression (score 0-2) and high expression (score 3) group ($P<0.05$ for all). The largest area under ROC curve (AUC) of T1-pre images (IDMAllDirection_offset4_SD), PVP (IDMAllDirection_offset1_SD), and T1-HBP (IDMomentAllDirection_offset4_SD) were 0.69(CI[0.55, 0.81]), 0.66(CI[0.52, 0.78]) and 0.77(CI[0.63, 0.87]), respectively, in identifying decreased OATP8 expression in HCC. T1-pre images (IDMAllDirection_offset4_SD) showed highest sensitivity (87.0%, CI[66.4%, 97.2%] vs 78.3% CI[56.3%, 92.5%], 65.2% CI[42.7%, 83.6%]) while T1-HBP (IDMomentAllDirection_offset4_SD) showed highest specificity (80.7% ,CI[62.5%, 92.5%] vs 48.4%, CI[30.2, 66.9], 51.6%, CI[33.1%, 69.8%]).

Conclusion: Whole-tumor Radiomics features based on Gd-EOB-DTPA enhanced MRI, especially the IDM on HBP images, offers a potential avenue toward preoperative evaluation of the decreased expression of OATP8 in HCC.

SS 9.4

Radiomics as a novel tool for primary nodal staging in rectal cancer

J.J.M. Van Griethuysen[1], D.M.J. Lambregts[1], S. Trebeschi[1], M. Maas[1], M.J. Lahaye[1], G.L. Beets[1], F.C.H. Bakers[2], R.G.H. Beets-Tan[1], H.J.W.L. Aerts[3]; [1]Amsterdam/NL, [2]Maastricht/NL, [3]Boston, MA/US

Purpose: To assess the potential of quantitative MR-imaging analysis using Radiomics for nodal characterization in primary rectal cancer staging.

Material and methods: 226 lymph nodes (from 34 rectal cancer patients who underwent MRI followed by surgical resection) were analyzed and matched node-by-node with histopathology. Short axis was measured for each node (on T2W-MRI) and nodes were manually segmented on T1W and T2W-MRI to extract 748 radiomic features (using PyRadiomics). Using principal feature selection, we selected the 25 features providing best complementary information to routine nodal size-measurements. Performance to distinguish between malignant and benign nodes was assessed with areas under the curve (AUC) per-feature using a binomial mixed effects logistic regression model, correcting for patient number. False detection rate (FDR) correction set at 10% was applied to correct for multiple testing.

Results: 17/226 nodes were malignant. Selected features were compared to (and combined with) nodal size-measurements using a bootstrap method with 100 iterations; the model was trained on a random subset of patients and tested on the remaining patients (train:test ratio 80:20). Average performance for nodal size-measurements was AUC 0.82. The best performing Radiomic-feature after FDR correction (gray level co-occurrence matrix (GLCM)-difference average; a measure of heterogeneity) resulted in an AUC of 0.83; the combination of this feature with nodal size resulted in an AUC of 0.85.

Conclusion: Radiomics may provide valuable quantitative information to characterize rectal cancer lymph nodes; particularly features reflecting nodal heterogeneity are promising. Although Radiomics slightly improves staging performance, the added benefit compared to routine size-based staging appears to be limited.

SS 9.5

Diffusion kurtosis MRI for evaluating inflammatory activity in ulcerative colitis: pilot study

J. Podgorska, K. Pasicz, E. Zagórowicz, B. Gołębiewski, P. Kuś, J. Jasieniak, P. Wieszczy, A. Anysz-Grodzicka, J. Pałucki, E. Fabiszewska, W. Skrzyński, P. Kukołowicz, A. Cieszanowski; Warsaw/PL

Purpose: To assess the efficacy of diffusion kurtosis imaging (DKI) in the assessment of inflammatory activity of ulcerative colitis (UC).

Material and methods: 17 patients with UC underwent 3T magnetic resonance DKI (b values of 0-2000 s/mm^2) within a short time (1-6 days) of endoscopic evaluation and with no bowel preparation. The inflammatory activity of up to 5 bowel segments (rectum, sigmoid, descending, transverse, ascending colon) was graded on endoscopy with Mayo score. Apparent diffusion for non-Gaussian distribution (DK) and apparent kurtosis coefficient (K) on DKI as well as apparent diffusion coefficient (ADC) on diffusion weighted imaging (DWI) were correlated with Mayo score. T-test was used to compare the groups.

Results: In total 54 bowel segments: endoscopically inactive (n=18) and with mild to severe activity (Mayo 1-3) (n=36) were analysed. Statistically significant differences between inactive and active disease were found in DK (mean = $2.3\text{x}10^{-3}$ mm^2/s, standard deviation (SD) = $0.61\text{x}10^{-3}$ mm^2/s and mean = $1.81\text{x}10^{-3}$ mm^2/s, SD = $0.51\ \text{x}10^{-3}$ mm^2/s respectively, $p=0.003$) and ADC (mean = $1.3\ \text{x}10^{-3}$ mm^2/s, SD = $0.27\text{x}10^{-3}$ mm^2/s and mean = $1.15\text{x}10^{-3}$ mm^2/s, SD = $0.23\text{x}10^{-3}$ mm^2/s respectively, $p=0.041$). No significant difference was found in K. Overlapping of parameters was less significant in DK than in ADC.

Conclusion: DKI of UC correlates with disease activity might be superior to Gaussian DWI model for assessment of the inflammatory activity.

SS 9.6

withdrawn by the authors

SS 9.7

Consistency of MR radiomic features on T2-weighted imaging of the liver

J. Santinha, J.M.G. Lourenço, I. Santiago, C. Matos, N. Papanikolaou; Lisbon/PT

Purpose: To assess the intra-observer, inter-observer and test-retest repeatability of radiomic features on T2-weighted magnetic resonance imaging of the liver.

Material and methods: Two axial 2D turbo-spin-echo T2-weighted abdominal acquisitions were acquired, with a minimum interval of 15 minutes between acquisitions, in 14 different patients (8 men; mean age=59.5 years) performing an abdominal MRI examination, in a „scan-rescan" design. Examinations were performed in a 1.5T Ingenia Philips scanner with the following parameters: slice thickness=5mm; gap=1mm; echo time=80ms; repetition time=850ms; flip angle=90º; Bandwidth=507Hz; echo train lenght=72. Two radiologists manually segmented the whole liver (VOI) twice in both acquisitions from each patient. A total of 2247 radiomic features (shape, first order, glcm, glrlm, glszm, gldm and ngtdm of the original and filtered images - exponential, logarithm, square, square root, two levels of wavelet and Laplacian of Gaussian with 1-,3-, 5-mm) were extracted from each VOI using the Pyradiomics package. The intra-observer, inter-observer, and test-retest repeatability were assessed using the intraclass correlation coefficient (ICC). An ICC≥0.81 was considered excellent.

Results: 1084 features for Reader 1 and 1053 features for Reader 2 showed excellent intra-observer repeatability (mean=47.5%) with 1017 (mean=95.2%, 45.3% of total) overlapping features. 1090 (48.5%) features showed excellent inter-observer repeatability and 1258 (56.0%) features showed excellent test-retest repeatability. A total of 930 (41.4%) features (wavelet filters and original≥100, firstorder=192 and glcm=241) showed excellent repeatability for intra-observer, inter-observer and test-retest repeatability.

Conclusion: Our results indicate that, for T2-based whole-liver analysis and after accounting for intra-observer, inter-observer and test-retest variability, less than half of radiomics features preserve an excellent repeatability. These „stable" features may, therefore, be more „trustworthy" for T2-based whole-liver radiomics analysis.

SS 9.8

Texture analysis of preoperative CT images for prediction of liver volume regeneration after major hepatectomy in living donor transplantation

J.E. Kim[1], J.H. Kim[1], S.J.H. Park[1], S.-Y. Choi[2], J.S. Bae[1], S.J. Jeon[1], J.K. Han[1]; [1]Seoul/KR, [2]Bucheon/KR

Purpose: To predict the rate of liver regeneration after donor hepatectomy using preoperative laboratory test and computed tomography (CT) texture analysis in living donor transplantation.

Material and methods: 112 living donors (M:F = 79:33, 31 years) who performed preoperative CT were included in this study. After transplantation, follow-up CT was performed after median 123 days. We measured the volume of future remnant liver (FLR) on preoperative CT and volume of the remnant liver (LR) on follow-up CT. Regeneration index (RI) was calculated using following equation: $[(V_{LR}-V_{FLR})/V_{FLR}] \times 100$. Texture analysis regarding FLR was semiautomatically performed. We used a stepwise multivariable regression to assess associations of laboratory results and texture parameters in relation to RI and make the best fit predictive model.

Results: The mean RI was 110.7 ± 37.8%, highly variable ranging from 22.4% to 247.0%. Among texture parameters, standard deviation, variance, volume of FLR and grey level co-occurrence matrices (GLCM) contrast were found to have significant correlations between RI in univariable analyses. In a multivariable analysis adjusting for other factors, a smaller volume of FLR (ß -0.17, 95% CI -0.22 to -0.13) and lower GLCM contrast (ß -1.87, 95% CI -3.64 to -0.10) were associated with higher RI. The regression equation predicting RI was following: RI = 203.82 + 10.42 x preoperative serum total bilirubin (mg/dL) – 0.17 x V_{FLR} (cm^3) – 1.87 x GLCM contrast (×100).

Conclusion: In our study, the volume of FLR and GLCM contrast were independently associated with the rate of liver regeneration. CT texture analysis can be useful in predicting liver regeneration for the donors undergoing right hepatectomy.

SS 9.9

Multiparametric combined fluorodeoxyglucose-positron emission tomography (FDG-PET)/CT and MR imaging to predict response to chemoradiotherapy in rectal cancer: whole tumor versus sub-volume analysis

N. Schurink[1], M. Berbee[2], J. Van Griethuysen[1], W.J.C. Van Elmpt[2], M. Maas[1], M.J. Lahaye[1], F.C.H. Bakers[2], R.G.H. Beets-Tan[1], D.M.J. Lambregts[1]; [1]Amsterdam/NL, [2]Maastricht/NL

Purpose: To assess the individual and complementary performance of quantitative parameters from pre-treatment multiparametric MRI and FDG-PET/CT to predict treatment response in rectal cancer.

Material and methods: A pilot group (n=20) underwent multiparametric MRI (T2W + diffusion weighted imaging (DWI); b0,100,500,1000) and FDG-PET/CT before neoadjuvant treatment + surgery. Images were anatomically co-registered using rigid + non-rigid registration. Whole-tumor volumes were segmented on T2W-MRI and transferred to the other modalities/sequences; each tumor was additionally divided into 7mm^3 sub-volumes. The following parameters were calculated per-tumor and sub-volume: T2-texture (uniformity/entropy), T2-signal intensity (SI), apparent diffusion coefficient (ADC) (mean/max/min/median/10th & 90th percentile), standard uptake value (SUV) (mean/max/median), CT-Hounsfield units (HU). Performance to predict poor response (=Mandard tumor regression grade (TRG)3-5) vs. good response (TRG1-2) was calculated using receiver operating characteristic (ROC)-analysis for [1] each individual parameter (whole-tumor), [2] multiparametric combination of the 5 best-performing parameters (whole-tumor), and [3] the proportion (%) of 'poor-response' sub-volumes within the tumor. Sub-volumes were defined as 'poor response' when ≥4 (out of 5) parameters within that sub-volume were indicative of TRG3-5, using a cut-off derived from dichotomisation by median split.

Results: Best single predictive parameters were T2-uniformity (area under curve (AUC)0.78), T2-SI (AUC0.70), ADCmax (AUC0.76), SUVmax (AUC0.78) and SUVmean (AUC0.73). Combined multiparametric performance (whole-tumor) was AUC0.91. The proportion of 'poor-response' sub-volumes resulted in AUC0.74.

Conclusion: Multiparametric analysis of quantitative MRI and FDG-PET/CT data has potential added value to predict response to neoadjuvant treatment. If there is a potential benefit for performing sub-volume (or voxel-wise) analysis, this needs to be established by further and larger studies; with our current method, we have so far not demonstrated a clear added value.

SS 9.10

Academic-industry collaborations involving quantitative imaging biomarkers in drug development clinical trials

M.S. Middleton, J. Cui, W.C. Henderson, J.C. Hooker, G. Hamilton, N. Szeverenyi, C. Sirlin; La Jolla, CA/US

Purpose: To describe an academic-industry collaboration paradigm developed over ten years while acting as a Radiology Coordinating Center (RCC) for drug development clinical trials involving quantitative imaging biomarkers (QIBs) such as MRI hepatic proton density fat fraction (PDFF), magnetic resonance elastography (MRE) liver stiffness, and magnetic resonance spectroscopy (MRS) fat tissue spectral characteristics. Our role as RRC for these complex, collaborative studies required iterative refinement of project planning, workflow, and management.

Material and methods: We describe non-disclosure agreements and contracts, statements of work and budgets, regulatory issues, conflicts of interest, site selection and training, intake quality control (QC), analysis, analysis QC, results reporting, protocol deviations and violations, and standard operating procedures.

Results: We have acted as an RCC for 21 industry clinical trials involving liver QIBs, and four industry clinical trials involving MRS of the abdomen, thigh, and lower leg muscles. These studies were conducted at over 400 sites worldwide involving over 5,000 MR exams using the five main MR manufacturers for PDFF and the three MR manufacturers with MRE capability. Collectively, these exams have involved almost every conceivable combination of scanner type and sequence parameter settings appropriate for the measured QIBs. We have developed robust templates for an imaging manual, an RCC charter, and billing log and results-reporting spreadsheets.

Conclusion: The methods, templates, and other study materials developed in collaboration with the pharmaceutical industry have helped us plan and manage new industry studies involving QIBs. Many of these concepts may be generalizable to other core labs and to other clinical trials using quantitative biomarkers, within and outside the field of radiology.

11:00 - 12:30 **Wicklow Hall 2A**

Scientific Session SS 10

Liver: focal and diffuse liver pathologies, intervention and transplantation

SS 10.1

Gadoxetic acid-enhanced MRI before primary liver transplantation to predict recurrence of HCC

S. Lee, K.W. Kim, W.K. Jeong; Seoul/KR

Purpose: We performed a multicenter retrospective survey to investigate the prognostic value of preoperative gadoxetic acid-enhanced MRI in predicting HCC recurrence after liver transplantation (LT).

Material and methods: From two large LT centers, data was collected from 140 recipients with HCC who underwent primary LT and pretransplant gadoxetic acid-enhanced MRI between January 2009 and December 2013.

Results: The 1-, 3-, and 5-year recurrence-free survival rates were 91.3%, 85.4%, and 82.4%, respectively. Multivariate analysis revealed that being outside the Milan criteria (HR, 3.062; 95% CI, 1.309–7.159; P = 0.010) and peritumoral hypointensity on hepatobiliary phase (HBP) (HR, 10.268; 95% CI, 4.248–24.820; P < 0.001) were independent predictors of HCC recurrence. The accuracy in categorization of the Milan criteria on pretransplant MRI was 92.9% in correlation with the explanted liver. Peritumoral hypointensity on HBP was significantly associated with worse tumor grade and microvascular invasion (P = 0.038 and P < 0.001, respectively). Using a combination of the Milan criteria and peritumoral hypointensity on HBP, preoperative MRI further stratified the risk of tumor recurrence after LT (P < 0.001), and 5-year recurrence-free survival rates for patients outside of the Milan criteria and non-peritumoral hypointensity on HBP were comparable to those within the Milan criteria (89.0% vs. 75.9%) (P = 0.090).

Conclusion: Pre-transplant MRI using gadoxetic acid offers not only precise morphologic tumor stage, but also additional biologic tumor behavior on the risk of HCC recurrence after LT. Patients outside of the Milan criteria with non-peritumoral hypointensity on HBP may achieve acceptable outcomes comparable to that of patients within Milan criteria.

SS 10.2

Radiological-pathological correlation of pre-transplant imaging and explanted livers: American College of Radiology (ACR) Liver Imaging Reporting and Data System (LI-RADS) 2017 category versus Organ Procurement and Transplantation Network (OPTN) class in the diagnosis of HCC

C.M. O Brien, A.C. O'Brien, P.A. McCormick, N. Nolan, S.J. Skehan, R. Ryan, D.E. Malone, R. Gibney; Dublin/IE

Purpose: To evaluate concordance of the LI-RADS 2017 and OPTN-United Network for Organ Sharing (UNOS) systems in the diagnosis of hepatocellular carcinoma (HCC).

Material and methods: Liver transplant (OLT) patients with a pre-operative diagnosis of HCC and explants with HCC on pathology from 01/01/2014 to 09/09/2017 were retrospectively identified using the OLT database. Pre-OLT CT/MRI reports were reviewed. In patients with LI-RADS 5, 4/5, 4 or 3 lesions, the descriptions in the reports were used to categorize the lesions using the LI-RADS 2017 (LR) and OPTN-UNOS systems and the histopathology coding of explanted livers was reviewed. Data were collated in an MSExcel spreadsheet and analysed on a per patient basis.

Results: 49 OLT patients met selection criteria. LR and OPTN scores were assigned to all patients. 39/49 with HCC were LR-5. Of these, 38/49 were OPTN-5, 1 did not meet arterial enhancement criteria and in retrospect was an LR-4 lesion. OPTN subclasses were: 5B 16; 5A 9; 5A-g 4; 5X 2; 5T 7. LR-4 or LR-4/5 nodules were present in 5/49 and 1/49 patients with proven HCC. 3/6 had prior TACE and were OPTN-5T. 3/6 were not OPTN 5, all patients had HCC. 4/49 were LR-3; none were OPTN 5.

Conclusion: No discrepancies were found between the 2017 ACR LI-RADs 5 and OPTN-UNOS 5 lesion classification systems in these HCC patients. Meticulous adherence to technical and interpretative aspects of both systems is essential. An advantage of LI-RADS vs OPTN-UNOS is that LI-RADS 4 (probable HCC) lesions not meeting OPTN 5 criteria are identified for close follow-up.

SS 10.3

The relationship between the location of the portal vein thrombus, the patency of the portal veins, and the coexisting disease

K. Ibukuro, G. Ogasawara, H. Fukuda, K. Tobe, M. Kishino; Tokyo/JP

Purpose: To clarify the relationship between the location of the portal vein thrombus, the patency of the portal vein, and the coexisting disease.

Material and methods: We retrospectively reviewed 48 patients with portal vein thrombus observed on contrast-enhanced CT scans for six years. The coexisting diseases were classified as (A) liver cirrhosis (LC) (n=29) and (B) inflammatory diseases (Inf) including cholangitis or cholecystitis (n=13) and hepatic abscess (n=6). The locations of the thrombus and the patency of the portal vein were classified as peripheral (second-order division of intrahepatic portal vein, n=18) and central (n=30), complete obstruction (n=20) and patent (n=28), respectively. We reviewed the presence of ascites, esophageal varices, gastro- or spleno-renal shunt, and Child classification. The logistic regression analysis was used to identify the statistically significant characteristics for the location of the thrombus and the patency of the vein. The level of significance was set to 5%. The Cramér's V was measured for the association between the location, the patency, and the coexisting disease.

Results: The coexisting disease was the primary factor that affected the location of the thrombus (odds ratio: 32; LC vs. Inf) and the patency (odds ratio: 18; LC vs. Inf). The V were as follows: 0.693 (the coexisting disease and the location), 0.612 (the coexisting disease and the patency), 0.306 (the location and the patency).

Conclusion: The coexisting disease had the most important role for the location of the portal vein thrombus and the patency of the portal vein.

SS 10.4

Assessment of liver function in patients with HCC using perfusion-weighted MRI with gadolinium-ethoxybenzyl-diethylenetriamine pentaacetic acid

T. Duan, J. Chen, X. Lin, B. Song; Chengdu/CN

Purpose: To prospectively evaluate liver function in patients with HCC using perfusion-weighted magnetic resonance imaging (PW-MRI) with gadolinium-ethoxybenzyl-diethylenetriamine pentaacetic acid (Gd-EOB-DTPA).

Material and methods: PW-MRI was performed on 41 HCC patients on a 3.0 Tesla MR scanner. The perfusion data were acquired using a prototype radial stack-of-stars 3D spoiled gradient echo pulse sequence with golden-angle radial sampling schemes over the course of 6.25 minutes. Post-processing of PW-MRI data was performed on an in-house software O.K. (Omini-Kinetics). A 2-compartment 2-input pharmacokinetic model was chosen to generate haemodynamic curving. We applied an extended Toft's linear model to generate the maps of K_{trans}, K_{ep}, V_e and the semi-quantitative parameters of time-to-peak (TTP), max concentration and max slope. Perfusion parameters and volumes of normal hepatic parenchyma were conducted, then the products of perfusion parameters and volume were calculated. Indocyanine green retention at 15 min (ICG R-15) and model for end-stage liver disease (MELD) scores were also recorded. PW-MRI parameters, volumes and products were correlated with both ICG R-15 and MELD scores using Spearman rank correlation analysis.

Results: The product of TTP and volume showed poor correlations with ICG R-15 (rho=-0.367, p=0.046). Meanwhile, K_{trans} (rho=0.496, p<0.001), K_{ep} (rho=0.930, p<0.001), max slope (rho=0.342, p=0.033), product of K_{trans} and volume (rho=0.898, p<0.001), product of K_{ep} and volume (rho=0.898, p<0.001) and product of max slope and volume (rho=0.388, p=.015) correlated significantly with MELD scores.

Conclusion: Measures of liver function obtained by Gd-EOB-DTPA PW-MRI with tracer kinetic modelling may provide a suitable method for the evaluation of liver functional reserve.

SS 10.5

Contrast-enhanced oncologic staging MRI of abdomen and pelvis with a hepatocyte-specific agent in a large-bore MR scanner: optimizing extrahepatic tumor evaluation in neuroendocrine neoplasms

U. Fehrenbach[1], U. Fahlenkamp[1], V. Prasad[1], M. Pavel[2], D. Geisel[1], T. Denecke[1]; [1]Berlin/DE, [2]Erlangen/DE

Purpose: Liver-specific MR contrast agents in neuroendocrine neoplasms (NEN) have shown its advantages in evaluation of hepatic tumor burden. However, a standard scan protocol is insufficient in extrahepatic and especially pelvic tumor evaluation. The aim of the study is to evaluate an MRI shuttle protocol with fast 3D-T1w sequences and hepatocyte-specific contrast (Gd-EOB) to enable imaging abdomen and pelvis in optimal first-pass contrast phases in the setting of a large-bore MRI scanner with shorter axial field of view.

Material and methods: 96 patients with NEN of the abdomen were scanned with the first pass (FP) pelvic protocol in a Gd-EOB MRI. FP pelvic sequence was acquired in between portal venous and venous liver phase. We compared pelvic vessel and tissue enhancement between FP and a standard equilibrium (EQ) pelvic sequence. Dynamic liver enhancement with the new protocol including FP pelvic sequence was compared to a standard protocol without additional sequence.

Results: The FP pelvic sequence showed improved vessel and tissue enhancement. Aortic (140.81 vs 116.43) and venous (89.92 vs 62.76) vessel enhancement in the lower abdomen showed significantly (p=0.000) higher signal intensities in FP pelvic than in the EQ phase. The FP sequence also showed significantly improved lymph node enhancement (57.84 vs 41.15; p=0.000). Dynamic liver enhancement in the FP protocol showed no significant differences to the standard protocol (57.48 vs 53.01; p=0.143).

Conclusion: Including a FP pelvic sequence in between portal venous and venous liver phase by shuttling of the patients' table enables improved tumor evaluation of the pelvis region in Gd-EOB MRI. Additionally, there was no quality loss in liver enhancement in the proposed FP pelvic protocol.

SS 10.6

MRI assessment of transarterial chemoembolization effects in patients with neuroendocrine hepatic metastasis

M. Lapteva, M.A. Shorikov, D. Frantsev, O. Sergeeva, E. Virshke, B. Dolgushin; Moscow/RU

Purpose: The purpose of the paper is to develop suitable transarterial chemoembolization effects (TACE) evaluation criteria in liver metastatic neuroendocrine tumor (mNET) patients on MRI.

Material and methods: 23 liver mNET patients (G1-9, G2-10, G3-2, unknown grade 2) who underwent 36 TACE procedures were enrolled in the study. 68 MRI studies performed 3-86 days before (median 28 days) and 23-147 days (median 61 days) after TACE were analyzed retrospectively. Using 1.5T MRI-scanner, we acquired: 1) 3DT1WIFS in axial plane before i.v. contrast injection and after in portal and delayed phases; 2) diffusion-weighted images with apparent diffusion coefficient (ADC) maps. We measured before/after TACE: 1) maximum necrotic/fibrotic zone diameter and solid component thickness on its periphery in the largest targeted lesion; 2) ADC and MR contrast agent accumulation dynamics (dSI) in regions of interest in tumor solid component.

Results: TACE effect according to response evaluation criteria in solid tumors (RECIST)(1.1) was evaluated as progressive disease in 8.3% cases, stabilization in 83.3% cases and partial response in 8.3% cases. The diameter of the fibrosis/necrosis areas before/after TACE demonstrated no changes (p=0.614), but solid component thickness on its periphery decreased significantly (p=0.003, median 16%). ADC values increased significantly in solid portions of mNETs after TACE (p=0.003). MR contrast agent accumulation of the lesions in portal phase decreased significantly after TACE (p=0.003, median 8.5%). Decrease of MR contrast agent accumulation in a solid part of the target lesions more than 10% after TACE is associated with a longer time to progression of the disease (p=0.025). There is an increase in MR contrast agent wash-out time in the solid part of the target lesions after TACE (p=0.032).

Conclusion: Parameters changed in liver mNET after TACE: 1) solid component thickness in cases of central necrosis/fibrosis (decrease); 2) ADC (increase); 3) ndSI T1WI in portal phase (decrease) and this is the positive prognostic factor; 4) MR contrast agent wash-out time (increase).

SS 10.7

Differentiation of focal nodular hyperplasia from HCC: the role of triple-phase arterial MRI

M. Gatti, R. Faletti, S. Rousset, L. Bergamasco, P. Fonio; Turin/IT

Purpose: To determine the value of triple-phase arterial imaging to differentiate focal nodular hyperplasia (FNH) from HCC.

Material and methods: The study population included 52 patients who had arterial enhancing hepatic lesions (a total of 72 lesions: 41 HCC and 31 FNH). All patients underwent triple-phase arterial phase MRI using hepatocyte-specific agents (Gd-EOB-DTPA). Images were reviewed by two radiologists in consensus: contrast enhancement ratios (CER), liver-to-lesion contrast ratios (LLC) and signal intensity (SI) were measured. The lesions were categorized based on the peak of LLC into the following groups: 1) angiographic, 2) early arterial and 3) late arterial. Data were analysed with Wilcoxon signed-rank test.

Results: There was no difference in CER between FNH and HCC patients ($p>0.09$). The SI_{HCC} increases through the different arterial phases 1) 242.08 --> 2) 251.84 --> 3) 253.95; however, the SI_{FNH} started to decrease in the late arterial phase 1) 303.21 --> 2) 326.03 --> 3) 323.72. LLC_{FNH} were significantly higher than LLC_{HCC} in the angiographic phase (41.3 vs. 25.0; $p=0.01$), whereas there were not different in the other phases ($p=0.20$ and $p=0.82$, respectively), this behaviour was paralleled by the subgroup divisions: 17 (55%) FNH were classified as the 1st group, 11 (35%) in the 2nd and only 3 (10%) in the 3rd; on the other hand, the HCC was homogeneously distributed (34%, 32% and 34%).

Conclusion: This study highlights the different enhancement patterns of HCC and FNH: FNH resulted more conspicuous in the angiographic phase and started its "wash out" in the late arterial phase; therefore, a multi-phase arterial phase MRI may be an adjunctive tool to further differentiate HCC from FNH.

SS 10.8

Reappraisal of rate and risk factors of complications after US-guided percutaneous liver biopsy: a retrospective analysis of 2405 biopsies

A. Maheux, S. Harguem, V. Vilgrain, M. Ronot; Clichy/FR

Purpose: To reappraise the rate and risk factors of complications after US-guided liver biopsy in a large single-center series of 2405 biopsies.

Material and methods: We analyzed 2405 liver biopsies performed in 2137 patients (58% males, mean age 54±15 yo) between January 2008 and December 2013. Biopsies were performed for the characterization of focal liver lesions or to assess suspected or known chronic liver disease. Clinical, laboratory, and technical data were recorded for all biopsies. For focal liver lesions, the following elements were also recorded: largest diameter, location, enhancement characteristics and pathological results. Occurrence of post-biopsy significant symptoms (any complaint motivating complementary imaging) and complications were noted. Complications requesting specific treatment (embolization or surgery) were considered as severe.

Results: 1283 (53%) biopsies targeted focal lesions and 1122 (47%) were performed for liver disease. Significant symptoms occurred after 134 biopsies (5.6%); the most frequent being pain (109/134). Complications occurred after 38 biopsies (1.6%); the most frequent being hemoperitoneum (n=21), subcapsular liver hematoma (n=11) and liver hematoma (n=6). One patient died. Severe complications were present in 13 patients. In univariate analysis, prothrombin time ($p=0.006$), creatinine serum level ($p<0.001$), lesion largest diameter ($p<0.001$) and tumor pathology ($p=0.040$) were associated with the occurrence of complications but not platelet count. In multivariate analysis, only the lesion largest diameter was retained (OR 1.014 [1.002-1.026], $p=0.018$).

Conclusion: Rate of complications after US-guided liver biopsy was low. Lesion largest diameter appears as the main risk factor of complication.

SS 10.9

Gadobenate dimeglumine-enhanced MRI in patients with ascitic effusion

M. Bonatti[1], G.A. Zamboni[2], F. Lombardo[1], R. Valletta[2], G. Bonatti[1]; [1]Bolzano/IT, [2]Verona/IT

Purpose: To evaluate the pharmacokinetics of gadobenate dimeglumine (Gd-BOPTA) in patients with ascitic effusion and to correlate it with the cause of the effusion.

Material and methods: We included in our institutional review board approved retrospective study 32 consecutive patients with ascites who underwent Gd-BOPTA-enhanced liver MRI (including hepatobiliary phase) on a 1.5T scanner in our Institution between January 2012 and December 2017. Clinical data were collected. Appearance of ascitic fluid (hypo-, iso- or hyper-intense in comparison to paravertebral muscle) was assessed on native and hepatobiliary phase gradient-recalled echo (GRE) T1-weighted images. Signal intensity of ascites and paravertebral muscle was measured by means of a $1cm^2$ round region of interest (ROI) on both phases; ascites/muscle signal-to-noise ratio (SNR) was calculated.

Results: The cause of ascites was portal hypertension in 23/32 patients, peritoneal carcinomatosis in 6/32 and recent major surgery in 3/32. On native images, ascitic fluid was hypointense in 90.6% of the cases and isointense in 9.4%, whereas in the hepatobiliary phase it was hypointense in 3.1% of the cases, isointense in 21.9% and hyperintense in 75% ($p<0.001$). Median ascites/muscle SNR was 0.54 in native phase and 1.59 in hepatobiliary phase with a median increase of 269% (range 158-748%) ($p<0.001$). Median SNR increase was 294% in patients with portal hypertension, 194% in patients with peritoneal carcinomatosis and 239% in those after surgery ($p>0.05$).

Conclusion: Gd-BOPTA is excreted in ascitic fluid, which significantly increases its signal intensity in hepatobiliary phase. No statistically significant differences were found between the different types of ascites.

SS 10.10

Evaluation of texture analysis for the differential diagnosis of focal nodular hyperplasia from hepatocellular adenoma on contrast-enhanced CT images

R. Cannella[1], A. Borhani[2], B. Rangaswamy[2], M.I. Minervini[2], A. Tsung[2], A. Furlan[2]; [1]Palermo/IT, [2]Pittsburgh, PA/US

Purpose: To investigate the value of texture analysis for the differentiation of focal nodular hyperplasia (FNH) from hepatocellular adenoma (HCA) on contrast-enhanced CT imaging.

Material and methods: This is a retrospective, institutional review board-approved study conducted in a single institution. A search of the medical records between 2008 and 2017 revealed 48 patients (47 females, 1 male) with 70 HCA and 50 patients (48 females, 2 males) with 62 FNH. All lesions were histologically proven and with available pre-operative CT imaging. Late hepatic arterial phase (HAP) and portal venous phase (PVP) images were used for texture analysis. A region of interest was placed on the largest tumor cross section and in the non-lesional right hepatic lobe. Textural features were extracted using a commercially available research software (TexRAD) which applies a 2-step filtration-histogram approach. The differences between textural parameters of FNH and HCA were assessed using the Mann-Whitney U test. A p value <0.05 was considered statistically significant.

Results: On HAP images, mean, standard deviation (SD), entropy, mean of positive pixels (MPP) and skewness were significantly higher in FNH than in HCA on both unfiltered ($p\leq0.006$) and filtered analysis ($p\leq0.02$). On PVP mean, MPP, skewness and kurtosis in FNH were significantly higher than in HCA ($p\leq0.006$) on unfiltered images, while mean, SD and entropy were significantly higher in FNH on filtered images ($p\leq0.03$). The analysis of the non-lesional liver did not show any significant difference between two groups.

Conclusion: Textural analysis parameters are significantly different between FNH and HCA. Imaging-based quantification of lesion heterogeneity may help in non-invasive differentiation of FNH from HCA.

11:00 - 12:30 **The Auditorium**

Scientific Session SS 11

Pancreas: focal and diffuse pancreatic pathologies including endocrine tumours

SS 11.1

Additional value of tumour growth rate in patients diagnosed with well-differentiated neuroendocrine tumours

C. Dromain[1], A. Sundin[2], P.S. Najran[3], H. Vidal Trueba[4], L. De Mestier[5], J. Crona[6], M. Opalinska[7], L. Carvalho[8], R. Franca[8], P. Borg[3], N. Vietti Violi[1], N. Schaefer[1], C. Lopez[4], D. Pezzutti[8], A. Lamarca[3], F. Costa[8], M. Pavel[9], M. Ronot[5]; [1]Lausanne/CH, [2]Stockholm/SE, [3]Manchester/UK, [4]Santander/ES, [5]Clichy/FR, [6]Uppsala/SE, [7]Krakow/PL, [8]Sao Paulo/BR, [9]Erlangen/DE

Purpose: To assess the impact of lesion measurements and inter-reader reproducibility on tumour growth rate (TGR) (% change in tumor volume/month) to predict patient outcome.

Material and methods: Baseline and 3-month (+/-1) images from patients with advanced, grade 1-2 neuroendocrine tumours (NETs) were retrospectively reviewed by 2 readers for TGR_{3m} calculation. Influence of number, location of lesions and tumor burden on TGR_{3m} on patient outcome (measured as progression-free survival (PFS)) was assessed by uni/multivariable Cox regression analysis. Spearman correlation and Kruskal-Wallis test were employed. Agreement between readers was assessed by the Lin's concordance coefficient (LCC) and kappa (KC).

Results: A total of 790 lesions measured in 217 patients were included. Median PFS was 22.9 months. On univariable analysis, number of lesions (</=>4), tumor burden and presence of liver metastases were significantly correlated to PFS. On multivariate analysis, ≥4 lesions (HR:1.89 (95%CI:1.01-3.57)), TGR_{3m} ≥0.8%/month (HR:4.01 (95%CI:2.31-6.97)) and watch-and-wait treatment correlated with shorter PFS. No correlation was found between TGR_{3m} and number of lesions employed for TGR calculation (rho: -0.2; p value: 0.1930). No difference in mean TGR_{3m} across different organs was shown (p value: 0.6). Concordance between readers was acceptable (LCC: 0.52 (95%CI: 0.38-0.65); KC: 0.57; agreement: 81.55%). TGR3m remained a significant prognostic factor when data from the second reader were employed (HR: 4.35 (95%CI: 2.44-7.79); p value<0.001) and regardless of second reader expertise (HR: 1.21 (95%CI: 0.70-2.09); p value: 0.493).

Conclusion: Our results suggest that number of measured lesions and TGR_{3m} value impact on PFS of patients with advanced NETs. The number of target lesions does not seem to affect the performance of TGR calculation. In addition, TGR3m role as a prognostic factor was maintained regardless of reader's expertise.

SS 11.2

Differentiation of pancreatic neuroendocrine tumor grade comparing 3D CT texture analysis and relative CT enhancement ratios

A. Sarno[1], G. Tedesco[1], V. Ciaravino[1], N. Cardobi[2], R. De Robertis[2], P. Tinazzi Martini[2], L. Landoni[1], S. Cingarlini[1], A. Scarpa[1], M. D'Onofrio[1]; [1]Verona/IT, [2]Peschiera del Garda/IT

Purpose: To evaluate the added value of 3D CT texture analysis compared to CT enhancement ratios in the study of pancreatic neuroendocrine tumors (pNETs).

Material and methods: 100 patients with pNETs were included in this study. All tumors were pathologically diagnosed after resection or by means of biopsy, so histological grade was available in all cases. There were 31 G1, 52 G2, and 17 G3 neoplasms with the presence of metastases in 53/100 (53%) cases. 3D CT texture analysis and a quantitative analysis of enhancement of CT studies were performed comparing the results with the tumor grading. CT texture analysis results (mean value, variance, skewness, kurtosis) and relative CT enhancement ratios were compared using Wilcoxon–Mann–Whitney correlation test.

Results: Included pancreatic neoplasms were located in the head of pancreas (42%), in the body–tail (52%) and 6 patients had entire involvement of the pancreatic gland (6%). CT texture analysis and CT quantitative analysis were done in all cases. Among the three grading tumors groups (G1, G2 and G3) kurtosis parameter resulted in statistically significant difference ($p < 0.05$) at CT texture analysis. Instead, there was no statistically significant difference in CT enhancement ratios between G1 and G2 groups at CT quantitative analysis.

Conclusion: CT texture analysis parameters can be more suitable to differentiate the three grading pNETs, compared to relative CT enhancement ratios.

SS 11.3

Location of liver metastases based on the site of primary pancreatic neuroendocrine tumour

C. Fabris, A. Bissoli, M.C. Ambrosetti, G.A. Zamboni, G. Mansueto; Verona/IT

Purpose: The presence of liver metastases from neuroendocrine tumors does not preclude surgery. Knowing the distribution of these metastases is important for treatment planning. Our purpose is to investigate whether the distribution of liver metastases from pancreatic neuroendocrine tumors (pNETs) is influenced by the "streamline phenomenon" within the portal vein.

Material and methods: Institutional review board approval was waived for this retrospective study. We reviewed retrospectively the CTs performed on 49 patients with pNETs (27 males, 22 females) and liver metastases. Patients were divided into 2 groups according to the pNET site: group A (11 patients) with a pNET in the head (mean age 50.3 years); group B (38 patients) with a pNET in the body–tail (mean age 59,3 years). Two readers in consensus evaluated tumor site, diameter, vascular invasion and number of metastases within each lobe. Student's and Fisher's tests were used as appropriate.

Results: Primary tumors in the body–tail (group B) were larger than those in the head (group A) (59.55 vs 39.82 mm; p=0.043). The splenic vein was more commonly involved in patients in group B. The number of liver metastases was higher in the right lobe in both groups (p=ns). The ratio of metastases in the right-to-left hemi-liver was 2.5:1 for group A compared with 1.79:1 for group B (p=0.0423).

Conclusion: As expected, tumors from all locations in the pancreas will give a higher number of metastases in the right lobe. The right-to-left ratio is, however, significantly different based on the site of the primary tumor.

SS 11.4

Pancreatic neuroendocrine tumor grade discrimination with enhancement pattern in the arterial phase: a meta-analysis

H. Yu, M. Li; Chengdu/CN

Purpose: To assess the diagnostic test accuracy for the discriminative potential of hypo-enhancement in the arterial phase to differentiate high-grade pancreatic neuroendocrine tumors (HGP) (World Health Organization [WHO] grade II or III) from low-grade pancreatic neuroendocrine tumors (LGP) (WHO grade I).

Material and methods: A systematic literature search up to November 2017 was performed to find relevant original studies. Retrieved hits were screened for inclusion and were evaluated with the revised tool for quality assessment for diagnostic accuracy studies (commonly known as QUADAS-2) by two researchers. Pooled sensitivity, specificity, area under receiver operating characteristic (AUROC) curve, and other measures were calculated using random effect models. Risk of heterogeneity was assessed for the appropriateness of meta-analysis.

Results: Fifteen studies involving 866 patients were included. The statistical heterogeneity was explained by imaging methods (CT/MR). The pooled AUROC was 0.7494 for discrimination of HGP from LGP, with 0.632 (95% CI: 0.567, 0.694) sensitivity and 0.688 (95% CI: 0.652, 0.724) specificity.

Conclusion: Hypo-enhancement in the arterial phase is a useful imaging feature to discriminate HGP from LGP.

SS 11.5

Pancreatic steatosis: quantitative analysis using MRI and correlation with visceral adiposity, diabetes mellitus, and chronic pancreatitis

T. Tirkes[1], T.A. Seltman[1], P.R. Territo[1], L. Li[2], S.A. Persohn[1], M. Sankar[1], C.Y. Jeon[3], E.L. Fogel[1]; [1]Indianapolis, IN/US, [2]Houston, TX/US, [3]Los Angeles, CA/US

Purpose: To determine the association between the pancreatic steatosis (PS), visceral adiposity, diabetes mellitus and chronic pancreatitis (CP) using MRI.

Material and methods: 118 patients were retrospectively categorized into normal (n=60), mild (n=21), moderate (n=27) and severe CP (n=10) groups based on clinical history and MRCP findings using the Cambridge classification as the diagnostic standard. PS was calculated by measuring signal intensity on the axial water and fat-only fractions of the 2-point DIXON MR images. Visceral and subcutaneous adipose tissues were separated and measured on axial MR image by manually outlining the anatomy using an image analyzer software.

Results: There was an association between the PS and distribution of the abdominal adipose tissue, with the strongest correlation being with adiposity within the visceral compartment (r=0.48). Higher visceral adiposity and PS were also associated with CP; PS in the mild (24%), moderate (22%) and severe CP (21%) groups were significantly higher (p<0.0001) than the normal group (15%). PS between the CP groups was similar (p=0.48). Smoking (p=0.003) and alcohol (p=0.02) were significant risk factors for CP. Patients who developed type 2 diabetes showed higher PS (p=0.01), higher visceral (p=0.01) and higher subcutaneous adiposity (p=0.002) as well as atrophy of the tail (p=0.0009). There was a weak positive correlation between the PS and age in the normal group (r=0.33).

Conclusion: Pancreatic steatosis quantitatively measured by the MRI showed a moderate positive correlation with visceral adiposity and was associated with CP and type 2 diabetes. Prospective evaluation in well-phenotyped patients is needed to confirm these results.

SS 11.6

Pancreatic steatosis is associated with restriction of pancreatic exocrine function

J.-P. Kühn[1], M.-L. Kromrey[2], R.-T. Hoffmann[1], M. Laniado[1], N. Friedrich[2]; [1]Dresden/DE, [2]Greifswald/DE

Purpose: Recent research is now focused on the clinical significance of pancreatic steatosis. The purpose was to investigate if pancreatic steatosis is associated with depression of pancreatic exocrine function.

Material and methods: 1,458 volunteers aged 21 to 88 years (777 women) underwent an MRI of the pancreas, and organ fat content was quantified. Exocrine pancreatic function was categorized by fecal elastase using defined cut-offs (normal function: >200 µg/g, n=1,319; moderate/manifest restriction: <200µg/g, n=139). Statistical analysis to associate pancreatic fat content and fecal elastases includes a linear regression. Analyses were adjusted for known confounders for pancreatic steatosis, such as age sex and body mass index (BMI).

Results: Overall mean (± standard deviation) of pancreatic fat content was 7.50±3.78%. Significant higher levels were found in subjects with a restriction of pancreatic exocrine function (9.36±4.95%) compared to subjects with normal function (7.30±3.59%) (p<0.01). Linear regression analyses showed an inverse association between pancreatic fat and fecal elastase levels in the whole study population [beta: -7.19 (standard error: 1.39); p<0.01] as well as in the subgroup of subjects with normal function [-4.26 (1.32); p<0.01]. Among subjects with restriction in exocrine pancreatic function, a trend towards an inverse relation was detected [-1.28 (0.84); p<0.13].

Conclusion: There is an inverse relation between pancreatic fat content and fecal elastases suggesting an association of pancreatic steatosis with a restriction of pancreatic exocrine function.

SS 11.7

Intra-observer and inter-observer agreement on MRI and MRCP features of chronic pancreatitis

T. Tirkes[1], A. Dasyam[2], Z. Shah[3], N. Takahashi[4], G. Tang[2], D. Yadav[2], K. Vipperla[2], P. Greer[2], D. Conwell[3], M. Topazian[4], E.L. Fogel[1]; [1]Indianapolis, IN/US, [2]Pittsburgh, PA/US, [3]Columbus, OH/US, [4]Rochester, MN/US

Purpose: To determine intra- and inter-observer variability of MRI/MRCP for evaluation of chronic pancreatitis (CP).

Material and methods: This ancillary study of the Consortium for the Study of Chronic Pancreatitis, Diabetes, and Pancreatic Cancer was performed at four academic institutions. Anonymized MRI/MRCP scans of 32 patients, being evaluated for CP, were collected from one academic institution and reviewed by three abdominal radiologists from other institutions. These radiologists were asked to repeat the review two months later after scans were re-assigned a different case number.

Results: Intra-observer agreement for Cambridge category varied from poor to excellent (kappa 0.33, 0.59, 0.81; concordance 47%, 69%, 84%). When individual imaging findings were analyzed, intra-observer agreement was poor to good for pancreatic atrophy (kappa 0.33, 0.66, 0.67; concordance 44%, 53%, 66%), moderate to excellent for pancreatic duct (PD) caliber (kappa 0.51, 0.65, 0.85; concordance 44%, 69%, 91%) and moderate to excellent for PD irregularity (kappa 0.45, 0.72, 0.89, concordance 66%, 69%, 89%). Inter-observer for Cambridge category was moderate (kappa=0.52). Inter-observer agreement for individual imaging findings was poor for atrophy (kappa=0.32), PD caliber (kappa=0.23), and PD irregularity (kappa=0.20). Patients were balanced in gender (50% female) with a median age of 50 years (IQR=37–58).

Conclusion: There is mostly moderate, however, very variable intra- and inter-observer agreement for grading of CP using the Cambridge classification. A more robust, less subjective and more quantitative classification system, specifically designed for MRI/MRCP seems necessary. This would allow improved categorization of CP patients for clinical and research purposes.

SS 11.8

MRI and MRCP features of chronic pancreatitis in patients with or without pancreas divisum abnormality and their relationship with patients' age

M.L. Monti, G.A. Zamboni, L. Bertuzzo, R. Pozzi Mucelli, G. Mansueto; Verona/IT

Purpose: To compare the MRI and MRCP features of chronic pancreatitis (CP) in patients with or without pancreas divisum (PD) and to determine their relationship with patient age.

Material and methods: We retrospectively reviewed 175 consecutive patients (mean age 52 years) with symptomatic CP who underwent MRI and MRCP. 86 had CP associated with pancreas divisum and 89 had CP without PD (biliary, alcoholic, post-inflammatory, genetic, idiopathic). Both groups of patients were stratified by age: <40 years (26 PD; 33 non-PD), 41–60 years (27 PD; 28 non-PD), >60 years (33 PD; 32 non-PD). Two readers in consensus evaluated the scans for: morphological changes, signal intensity abnormalities, pancreatic ducts changes, disease distribution. All MRI features were compared across age groups using Chi-square tests.

Results: The pancreatic parenchyma was significantly more often T1-hypointense in non-PD than in PD patients (p<0,0001). The degree of parenchymal thinning and irregularity of parenchymal margins was significantly higher in non-PD patients in the groups aged <40 and 41–60 (p<0.0001) while no difference was observed between PD and non-PD patients aged >60 (p=ns). The main pancreatic duct (MPD) was significantly more often dilated in non-PD patients, in all age groups (p=0.0031). Filling defects were more common in non-PD patients (p<0.0007). A significant association was found between parenchymal T1-hypointensity, MPD dilation and filling defects and increasing age in non-PD patients compared to PD patients in all age groups (p<0.001).

Conclusion: Patients with PD show less severe morphological alterations than patients affected by other forms of chronic pancreatitis; these morphological alterations are significantly associated with increasing age.

SS 11.9

Value of MRCP for the detection of intraductal papillary mucinous neoplasm of the pancreas

V. Grossarth, J. Boddenberg, N. Ziayee, F. Verfürth, T. Lauenstein; Düsseldorf/DE

Purpose: To assess the diagnostic value of MRCP for the detection of intraductal papillary neoplasm (IPMN) and to compare the results with endoscopic retrograde cholangiopancreatography (ERCP), endosonography and histopathology as the standard of reference.

Material and methods: In this retrospective study, 98 patients with suspected IPMN were analyzed. All subjects underwent an MRI examination on a 1.5T scanner (Magnetom Avanto, Siemens) including 3D MRCP sequences. Two radiologists evaluated MRI data in a consensus mode regarding the presence of main duct (MD) or side branch (SB) IMPN. ERCP, endosonography and histopathology were performed within two weeks of MRI and served as a standard of reference.

Results: Presence of IMPN was revealed in 80 of 98 patients. Overall sensitivity and specificity of MRCP amounted to 97% and 62%, respectively. While sensitivity for the depiction of SB IPMN was as high as 97%, only 77% of MD IPMN was correctly identified by MRCP.

Conclusion: MRCP is an accurate tool for the detection of IPMN in general. However, the diagnosis of MD IPMN should be verified in a clinical setting by further diagnostic tools since therapeutic options strongly depend on the correct diagnosis. The only moderate specificity of MRCP may be related to the misdiagnosis of IPMN as other cystic pancreatic lesions.

SS 11.10

MRI follow-up of intraductal papillary mucinous neoplasia: can we use a non-gadolinium-enhanced MRI protocol?

L. Bertuzzo[1], G.A. Zamboni[2], C. Fabris[2], R. Pozzi Mucelli[2], G. Mansueto[2]; [1]Santorso-VI/IT, [2]Verona/IT

Purpose: To assess whether non-contrast MRI can be safely used to follow up patients with intraductal papillary mucinous neoplasia (IPMN).

Material and methods: Institutional review board approval was waived for this retrospective study. We evaluated 138 patients (48M, 90F, average age 64.5 years) with an initial diagnosis of IPMN without signs of malignancy (128 branch-duct IPMN, 10 combined IPMN). All patients underwent at least two consecutive MRI/MRCP with gadolinium in our center with an average follow-up of 12 months. For each patient, one reader evaluated, in separate sessions, in the non-contrast and post-contrast scans: cyst size, walls/septa thickening, mural nodules, main pancreatic duct (MPD) dilation and contrast enhancement.

Results: We detected 376 cysts with a mean size of 10.9mm (5-29mm). Patients had a median of 2 cysts each (range 1-20; mean 2.7). The MPD was dilated in 22 patients, with a mean caliber of 4.9mm (4-9mm). In the first MRI available, in the non-contrast scans, 356 (94.7%) lesions did not show suspicious signs. We detected walls/septa thickening in 4 cysts and endoluminal defects in 16: 15 were classified as debris because of their dependent position, 1 as mural nodule. After contrast administration, none of these showed enhancement. At the next available follow-up MRI, in the non-contrast scans, 360 (95,7%) lesions did not show any changes, 11 (3%) showed a slight increase in size and 5 (1,3%) showed signs of progression. This was confirmed in the post-contrast scans.

Conclusion: At follow-up, non-contrast MRI would have been enough to exclude signs of malignant evolution in 98.7% cysts and 96.4% patients.

11:00 - 12:30 **The Liffey A**

Scientific Session SS 12
CT colonography and colonic imaging

SS 12.1
Performance and evaluation in CTC screening
A.E. Obaro[1], A. Plumb[2], R. Baldwin-Cleland[1], C. Ugarte-Cano[1], S. Halligan[2], D. Burling[1]; [1]Harrow/UK, [2]London/UK

Purpose: To implement a structured CTC training programme with individualized feedback and assess radiologist attitudes to the programme and CTC quality metrics.
Material and methods: CTC reporting radiologists were randomised to either an intervention group (received one-day, 1:1 CTC training and feedback on test performance) or a control group (no training or feedback). Both groups took four CTC assessments to assess detection of colorectal cancer (CRC) and polyps >5mm. Tests were administered at baseline, 1 month after workshop, 6 months and 12 months. CTC workload and views on CTC quality metrics were obtained via questionnaires.
Results: 97 radiologists have been recruited and have a wide range of CTC reporting experience, from less than 50 cases (2 of 97, 2%) to over 3000 (10 of 97, 10%). Most radiologists would find knowledge of their polyp detection rate valuable or very valuable (92 of 97, 95%). 51 radiologists are randomised to the intervention group. Of these, 28 have taken baseline test and attended the workshop. 71% (20 of 28) found the baseline test difficult, and all either agreed (9 of 28, 32%) or strongly agreed (19 of 28, 68%) that the workshop provided useful feedback regarding their baseline test performance as well as additional learning opportunities (21 of 28, 75%, strongly agreed). 96% (27 of 28) felt motivated to independently improve their CTC performance.
Conclusion: Early results demonstrate that a 1:1 CTC training workshop is well received and motivates radiologists to improve their practice. Radiologists would find knowledge of their validated polyp detection rate very valuable.

SS 12.2
Patient anxiety prior to a first CT examination to investigate abdominal malignancy: is CTC different from standard abdominal CT?
D.J.M. Tolan[1], C. Roe[2], C.G.D. Clarke[2]; [1]Harrogate/UK, [2]Leeds/UK

Purpose: This study evaluates patients undergoing CT for the first time and whether patients undergoing CTC have different levels of anxiety than those having standard CT of the abdomen and pelvis (CTAP) when performed as a search for cancer.
Material and methods: Adult patients referred for either CTC or CTAP (single, dual or triple phase) were eligible for this pilot study. 60 consecutive eligible patients were recruited (30 in each group). Participating patients completed the state–trait anxiety inventory (STAI) questionnaire in the department prior to CT scan. The study was granted health research authority ethics approval.
Results: Patients were recruited between March and October 2017. The CTC group was older (CTC mean 77.7, range 63-90 vs. CTAP mean 56.6, range 25-81, p=<.00001) and had more females (CTC n=23/30; 76.6% vs CTAP n=13/30; 43.3%, p=0.008). However, there was no significant difference in the baseline 'T-anxiety' measure (mean CTC 36.3 vs CTAP 34.6; p=0.42). The immediate pre-scan 'S-anxiety' was significantly higher for CTC (mean CTC 42.73 vs CTAP 33.73; p=0.00614). Patients having CTC have significantly higher anxiety levels before the scan from baseline levels (CTC mean T-anxiety 36.3, S-anxiety 42.73, p=0.004296).
Conclusion: Patients experience significant anxiety prior to CTC over those attending for CTAP when investigating cancer. Further work is required to identify the impact of anxiety on patient perception of care and effective approaches for managing patient anxiety in those having CTC.

SS 12.3
CTC in patients undergoing surgical management for deeply infiltrating endometriosis
S. Liddy, E. O'Dwyer, R. Sarkar, A. O'Neill, J. Feeney; Dublin/IE

Purpose: To determine the value of CTC in predicting the need for bowel resection and stoma formation in patients undergoing surgical management for deeply infiltrating endometriosis.
Material and methods: A retrospective review of all patients who underwent surgical management of deeply infiltrating endometriosis at a tertiary referral centre over a 12-month period. CT colongraphy was correlated with intraoperative findings. Data recorded included patient demographics, medical history, sites of disease involvement, the plane of contact between the bowel and the surrounding organs and/or endometrial deposits, the presence of luminal narrowing and the surgical procedure undertaken. A per-patient and per-lesion analysis was performed using the Student's t test, chi-square test and one-way analysis of variance.
Results: Eighteen patients with a total of 25 sites of bowel involvement underwent surgery in the 12-month period. The mean age was 39. Sites of bowel involvement included rectal (13/25), rectosigmoid (3/25), sigmoid (7/25) and caecal (2/25). The mean plane of contact was 1.9 cm. Luminal narrowing was present at 8/25 sites of bowel involvement. A longer plane of contact was associated with a need for bowel resection (2.6 vs 1.7 cm, p=0.04). Factors not associated with bowel resection included patient age (38 vs 39, p=0.44), multifocal disease, site of bowel involvement and the presence of luminal narrowing (2/7 vs 8/18, p=0.8).
Conclusion: A longer segment of bowel involvement may be predictive of a need for bowel resection and stoma formation in patients undergoing surgical management for deeply infiltrating endometriosis.

SS 12.4
MR-enema (MR-e) and CTC in the diagnosis of recto-sigmoidal endometriosis: a preliminary comparative evaluation
E. Biscaldi, F. Barra, C. Scala, V. Vellone, S. Ferrero; Genova/IT

Purpose: To compare the accuracy of MR-e and CTC in detecting and evaluating recto-sigmoid endometriosis.
Material and methods: We collected the patients following these inclusion criteria: reproductive age, suspicion of deep pelvic endometriosis on the basis of symptoms and vaginal examination, presence of gastrointestinal symptoms, no previous radiological imaging. Patients underwent laparoscopy within 3 months from the diagnostic procedures. Radiological findings were compared with surgery and histology.
Results: Out of 85 women included, 52 had rectosigmoid endometriotic nodules (61.2%). The sensitivity, specificity, positive predictive value, negative predictive value, likelihood ratio positive and likelihood ratio negative of MR-e and CTC in the diagnosis of recto-sigmoid endometriosis were 88.46% (95%C.I., 76.56%-95.65%), 90.0% (73.47%-97.89%), 93.88% (83.92%-97.83%), 81.82% (67.75%-90.60%), 8.85 (3.01-26.0), 0.13 (0.06-0.27) and 92.31% (81.46%-97.86%), 93.75% (79.19%-99.23%), 96.0% (86.22%-98.93%), 88.24% (74.44%-95.08%), 14.77 (3.85-56.64), 0.08 (0.03-0.21), respectively. No significant difference was appreciated in the accuracy of the two techniques in the diagnosis of rectosigmoid endometriosis (p = 0.607; McNemar's test). CTC was more effective in evaluating the distance between the nodule and the anal verge in all cases, it was less precise in evaluating the depth of the lesions in the intestinal wall. CTC was more panoramic in whole colon evaluation.
Conclusion: CTC is competitive with MR-e in this diagnosis. CT software also allows measurement of the distance of the nodule from the anal verge. CTC is probably still limited in evaluating the depth of penetration of the nodule in the intestinal wall, due to the lack of contrast resolution. In the future, CTC may be implemented with iodinated medium injection to boost its diagnostic yield.

SS 12.5

Incidence of clinically significant perforation at low-dose non-contrast CT and its value prior to same day CTC following incomplete colonoscopy

A. O'Shea, M. Morrin, M. Lee, E. Thornton, T.É. Murray; Dublin/IE

Purpose: Routine low-dose non-contrast CT of the abdomen and pelvis has been recommended prior to same-day completion CTC to assess for occult perforation at preceding incomplete colonoscopy, before insufflation at CTC. The aim of our study is to examine the incidence of clinically significant perforation at low-dose CT. We also examine the benefits of low-dose pre-scan in assessing adequacy of bowel preparation and identifying any other relevant contraindications to CTC.

Material and methods: We conducted a retrospective review of all low-dose non-contrast CTs performed following failed colonoscopies over a one-year period (n=135). We also assessed the adequacy of bowel preparation on a scale of 1-5, in order of increasingly adequate preparation. Incidentally noted contraindications to CTC were also recorded.

Results: One perforation (which was extraperitoneal) was identified on low-dose CTC. However, 6 patients were found to have contraindications to CTC including acute diverticulitis and acute colitis. Overall, the bowel preparation was felt to be adequate (≥ 3) in 96% percent of patients. 5 patients (0.04%) had their CTC postponed due to poor bowel preparation.

Conclusion: While the incidence of perforation identified at low-dose pre-scan is low, there may be additional benefits to a low-dose non-contrast CT prior to insufflation including assessment of adequacy of bowel preparation and identifying other contraindications to same-day CTC.

SS 12.6

7 T MRI for fibrosis evaluation in a radiation-induced murine model of colitis

M. Zappa[1], S. Doblas[2], D. Cazals-Hatem[1], F. Milliat[3], P. Garteiser[1], M. David[1], V. Vilgrain[1], B. Van Beers[1], E. Ogier-Denis[2]; [1]Clichy/FR, [2]Paris/FR, [3]Fontenay-Aux Roses/FR

Purpose: Crohn's disease transmural bowel wall inflammation can lead to fibrosis causing luminal narrowing and fistula which are the main indications to surgery. The aim of our study was to evaluate MRI to distinguish submucosal from transmural fibrosis using an original murine model of radiation-induced colitis.

Material and methods: Colitis was induced with localized single-dose radiation (27 Gy). We included an inflammation group of 24 rats with pathologic features of severe acute inflammation associated with minimal submucosal fibrosis and a mixed group of 39 rats with pathological features of severe inflammation associated with transmural fibrosis, obtained two and twelve weeks after irradiation, respectively. Fat-suppressed T2- and T1-weighted, diffusion-weighted, magnetization transfer and perfusion using arterial spin labelling (ASL) technique 7 T MRI was performed.

Results: MRI showed significant differences between inflammation and mixed groups in normalized to muscle signal intensity on T2-weighted images (4.2 vs 3.1, P< 0.0001) and T1-weighted images (1.4 vs 1.3, P=0.0003), ADC (2.17×10^{-3} vs 1.69×10^{-3} mm^2/s, P<0.0001), magnetization transfer ratio (35 vs 42%, P<0.0001) and perfusion (60 vs 38 mL/min/100g, P=0.0009). Monoparametric analysis with the best area under the curve (AUC) to differentiate the two groups included T2-weighted signal intensity, apparent diffusion coefficient (ADC) and magnetization transfer ratio. The combination with the best global predictive value (94%) included all parameters but T1-weighted parameter (AUC 0.94).

Conclusion: MR multiparametric analysis was able to distinguish transmural from submucosal fibrosis in our radiation-induced model. This model could be used to evaluate antifibrotic treatments currently under development.

SS 12.7

MRI parameters for prediction of sigmoid carcinoma in patients with background of diverticular disease: a retrospective study

E. Savoldi[1], A. Higginson[2], R. Beable[2], C. Ball[1]; [1]Cosham/UK, [2]Portsmouth/UK

Purpose: To retrospectively identify morphologic-specific findings at MRI in the differentiation of mass-like diverticular disease from sigmoid carcinoma, in patients with background of diverticular disease and sigmoid stricture at CT.

Material and methods: The cohort consisted of 37 patients with thickening/stricture of the sigmoid colon at CT, representing diverticular disease (n = 32) or sigmoid carcinoma (n = 5). MRI studies were scored according to the presence or absence of potential discriminators. Patients underwent CT, T2-weighted and diffusion-weighted MRI. Sensitivity, specificity, positive predictive value (PPV), negative predictive value (NPV), and accuracy were calculated and MRI were retrospectively reviewed using three different parameters: diffusion restriction, loss of wall stratification and mucosal lesion.

Results: MRI showed high NPV (93%) and specificity (96%) and PPV and sensitivity of 75% and 60%, respectively, with an overall accuracy of 91%. Diffusion restriction had a sensitivity, specificity, and PPV of 100%, 96% and 83%, respectively, for the diagnosis of cancer. Loss of wall stratification had a sensitivity, specificity, and PPV of 60%, 96%, and 75%, respectively, while the presence of mucosal lesion had a sensitivity, specificity, and PPV of 80%, 100%, and 100%. The analysis of the three parameters may change the MRI accuracy at 97%.

Conclusion: Diverticular disease is best differentiated from carcinoma by the analysis of three parameters: preservation of the wall layering, the absence of restricted diffusion and the absence of mucosal mass with low T2 signal. MRI improves the differentiation between sigmoid cancer and diverticulitis. These encouraging results need to be confirmed in a larger study.

SS 12.8

Does the abdominal deep subcutaneous fat distribution influence complication rate and mortality after elective surgery for colorectal cancer?

E. Frostberg, Y. Manhoopi, M.R. Pedersen, H. Rahr, S.R. Rafaelsen; Vejle/DK

Purpose: Intraabdominal visceral adipose tissue is associated with high risk of developing arteriosclerosis, and cardiovascular co-morbidity is associated with high complication and mortality rates after colorectal cancer surgery. According to the new literature, the deep subcutaneous adipose fat (dSAT) is like the intraabdominal visceral adipose tissue. The aim of this study was to evaluate if the dSAT, measured by a regular CT scan, may be used as a predictor for complications and mortality after colorectal cancer surgery.

Material and methods: Preoperative CT scans of 344 patients who underwent colorectal cancer surgery in the years 2010 and 2011 were examined retrospectively. Measurements of the dSAT were collected. Clinical data regarding patient characteristics, postoperative surgical and medical complications and survival data were retrieved. The radiological measurements were used as explanatory variables in fitted logistic and Cox regression models.

Results: 325 patients were eligible for the study. The dSAT had a significant relationship with body mass index, and body mass index had a significant association with surgical complications (OR: 1.09, p=0.01). Surgical complication had a strong impact on medical complication (OR:5.9, p=0.0001). Union for international cancer control (UICC) stage, age and co-morbidity had a significant association with long-time survival. The radiological measurement of the dSAT did not have an impact on surgical or medical complications, nor did it have an association with long-time survival.

Conclusion: Measuring the thickness of the dSAT in a preoperative setting does not have any impact on postoperative surgical or medical complications nor long-time survival in colorectal cancer patients treated with elective surgery.

SS 12.9

Model-based iterative reconstruction in ultralow-dose CTC: diagnostic performance and influence on computer-assisted diagnosis

S. Barbieri, G. De Paoli Barbato, E. Raimondi, M. Bassi, A. Deledda, M. Tilli, R. Rizzati, M. Giganti, G. Benea; Ferrara/IT

Purpose: To compare the perfomance of standard dose (SD) and ultralow dose (ULD) in CTC using hybrid-iterative reconstruction (HIR) and model-based iterative reconstruction (MBIR), and to assess the effect of different reconstruction algorithms on computer-aided diagnosis (CAD).

Material and methods: We evaluated 50 patients (31 males, 19 females, mean age 69.7) through CTC with SD (120kV, 50mAs 4.6±1.3mSv) and ULD (120kV, 10mAs, 0.95±0.2mSv); images were reconstructed with both HIR and MBIR. A commercial CAD system was applied complementary to all reconstructions. Two independent radiologists reviewed all obtained images separately and in random order to avoid recall biases. The two readers recorded colonic findings (polyps/cancer), extracolonic findings and CAD detections. Polyps (p) were classified by size (p<5mm, 5≤p<10mm, p≥10mm), shape (flat, sessile, pedunculated) and location (rectum, sigmoid, descending, transverse, ascending, cecum). Only relevant extracolonic findings (C-RADS: E4) were recorded. CAD results were reported and significant findings were selected.

Results: 9 polyps were found in 8 patients from: six <5mm, two ≥5_<10mm and one ≥10mm; 8 were pedunculated and 1 flat 2 were in cecum, 3 ascending, 2 transverse, 1 descending, 1 sigmoid tract; colonic-finding records were superimposable for both radiologist with SD reconstructions and with ULD MBIR reconstruction; 11 extracolonic findings E4 were recorded with SD, 2 with ULD (AAA, hiatal hernia). Colonic findings were confirmed by optical colonoscopy.

Conclusion: CTC with ULD and MBIR reconstructions showed promising results in terms of diagnostic performance and inter-reader reproducibility for intra-colonic findings. CAD detection of significant findings was unaffected by acquisition protocol or reconstruction algorithm.

SS 12.10

Dynamic MR of the pelvic floor: impact of the pubococcygeal line on the grading of pelvic floor descent

S. Picchia[1], M. Rengo[2], D. Bellini[1], M. Montesano[1], A. Laghi[2]; [1]Latina/IT, [2]Rome/IT

Purpose: To evaluate the impact of three methods for drawing the pubococcygeal line (PCL) on the grading of pelvic floor descent with MR.

Material and methods: Female patients with suspected pelvic floor dysfunction were prospectively included in the study. All exams were acquired on a 1.5 Tesla MR with patient in supine position. Rectum and vagina were filled with 200 ml and 50 ml of ultrasound gel, respectively. A distended bladder was required. The acquisition protocol included turbo spin echo (TSE)-T2-weighted sequences on the three planes for morphological evaluation. A steady-state sequence (True-FISP) in the midsagittal plane was acquired during straining and defecation, acquiring 1 image/sec. The anterior point of all PCL was the pubic symphysis, while posterior points were the tip of the coccyx (PCLtip), the sacrococcygeal joint (PCLsc) and the last coccygeal joint (PCLcc). The grade of pelvic floor descent was measured with the M-line according to the HMO system, traced perpendicularly from the PCL to the posterior end of the H-line. Measurements of M-line were compared as differences of absolute measures and differences of grading.

Results: The final population consisted of 29 consecutive patients (mean age 56.07yy±10.52). M-line measured using PCL tip was significantly smaller than PCLsc or PCLcc in all measurements. The grading of pelvic floor relaxation, using PCLtip, was underestimated in 13 patients (44%) at rest, in 19 patients (65%) during straining and in 16 patients (55%).

Conclusion: A significant underestimation of the pelvic floor descent was observed when the M-line was measured using the PCLtip as reference. The use of PCLsc or PCLcc should be used to quantify the pelvic floor descent.

11:00 - 12:30 **Liffey Hall 1**

Scientific Session SS 13

Diffuse and chronic liver disease

SS 13.1

Liver imaging findings in adult patients with Fontan circulation

H.K. Yang, H.-J. Jang, R.M. Wald, S.-J. Yoo, T.K. Kim; Toronto, ON/CA

Purpose: To describe liver imaging findings and complications on CT or MRI in adult patients with Fontan circulation and to investigate as to whether hepatic imaging features show correlation with post-Fontan duration, age or serum hepatic function tests.

Material and methods: Our institutional review board approved this retrospective study with waiver of informed consent. Two blinded abdominal radiologists retrospectively reviewed the abdominal CT (n = 21) and MR (n = 16) images of 37 adults (mean age, 30 years; 14 men and 23 women) with Fontan circulation (mean post-Fontan duration, 23 years). Biochemical hepatic function tests within 6 months of CT or MR examinations were used for analysis.

Results: Inhomogeneous, reticulated-mosaic pattern of hepatic parenchymal enhancement, lobulated hepatic contour, blunt margin, and hypertrophy of the left lateral section were seen in 86% (32/37), 96% (34/37), 95% (35/37) and 73% (27/37) of patients, respectively. Among the analyzed 25 arterial hyperenhancing nodules in 16 patients, 2 nodules (8%, 2/25) in 2 patients (13%, 2/16) were hepatocellular carcinomas (HCCs) and the remaining 23 nodules in 14 patients were diagnosed as focal nodular hyperplasia (FNH)-like nodules. The diameter of inferior vena cava showed significant positive correlation with post-Fontan duration, age and laboratory hepatic function test.

Conclusion: Imaging findings of adult patients with decades of Fontan circulation were characterized by reticulated-mosaic pattern of parenchymal enhancement, lobulated contour, blunt margin, and hypertrophy of the left lateral section. Arterial-phase hyperenhancing FNH-like nodules are commonly seen, but HCC can infrequently occur.

SS 13.2

Evaluation of two-point Dixon water-fat separation for gadoxetic acid-enhanced MRI-based estimation of liver function

M. Haimerl, S. Poelsterl, C. Stroszczynski, P. Wiggermann; Regensburg/DE

Purpose: To evaluate the impact of intrahepatic fat on gadoxetic acid (Gd-EOB-DTPA)-enhanced T1 relaxometry for the estimation of liver function using T1-weighted volume-interpolated breath-hold examination (VIBE) sequence with Dixon water-fat separation.

Material and methods: 74 patients underwent Gd-EOB-DTPA-enhanced T1 relaxometry and ^{13}C-methacetin breath test (^{13}C-MBT) for the evaluation of liver function. Prior to ($T1_{pre}$) and 20 minutes after the intravenous administration of Gd-EOB-DTPA ($T1_{post}$), a T1-weighted VIBE sequence with Dixon water-fat separation and multiple flip angles (1°, 7°, and 14°) was used to generate both T1 maps (T1_in) of the in-phase component without fat separation and T1 maps merely based on the water component (T1_W). The reduction rates of T1 relaxation time (rrT1) between pre- and post-contrast images were evaluated for T1_in (rrT1_in) and T1_W (rrT1_W). ^{13}C-MBT values were correlated with $T1_{post}$ and rrT1.

Results: A constant significant decrease of rrT1 with progressive reduction of liver function could be shown for both T1_in ($p < 0.001$) and T1_W ($p < 0.001$). When patients are subdivided into 3 different categories of ^{13}C-MBT readouts, the groups can be significantly differentiated by their rrT1_in and rrT1_W values ($p<0.005$). Simple regression model showed a log-linear correlation of ^{13}C-MBT values with $T1\_in_{post}$ ($r = 0.566$; $p<0.001$), $T1\_W_{post}$ ($r = 0.568$; $p<0.001$), rrT1_in ($r = 0.726$; $p < 0.001$) and rrT1_W ($r = 0.766$; $p<0.001$).

Conclusion: Liver function as determined using ^{13}C-MBT can be estimated from Gd-EOB-DTPA-enhanced MR-relaxometry more accurately when intrahepatic fat is taken into account. Here, T1_W maps are significantly superior to T1_in maps without separation of fat.

SS 13.3

Disodium gadoxetate-enhanced liver MRI in cirrhotic patients: can clinical parameters predict suboptimal hepatobiliary phase enhancement?

S.P. Walker, D. Wilson, H. Ramotar, C.R. Smith, R. Albazaz, M.B. Sheridan, J.A. Guthrie; Leeds/UK

Purpose: The potential added value of disodium gadoxetate (Gd-EOB-DTPA) is its active uptake by hepatocytes to provide a hepatobiliary phase (HBP) aiding detection and characterisation of focal liver lesions. Predicting suboptimal HBP enhancement would be advantageous so as to select a different contrast medium saving expense and room time. This study evaluates the relationship of clinical parameters to HBP enhancement using Gd-EOB-DTPA in cirrhotic patients.

Material and methods: Cirrhotic patients undergoing Gd-EOB-DTPA MRI between January 2016 and December 2016 were retrospectively reviewed. Based on region-of-interest sampling, the liver signal intensity was calculated using the spleen as a reference. The liver spleen contrast ratio (LSCR) was then calculated and compared with basic patient characteristics and laboratory results.

Results: 127 patients were identified with an average HBP time of 19 minutes 31 seconds. Twelve patients were excluded due to incomplete availability of clinical parameters. Multiple logistic regression analysis revealed that bilirubin (p=0.04), albumin (p=0.01), PT (p=0.02) and platelets (p=0.04) were factors predictive of HBP enhancement. These clinical parameters were also significant with a simple logistic regression analysis, except for platelets (p=0.86).

Conclusion: HBP enhancement in cirrhotic patients correlates with a number of clinical biomarkers, the strongest being albumin. Prospective identification of suboptimal HBP enhancement using such biomarkers could avoid the non-beneficial use of Gd-EOB-DTPA in cirrhotic patients thus saving money and resources in favour of alternative contrast medium.

SS 13.4

Assessing liver function: diagnostic efficacy of parenchymal enhancement and liver volume ratio during hepatobiliary phase of gadolinium-ethoxybenzyl-diethylenetriamine pentaacetic acid-enhanced MRI studies

A. Pecorelli, E.B. Orsini, C. Talei Franzesi, S. Famularo, L. Gianotti, D. Ippolito; Monza/IT

Purpose: To assess whether gadolinium-ethoxybenzyl-diethylenetriamine pentaacetic acid (Gd-EOB-DTPA)-enhanced MRI study is useful to determine liver function in comparison to Child-Pugh (CP), model for end-stage liver disease (MELD) and biochemical test.

Material and methods: All Gd-EOB-DTPA-enhanced MRI studies performed, between May 2011 and September 2017, to characterize focal liver lesion were retrospectively reviewed. Patients were divided into study and control group according to the presence/absence of liver cirrhosis. Signal intensity was calculated as the rate of liver-to-muscle ratio on contrast-enhanced T1-GE sequences in portal (SI-POR) and hepatobiliary phase (SI-HEP) and then normalized for liver volume (SI-POR/LV and SI-HEP/LV).

Results: A total of 303 Gd-EOB-DTPA-enhanced MRI studies, performed in 221 consecutive patients, were included. Cirrhosis was present in 191 (63.0%) MRI studies. SI-HEP was significantly lower in cirrhotic than in non-cirrhotic patients (0.55±0.29 vs 0.66±0.40, p=0.004), while no difference was found in SI-POR. SI-HEP progressively decreased from CP-A group to CP-C (0.59±0.28 to 0.25±0.19, p<0.0001) and from MELD≤10 to MELD 19-24 (0.58±0.30 to 0.54±0.49, p=0.773). SI-HEP had a good performance in distinguishing CP-A from CP-B/C patients (AUC=0.75; 95%CI=0.66-0.83). Among biochemical parameters, a moderate correlation was found between SI-HEP and total bilirubin (R=-0.324), GOT (R=-0318) and albumin (R= 0.320). Comparable results were observed when SI-HEP was normalized for liver volume.

Conclusion: SI-HEP of Gd-EOB-DTPA-enhanced MRI studies can be used to effectively evaluate liver function. In clinical practice, this imaging technique could be performed both to correctly characterize liver lesions and to assess the severity of liver disease especially in the perspective of surgical treatment.

SS 13.5

Assessment of liver function in patients with chronic liver diseases using different parameters of gadoxetic acid-enhanced hepatobiliary phase imaging: a comparison study

L.B. Beer, N. Bastati-Huber, S. Pötter-Lang, D.P. Stoyanova, M. Elmer, D. Tamandl, A. Ba-Ssalamah; Vienna/AT

Purpose: To evaluate the correlations between different hepatobiliary phase (HBP) image scores using gadoxetic-acid (GA) uptake and the albumin-bilirubin (ALBI) grading system, in patients with chronic liver disease.

Material and methods: This retrospective institutional review board approved study included 220 patients (139 male, 81 female, mean age 54.9 ±14.3 years) with chronic liver disease who had undergone GA-enhanced MRI of the liver between 2011 and 2015. Relative liver enhancement (RLE), hepatic uptake index (HUI), contrast uptake index (CUI), and liver-to-spleen contrast ratio (LSC) were calculated using unenhanced and GA-enhanced HPB images, 20 minutes after administration of the contrast material. ALBI grading was used as a clinical score for correlation with disease severity. Correlation coefficients between different factors were calculated using Pearson's correlation coefficient.

Results: The highest correlation coefficients were observed between RLE-CEI (R=0.904, p<0.001), RLE-LSC (R = 0.782, p<0.001), and CUI–LSC (R=0.787, p<0.001). Correlation strength between HUI and RLE, CEI, and LSC was (R=0.564, R = 0.535, R = 0.434, respectively, p<0.001 for all). R values between the ALBI score and RLE, CUI, HUI, and LSC were -0.481. -0.442, -0.335, -0.416, respectively, indicating a moderate correlation.

Conclusion: A strong correlation between different MR-derived parameters using HBP imaging and the ALBI score, except for the HUI, was observed. These data indicate that, except for volume-based scores, such as the HUI, other MR-derived parameters are interchangeable for the evaluation of diffuse liver disease.

SS 13.6

Comparison of hepatic R2* and fat fraction obtained by pixelwise map methods to MRQuantif software results

A. Paisant, C. Chargeboeuf, J. Jouan, H. Saint-Jalmes, E. Bardou-Jacquet, Y. Gandon; Rennes/FR

Purpose: The aim was to compare the results of MRQuantif freeware using a generic 2D multi-echo gradient echo sequence (ME-GRE), previously validated against biopsy, to constructor sequences providing R2* and fat fraction (FF) maps.

Material and methods: After institutional review board (IRB), also known as an independent ethics committee (IEC), ethical review board (ERB), or researchIRB approval and written informed consent, on a 3.5-year period, we explored 619 patients for hepatic iron or fat quantification. For each we obtained a generic 2D ME-GRE with TE multiple of 1.2 ms and a constructor 3D ME-GRE providing a R2* or T2* and a FF maps, either Ideal-IQ (n=113) on a 1.5T MR450 (General Electric), 3D-Vibe-Dixon WIP (n=196) on a 3T Verio (Siemens) or mDixon-Quant (n=310) on a 3T Ingenia (Philips). We then compared (correlation and Bland-Altman) R2* and FF determined by MRQuantif to the value of the two maps, from the mean of 3 region of interests (ROI)s placed at the same location on the right liver. Discordant data were specifically analyzed by an expert.

Results: After exclusion of map reconstruction miscalculation errors (FF>50%, n=6), R2* and FF correlations of MRQuantif to 1.5T Ideal-IQ were r^2=0.6 and 0.6, to 3T Vibe-Dixon were r^2=0.76 and 0.31 or to 3T mDixon-Quant were r^2=0.94 and 0.87, respectively. Correlations increased greatly when excluding high liver iron overload with still clinically significant map results errors. 3T R2* maps were not accurate above 200 µmol of iron/g liver.

Conclusion: R2* and FF maps are less robust than the ROI analysis proposed by MRQuantif.org freeware.

SS 13.7

MRI hepatic fat quantification using various methods, at 1.5 and 3T, in comparison to quantitative histomorphometry

A. Paisant[1], J. Jouan[1], E. Bardou-Jacquet[1], E. Bannier[1], J. Boursier[2], C. Aubé[2], Y. Gandon[1]; [1]Rennes/FR, [2]Angers/FR

Purpose: To compare the results of different methods of quantification by MRI of the hepatic fat fraction (FF), at 1.5T and 3T, with the histological, semi-quantitative and especially quantitative measurement of steatosis.

Material and methods: 169 patients were prospectively included in 2 centers, one using a 1.5T Signa (GEMS), the other using a 3T Verio (Siemens) MRI. A 2D gradient echo multi-echo sequence (2D-ME-GRE), designed for hepatic fat and iron assessment, was used to quantify FF. MRquantif software calculated Dixon method (dual-echo, triple-echo or with T2* correction) and „complex" method taking into account a 3-peak spectral modeling of the fat. All patients had a liver biopsy with semi-quantitative assessment and a quantitative measurement of FF by determining the percentage of surface of the fat vacuoles. Analyses used were Spearman test and Bland-Altman comparison.

Results: MRI and quantitative FF were well correlated: Dixon dual-echo (ρs=0.95, p<0.001 at 1.5T; ρs=0.87, p<0.001 at 3T), triple-echo (ρs=0.95, p<0.001 at 1.5T; ρs=0.93, p<0.001 at 3T), corrected by T2* (ρs=0.94, p<0.001 at 1.5T ; ρs=0.94, p<0.001 at 3T), complex (ρs=0.94, p<0.001 at 1.5T; ρs=0.94, p<0.001 at 3T). The biases calculated by the Bland-Altman method were closed to 0. Correlation of semi-quantitative histological assessment to MRI FF and also to quantitative histological FF was weaker.

Conclusion: Using a 2D-ME-GRE sequence, MRQuantif freeware provides a good evaluation of FF compared to a really quantitative gold standard at 1.5T and 3T. MRI FF assessment is a better gold standard than the semi-quantitative histological grading.

SS 13.8

Liver MR relaxometry: basic rules for clinical application and reference values when analyzing T1 and T2* maps

V.C. Obmann, N. Mertineit, C. Marx, A. Berzigotti, J. Heverhagen, A. Christe, A.T. Huber; Bern/CH

Purpose: To determine T1 mapping reference values of the liver at 3T with respect of hepatic fat, fibrosis and iron content, as well as susceptibility-induced liver effects from the adjacent lung parenchyma.

Material and methods: 143 patients without solid liver lesions >1cm on contrast-enhanced abdominal CT scans underwent multiparametric MR imaging on a Siemens Verio 3T magnet including T1-/T2*-mapping, proton density fat fraction (PDFF) quantification and MR elastography. The population was divided into negative patients without fibrosis (shear modulus <2.8 kPa) and steatosis (PDFF<10%) and positive patients with fibrosis and/or steatosis. T1 values were compared between liver segments and groups. Multivariate analysis was used to statistically correct T1 for T2*. Mann-Whitney U test between segments and groups was performed.

Results: In negative patients, T2*-time was a significant confounder for T1-time (p<1^15), while age and sex (p=0.722, 0.687) were not. T1 and T2 relaxation times were shorter in lung-adjacent liver segments as compared with non-lung-adjacent segments (mean of differences 33 ms, p<0.001 for T1). Normal T1 in reference patients' non-lung-adjacent segments was 780±83 ms. In positive patients with steatosis and fibrosis, T1 was significantly higher (p=0.011 or less). When correcting T1 for T2*, this discrimination between positive and negative patients could be improved (p<0.001 for all comparisons).

Conclusion: When analyzing T1 maps in the liver at 3T, non-lung-adjacent segments should be measured due to susceptibility effects of the adjacent lung. Liver iron content as indicated by T2*-shortening is a major confounder of T1 time.

SS 13.9

Liver surface nodularity quantification from routine CT images for the detection of clinically significant portal hypertension

R. Sartoris[1], P.-E. Rautou[1], L. Elkrief[2], V. Vilgrain[1], M. Ronot[1]; [1]Clichy/FR, [2]Geneva/CH

Purpose: To determine whether quantification of liver surface nodularity (LSN), a computer-based marker derived from routine CT images, can estimate the presence of clinically significant portal hypertension (CSPH) in patients with cirrhosis, and to compare LSN with other existing non-invasive tests.

Material and methods: This retrospective study included 189 patients with cirrhosis who underwent hepatic venous pressure gradient (HVPG) and abdominal CT, including 102 (54%) with CSPH. LSN was measured on CT and other available non-invasive tests were performed, namely liver and spleen volumes, liver-to-spleen volume ratio, platelet/spleen diameter, Iranmanesh score, aspartate aminotransferase/platelet ratio index (APRI), Fibrosis-4 (FIB-4). Technical success rate and measurement time were calculated. Area under receiver operating characteristic (AUROC) and DeLong test were used. Results were validated in an independent external cohort of 78 patients with biopsy-proven cirrhosis.

Results: Technical success rate of LSN was 93%; measurement time was 113±36.3 seconds. LSN quantification was correlated to the HVPG (r=0.75; p<.001). Patients with CSPH had a significantly higher LSN score than those without (3.22±0.59 vs. 2.44±0.34; p<.001). A cut-off value of 2.76 had a positive predictive value of 88% for CSPH. AUROC of LSN for the estimation of CSPH was 0.88. This was significantly higher than that of other available non-invasive tests (all p<.001). Cut-off value 2.76 was validated in the independent external cohort.

Conclusion: Non-invasive CT-based LSN quantification rapidly and accurately detects CSPH. This strategy could be particularly useful to evaluate portal hypertension before liver surgery.

SS 13.10

Modern MRI in the diagnostic workup of cystic fibrosis-associated liver disease

S. Pötter-Lang, K. Staufer, P. Baltzer, D. Tamandl, N. Bastati-Huber, D. Muin, L. Kazemi-Shirazi, A. Ba-Ssalamah; Vienna/AT

Purpose: To identify independent imaging features and establish a diagnostic algorithm for early diagnosis of cystic fibrosis-associated liver disease (CFLD) in CF patients as compared with a control group (CG) on gadoxetic acid-enhanced MRI.

Material and methods: A total of 90 adult patients were enrolled, 50 with CF and 40 of the CG. The CF group was divided into two subgroups, the retrospective or test subgroup (n = 33) and the prospective or validation subgroup (n = 17). The CG (patients with normal liver enzymes, but no more than benign focal liver lesions) was divided also accordingly (27:13). MRI variables including quantitative and qualitative parameters were used to distinguish those with CFLD from the CG using the clinical criteria by Debray et al. Fifteen qualitative single-lesion CF descriptors were defined. Two readers independently evaluated the images. Univariate statistical analysis was performed to obtain the significant imaging features that differentiate CF patients from the CG. Subsequently, a multivariate classification analysis using the chi-squared automatic interaction detector (CHAID) methodology was performed to identify the most important descriptors. Diagnostic performance was assessed by receiver-operating characteristic (ROC) analysis.

Results: Three independent imaging descriptors distinguished CFLD from CG: a) the presence of altered gallbladder morphology (GBAM); b) periportal tracking (PPT) and c) periportal fat deposition (PPFD). Prospective validation of the classification algorithm demonstrated a sensitivity of 94.1% and specificity of 84.6% for discriminating CFLD from the control cohort.

Conclusion: We identified 3 independent imaging features that could potentially diagnose early-stage CFLD on unenhanced MRI.

11:00 - 12:30 **Wicklow Hall 2A**

Scientific Session SS 14

Technical advances in abdominal imaging

SS 14.1

withdrawn by the authors

SS 14.2

Diagnostic accuracy of whole body 18F-fluorodeoxyglucose positron emission tomography-MR in HCCs: comparison of local and metastatic staging with chest-abdomen-pelvic CT and liver MRI

M. Vermersch[1], B. Emsen[1], S. Mulé[1], J. Chalaye[1], A. Monnet[2], E. Hérin[1], F. Pigneur[1], L. Baranes[1], H. Regnault[1], G. Amaddeo[1], A. Laurent[1], A. Rahmouni[1], E. Itti[1], A. Luciani[1]; [1]Creteil/FR, [2]Saint Denis/FR

Purpose: To assess the diagnostic accuracy and therapeutic management impact of whole body 18F-fluorodeoxyglucose positron emission tomography-MRI (WB-18FDG-PET-MR) for local and whole body staging of HCCs.

Material and methods: 36 consecutive patients followed for HCC were included in this retrospective study. All patients underwent WB-18FDG-PET-MR (Biograph mMR) which included whole body sequences (simultaneous multislice with blipped Controlled Aliasing in Parallel Imaging Results in Higher Acceleration sequence design (SMS diffusion-weighted imaging (DWI)), unenhanced and post contrast 3DT1 Dixon VIBE) simultaneously acquired with PET data (25 minutes acquisition overall), and dedicated liver sequences (SMS intravoxel incoherent motion (IVIM) DWI, T2, multiphasic 3DT1 VIBE). The accuracy of WB-18FDG-PET-MR for HCC detection, local—biliary, vascular involvement—regional N staging, and distant staging was compared to that observed with chest-abdomen-pelvis (CAP) CT and liver MRI, with pathology, follow-up or consensus interpretation of all available data as the reference standard.

Results: Overall, 55 HCC and 7 metastatic sites were documented in 33 patients. Sensitivity, specificity, positive predictive value (PPV) and negative predictive value (NPV) of WB-18FDG-PET-MR were 100% for liver HCC detection, local and regional staging. The sensitivity of WB-18FDG-PET-MR was 100%, specificity 97%, PPV 83%, NPV 100% and accuracy 97% for detection of metastatic patients. WB-18FDG-PET-MR led to changes in therapeutic management in 14% of patients (5/36), 2 by detection of additional HCC and 3 by detection of additional metastatic sites.

Conclusion: One-stop-shop WB-18FDG-PET-MR improves local and distant HCC tumor staging compared to CAP CT and liver MRI performed separately, with significant impact on patient treatment management.

SS 14.3

withdrawn by the authors

SS 14.4

Virtual unenhanced imaging of the liver derived from 160mm rapid-switching dual-energy CT: comparison of image quality and solid liver lesion conspicuity with true unenhanced images

M. Lacroix[1], S. Mulé[1], E. Hérin[1], F. Pigneur[1], P. Richard[2], B. Zegai[1], L. Baranes[1], M. Djabbari[1], F. Brunetti[1], N. De Angelis[1], A. Laurent[1], A. Rahmouni[1], A. Luciani[1]; [1]Creteil/FR, [2]Buc/FR

Purpose: To compare virtual unenhanced images derived from arterial (VUEart) and portal-venous phases (VUEport) with native unenhanced (NU) acquisitions in patients with suspected solid liver tumors (SLT) imaged on a rapid-switching single-source 160mm dual-energy CT (rsDECT).

Material and methods: 73 patients with 52 SLT who underwent a multiphasic abdominal rsDECT were included in this institutional review board approved retrospective study. Both NU (120kVp, 40mm, Pitch 1.375, rotation 0.7s, ASIRv 40%), VUEart and VUE port (80 kVp-140 kVp; 80mm collimation, pitch 0.992, rotation time 0.8s, ASIRv 50%) were reconstructed from raw data. Both qualitative detectability of SLT on a 4-point scale and quantitative analyses of liver and erector-spinae muscles mean+SD densities, and lesion-to-liver contrast-to-noise-ratio (CNR) were compared on NU, VUEart and VUEport (Kruskal–Wallis, Dunn, Kolmogorov–Smirnov).

Results: The mean liver density was significantly lower on VUEart and VUEport than on NU (respectively, 56.7±6.7 and 57.9±6 vs 59.6±7.5; $p<0.01$), but was similar on VUEart and VUEport ($p=0.09$). The mean muscle density was significantly lower on VUEart and VUEport than on NU (respectively, 47.1±5.4 and 48.4±5.3 vs 51.8±5.2; $p<0.0001$), but was similar on VUEart and VUEport ($p=0.5$). The lesion-to-liver CNR was significantly higher on VUEart and VUEport than on NU (respectively, 1.7±1 and 1.6±1.1 vs 0.9±0.6; $p<0.001$), but was similar on VUEart and VUEport ($p>0.9$). Lesion conspicuity was significantly higher on VUEport images than on NU ($p=0.004$).

Conclusion: rsDECT-derived VUE improves lesion-to-liver CNR and image quality and could replace true unenhanced acquisitions in this oncology setting.

SS 14.5

Accuracy of multi-parametric MRI in the diagnosis and grading of intestinal acute graft-versus-host disease after allogenic bone marrow transplantation

D. Vitale, F. Maccioni, V. Buonocore, D. Bencardino, M. Lopez, A.P. Iori, C. Catalano; Rome/IT

Purpose: The diagnosis of intestinal acute graft-versus-host disease (a-GVHD) after allogenic bone marrow transplantation is based on clinical symptoms, CT findings and biopsies. We assessed MRI diagnostic accuracy.

Material and methods: We performed a prospective study on 35 patients (range 9-69 years) with clinical suspicion of intestinal a-GvHD, who underwent clinical-endoscopic, histological and multi-parametric MRI evaluation. Inclusion criteria: intestinal symptoms within 100 days from transplantation, <2 weeks between MRI and clinical-endoscopic evaluation. The following MRI features were evaluated: small and large bowel wall thickening, T2 signal and gadolinium enhancement of the intestinal wall, mesenteric lymph nodes, peritoneal effusion, comb-sign and restricted diffusion. Histology, clinical-endoscopic data and follow-up were considered as gold standard for diagnosis and staging. Sensibility, specificity, accuracy and Cohen's kappa were calculated.

Results: In 21/35 (60%), a-GvHD was confirmed at histology and follow-up. In true-positive patients, MRI showed significant continuous wall thickening in 76.2%, stratified wall contrast enhancement in 90%, comb-sign in 76%, increased number of mesenteric lymph nodes in 19%, and free intra-peritoneal fluid in 57.2%. A significant correlation was found between the number of pathological intestinal segments and clinical grade of a-GvHD ($r=0.54$, $p=0.009$). The distal ileum was the segment most frequently involved (85.7%). MRI sensitivity was 90.5%, specificity 78%, the PPV 86%, NPV 84% and accuracy 85%. Furthermore, MRI detected early disease in 82% of patients without intestinal symptoms.

Conclusion: In patients with intestinal a-GvHD, MRI can diagnose and grade the disease with high accuracy, in both early and more advanced or severe stages.

SS 14.6

How low can we go? Assessment of the lowest CT enterography dose achievable with iterative reconstruction

M. Twomey[1], H. Javed[1], D. Mondal[2], S. Moghe[3], J. Sammon[1], P. Rogalla[1], L. Guimaraes[1]; [1]Toronto, ON/CA, [2]Oxford/UK, [3]Vernon Hills, IL/US

Purpose: To determine the maximum dose reduction achievable without sacrificing observer performance for the detection of Crohn's disease (CD) lesions in CT enterography (CTE) using filtered back projection (FBP), hybrid iterative reconstruction (H-IR) and a new model-based IR (MB-IR) algorithm.

Material and methods: 50 CTE studies performed in a 320 row scanner for known/suspicion of CD between July 2016 and July 2017 were included. A validated noise insertion tool was utilized to simulate 75%, 50% and 25% of original dose. Datasets were reconstructed with FBP, H-IR and 2 types of MB-IR (IR1 and IR2). Two fellowship-trained abdominal radiologists independently reported intestinal findings and assessed image quality (IQ), noise and sharpness using 5-point scales. Assessment of the full-dose dataset/endoscopic data by an experienced abdominal radiologist served as reference standard.

Results: Fifty patients with 48 CD lesions were included. Mean effective dose of the full-dose datasets was 3.9 mSv. At 50% & 75% dose, sensitivity was 98% for both readers and all reconstruction methods. At 25% dose sensitivities of FBP, H-IR, MB-IR were 88%, 92%, 88% for Reader 1 and 84%, 96%, 89% for Reader 2. Agreement was almost perfect (k=0.82). IQ of FBP was unacceptable and worse than H-IR and MB-IR ($p<0.05$) at all dose levels. Mean H-IR and MB-IR IQ scores were <3 (acceptable) at 50% and 75% dose. No significant difference was seen between H-IR and MB-IR1/2 ($p>0.1357$). MB-IR1 images were the sharpest, while MB-IR2 were less noisy ($p<0.05$).

Conclusion: Low-dose and ultralow-dose CTE can be performed with H-IR and MB-IR with acceptable image quality without compromising observer performance, providing knowledge facilitating confident implementation of lower dose CTE protocols using multiple CT platforms and reducing radiation exposure in this patient population.

SS 14.7

The effect of gadoxetic acid on image quality of multiple hepatic arterial phase imaging: comparison study with gadoteric acid-enhanced MRI

K.C. Sim, B.J. Park, H. Na Yeon, M.J. Kim, D.J. Sung, S.B. Cho; Seoul/KR

Purpose: To evaluate the effect of gadoxetic acid on image degradation of single-breath-hold, triple (first, second, and third) arterial phase acquisition of the liver compared with those obtained with gadoteric acid.

Material and methods: A total of 211 consecutive MR examinations were evaluated including triple arterial phase acquisition using 4D eTHRIVE Keyhole technique. 108 examinations were performed with gadoxetic acid and 103 examinations were performed with gadoteric acid. Two radiologists evaluated image qualities of the precontrast and triple arterial phases of both groups in a blinded fashion. Image quality on each phase was assessed in regard to image artifacts, sharpness of intrahepatic vessel, sharpness of liver edge, and overall image quality.

Results: Gadoxetic acid group shows better image score in the precontrast images, despite the compromised conditions such as cirrhosis, more ascites, and variable comorbid malignancies that could make more degraded image quality ($p < 0.05$). Image quality of triple arterial phases of gadoxetic acid-enhanced liver MRI was significantly degraded than those of gadoteric acid for artifact, sharpness of intrahepatic vessel, sharpness of liver edge, and overall quality in each arterial phases ($p < 0.05$). Overall image quality was gradually improved from first to third arterial phase ($p < 0.003$). Third arterial phase showed best image quality in both groups. Inter-rater reliability was high ($p < 0.001$).

Conclusion: Intravenous gadoxetic acid can have a detrimental effect on image quality of triple arterial phases MR imaging using 4D eTHRIVE keyhole technique. Third arterial phase images show best image quality regardless of the contrast media.

SS 14.8

Transient arterial phase respiratory motion-related artifact in liver MR imaging with gadoxetic acid vs. extracellular gadolinium: a within-patient cohort comparative study

E. Belmonte, A. Darnell, J. Rimola, A. Forner, V. Sapena, J. Bruix, C. Ayuso; Barcelona/ES

Purpose: To compare the frequency and severity of transient arterial phase (TAP) respiratory motion-related artifact following gadoxetic acid (EOB) and extracellular gadolinium (Ec-Gd) in a cohort of cirrhotic patients.

Material and methods: Eighty-two cirrhotic patients from prospective series underwent liver MR with EC-Gd and EOB within 1 month. Two readers, blinded to all data, assigned a respiratory motion-related sore (0 [none], 1 [mild, no impact on reader confidence interpretation], 2 [moderate, causing decrease in reader confidence interpretation], and 3 [sever, non-diagnostic]) for non-enhanced, arterial and portal venous phase. Scores for each phase were averaged, and definitions for TAP, severe TAP and post-contrast motion-related artifacts were established. The frequency of motion-related artifacts was compared for each pair of examinations.

Results: The mean motion scores for EC-Gd and EOB for non-enhanced phase were 0.68 vs 0.73 ($p=0.3$), for arterial phase 0.91 vs. 1.26 ($p<0.0001$), and for portal venous phase 0.73 vs. 0.87 ($p=0.04$). The frequency of TAP observed on EOB was superior to EC-Gd (19.5% vs. 6%; $p=0.013$), but there were no differences in frequencies for severe TAP ($p>0.99$) between both contrasts agents. EOB was associated with a higher frequency of post-contrast motion-related artifacts (7.3% vs. 0%; $p=0.03$).

Conclusion: TAP respiratory motion-related artifact is more frequently observed on liver MRI with EOB than with EC-Gd and it may affect 19.5% of the patients. However, the rate of severe TAP was very low and similar for both contrast agents.

SS 14.9

withdrawn by the authors

SS 14.10

Assessment of whole-body fat using MRI: a pilot study

J.-P. Kühn[1], N. Friedrich[2], M.-L. Kromrey[2], J. Effler[2], R.-T. Hoffmann[1], M. Laniado[1], R. Laqua[3]; [1]Dresden/DE, [2]Greifswald/DE, [3]Bern/CH

Purpose: To develop an algorithm to assess fat compartments of the whole body using confounder-corrected chemical shift-encoded magnetic resonance imaging (CSI-MRI).

Material and methods: Seventy-three volunteers aged 29 to 80 years (29 female) underwent a whole-body MRI including three-echo chemical shift-encoded sequences acquired in 5 steps. After confounder correction and stitching of steps, the whole-body proton-density fat fraction was acquired. Based on tissue fat content, we developed a post-processing for segmentation of fat compartments as well as for tissue fat quantification. Using this algorithm, two observers measured total body fat volume (TAT), subcutaneous fat volume (SAT), visceral fat volume (VAT), and liver fat content (LFC). Robustness of the algorithm was tested by evaluation of inter- and intraobserver variability using a Bland-Altman analysis. In addition, data were correlated with body mass index (BMI) and age using Spearmen correlation coefficients.

Results: TAT, SAT, FAT and LFC were successfully measured in all volunteers. There were no differences between two readings (mean bias (%)±standard deviation; TAT/SAT/FAT/LFC: -0.1±0.3/0.4±1.0/0.2±0.4/0.4±1.0) and both observers (TAT/SAT/FAT/LFC: 0.0±0.3/0.9±1.4/0.4±0.8/0.9±1.6). TAT showed the highest correlation with BMI ($r=0.88$, $p<0.01$), followed by SAT ($r=0.83$, $p<0.01$), VAT ($r=0.76$, $p<0.01$), and LFC ($r=0.61$, $p<0.01$). The order was not affected by sex; however, the correlation coefficients were generally higher in men than in women.

Conclusion: CSI-MRI is an excellent approach to assess whole-body fat volume and organ fat content. It opens new perspectives for clinical research in imaging of metabolic disorders.

11:00 - 12:30 **Wicklow Hall 2B**

Scientific Session SS 15

Liver and bile duct intervention: evaluating treatment response

SS 15.1

Preoperative CT findings for prediction of incomplete resection and poor survival in patients with gallbladder cancer

J.H. Kim[1], S.-Y. Choi[2], H.J. Park[1], H.W. Eun[1], J.K. Han[1]; [1]Seoul/KR, [2]Bucheon/KR

Purpose: To predict residual tumor (R) classification and poor survival in patients who underwent surgery for gallbladder cancer using preoperative CT.

Material and methods: From 2006 to 2012, 173 patients (M:F=96:77, 65.3years) with gallbladder cancer underwent CT and surgery. Two radiologists assessed CT findings including tumor morphology, location, T-stage, adjacent organ invasion, hepatic artery abutment, portal vein encasement, LN metastasis, metastasis, resectability, gallstone, and combined cholecystitis. R classification was categorized into no residual tumor (R0) and residual tumor (R1 or R2). We analyzed the correlation between CT findings and R classification. In addition, we followed up the patients up to 5 years and analyzed the relationship between each CT findings and overall survival using Cox regression analysis and Kaplan–Meier analysis.

Results: R classification included no residual tumor in 127 patients and residual tumor in 46 patients. 5-year survival was 44%. For prediction of R classification, hepatic invasion (Exp(B)=4.008, 95% CI, 1.22-6.39, p=0.014) and hepatic artery abutment (Exp(B)= 8.67, 95% CI, 3.24-25.21, p=0.001) were significant predictors for residual tumor. On survival analysis, residual tumor (Exp(B)= 2.68, 95% CI, 1.72-4.19, p=0.001), liver metastasis (Exp(B)= 6.18, 95% CI, 1.41-27.07, p=0.016), duodenum invasion (Exp(B)= 2.8, 95% CI, 1.61-4.87, p=0.001), and regional LN metastasis (Exp(B)= 6.18, 95% CI, 1.41-27.07, p=0.016) were significant predictors for poor survival.

Conclusion: Preoperative CT findings could aid planning surgery using the high-risk findings of residual tumor including hepatic invasion and hepatic artery abutment. In addition, CT can predict poor survival using important findings including liver metastasis, duodenum invasion, and regional LN metastasis.

SS 15.2

Diagnostic performance of dual-tracer positron emission tomography-CT with 18F-fluorodeoxyglucose and 11C-acetate versus modified response evaluation criteria in solid tumors in the assessment of residual viable tumours in HCC that received loco-regional therapy

K.W.H. Chiu, T.-T. Cheung, R. Lo, H. Yuan, L.W. Chan; Hong Kong/HK

Purpose: Dual-tracer positron emission tomography (DT-PET) with 11C-acetate (Ac) and 18F-fluorodeoxyglucose (FDG) have shown to be highly sensitive in the detection of HCC although thus far, it has only been applied to treatment-naïve patients. The aim of this study was to evaluate the diagnostic performance DT-PET in assessing HCC that had undergone loco-regional treatment.

Material and methods: Patients with HCC who received loco-regional treatment were retrospectively identified and included if they underwent CT or MRI and DT-PET within 3 months of resection of the lesion. All lesions were evaluated on cross-sectional imaging using the modified response evaluation criteria in solid tumours (mRECIST) and radiotracer uptake on PET were recorded and compared with histology.

Results: Fourteen patients with 30 HCC fulfilled the inclusion criteria; 11 underwent transarterial chemoembolization (TACE), 2 radiofrequency ablation (RFA) and 1 both RFA and TACE (median time from previous intervention 3 months, range 1-43 months). Residual tumour was present in 24 lesions on histology. Using mRECIST criteria, 16/30 lesions had complete response, 14 partial response/stable disease. FDG was avid in 15/30, Ac in 20/30 and DT PET in 22/30 lesions. The positive predictive values for both modalities were 100% and the sensitivities in detecting residual disease were 54.2% and 83.3% ($p<0.05$) for cross-sectional imaging and DT-PET, respectively.

Conclusion: mRECIST criteria on cross-sectional imaging under-detect residual viable tumour in HCC that had undergone loco-regional treatment. DT-PET is a sensitive modality that can be used as an alternative modality for the treatment reassessment especially in cases where patients' management may be altered.

SS 15.3

CT texture analyses can predict early regrowth after thermal ablation of colorectal liver metastases

D.J. Van Der Reijd, E. Klompenhouwer, M. Taghavirazavizadeh, F. Staal, F. Imani, D. Meek, M.C. De Boer, D.M.J. Lambregts, R.G.H. Beets-Tan, M. Maas; Amsterdam/NL

Purpose: To assess whether CT texture analysis can detect early regrowth of colorectal liver metastases (CRLM) one month after thermal ablation.

Material and methods: 38 patients with CRLM who underwent radiofrequency ablation (RFA) or microwave ablation (MWA) for lesions ≤3 cm were included. Ablation zones 1-month post-ablation were manually delineated on all slices on portal venous phase CT by an expert radiologist blinded to clinical outcome. A margin of 5 mm was mathematically added to the ablation zone and texture parameters (entropy, uniformity and mean grey-level intensity) were compared between patients with and without regrowth using multiple Laplacian of Gaussian filters (σ0.5-2.5). Analyses were performed with pyradiomics.

Results: 18/38 patients had a regrowth. Mean follow-up was 32 (standard deviation (SD) 27) months and mean time to regrowth was 9 (SD 8) months. Entropy of the ablation zone (AZ) and ablation margin (AM) were significantly lower in regrowths (mean 1.34 vs 1.71, p=0.004 and mean 1.47 vs. 1.81, p=0.044, respectively). Uniformity of both the AZ and AM were higher in regrowths (mean 0.45 vs. 0.37, p=0.004 and mean 0.42 vs. 0.35, p=0.03, respectively). These differences were found both for analyses with a filter of σ0.5 and without a filter. For mean grey-level intensity no significant differences were observed for neither the AZ nor AM (mean 1.22 vs 0.73, p=0.496 and -1.90 vs -2.04, p=0.874, respectively).

Conclusion: Patients with regrowth after ablation show a lower entropy and higher uniformity of the ablation zone and ablation margin 1-month post-ablation. CT texture analyses can help in identifying patients who are at risk for regrowth.

SS 15.4

Influence of pre-treatment tumor growth rate on the objective response of HCC treated with selective trans-arterial chemoembolization

Y. Purcell, R. Pommier, V. Roche, M. Dioguardi Burgio, A. Sibert, V. Vilgrain, M. Ronot; Clichy/FR

Purpose: To assess the influence of pre-treatment tumor growth rate ($_{pre}$TGR) on the objective response (OR) according to modified response evaluation criteria in solid tumors (mRECIST) criteria after a first session of selective trans-arterial chemoembolization (TACE) for the treatment of HCC.

Material and methods: Ninety-nine patients (91 male, 93%) with 148 tumors (mean 34±29mm), who underwent the first session of selective TACE for the treatment of HCC between 2011 and 2016, were included. preTGR was calculated as the percentage change in tumour volume per month (%/mo) on available CTs before treatment. OR was defined as a complete or partial response on a lesion-based analysis. preTGR cut-off for prediction of OR was identified by receiver operating characteristic (ROC) curve analysis.

Results: After one session of treatment 74 (50%), and 41 (28%) tumors showed complete (CR), or partial response (PR) while 29 (20%) and 4 (2%) showed stable (SD), or progressive disease (PD). The mean $_{pre}$TGR was 13±17 %/mo. It followed a U-shaped distribution with a mean 15±19, 13±16, 6±10, and 15±5 %/mo in tumors showing CR, PR, SD, and PD. After exclusion of tumors showing PD, $_{pre}$TGR was significantly higher in tumors with OR (mean14±18 %/mo) when compared to those showing SD (6±10 %/mo, p=0.03). A $_{pre}$TGR value of 6.5%/mo was associated with a sensitivity and specificity of 60% and 86% for the prediction of OR (Area under ROC of 0.67±0.05).

Conclusion: Pre-treatment TGR is highly variable in HCC before TACE with a U-shaped distribution for the prediction of tumor response. It provides insight into tumor biology that may be used during pre-treatment workup to help stratify patients.

SS 15.5

withdrawn by the authors

SS 15.6

Radiological tumor response and histopathological correlation of HCC treated with stereotactic body radiation therapy as a bridge to liver transplantation

K. Mastrocostas, S. Fischer, P. Munoz-Schuffenegger, H.-J. Jang, G. Sapisochin, L.A. Dawson, T.K. Kim; Toronto, ON/CA

Purpose: To assess the imaging appearance of HCC treated with stereotactic body radiation therapy (SBRT) as a bridging therapy prior to liver transplantation (LT), with pathological correlation.

Material and methods: 23 patients (20 males; mean age, 60 years) were included, with a total of 25 lesions assessed. CT and/or MRI imaging pre- and post-SBRT were reviewed by two independent radiologists, with a third reader resolving inter-observer differences. The target lesions were assessed for radiological response including change in size, change in attenuation in the portal venous phase on CT or signal intensity on MRI, and percentage necrosis if present. The radiological findings were compared to the tumor necrosis at explant as assessed by a pathologist.

Results: Of the 25 lesions, 15 lesions were classed as stable disease (SD), 8 lesions as partial response (PR) and 2 lesions as progressive disease (PD). Among the 15 SD lesions, all lesions were identified as having necrosis at explant pathology and imaging. Ten of these lesions were assessed as having imaging changes of necrosis concordant within 10% of the necrosis at pathology. Nine lesions were assessed at imaging as having >20% necrosis, all of which were concordant with the pathology findings, despite stable size. In only one case was necrosis at imaging >20% above that at explant pathology.

Conclusion: Current standard HCC response criteria such as response evaluation criteria in solid tumors (RECIST) underestimate the response of lesions to local therapy with SBRT. As the utility of SBRT as a focal therapy for HCC increases, further evaluation of the imaging findings of response is required.

SS 15.7

Factors associated with tumor progression after percutaneous ablation of HCC: results of a propensity score matching analysis comparing monopolar radiofrequency and microwaves

D. Bouda, V. Barrau, C. Garcia-Alba, V. Roche, M. Dioguardi Burgio, A. Sibert, V. Vilgrain, M. Ronot; Clichy/FR

Purpose: To identify risk factors for local and distant tumor progression after percutaneous thermal ablation of HCC with a focus on the comparison between microwave ablation (MWA) and monopolar radiofrequency ablation (RFA).

Material and methods: Data were reviewed from consecutive cirrhotic patients with very early/early HCCs who underwent image-guided percutaneous monopolar expandable RFA or MWA. Factors associated with local and distant tumor progression were identified using propensity score matching (PSM). Statistical analysis was performed with the Kaplan-Meier method using the log-rank test and Cox regression models.

Results: A total of 190 HCC (mean 23±8.6mm) in 149 patients (mean 63±11 y-o, 79% male) underwent RFA (n=90, 47%) or MWA (n=100, 53%). Secondary technical success rate was 97.4%. After a median follow-up of 24.6 months (interquartile range (IQR): 9.7-37.2), 43 (23%) HCC showed local progression (median time delay 13.4 months (IQR: 5.8-24.3)) and 91 (63%) patients had a distant progression (median time delay 10.4 months (IQR: 5.7-22). Cox model after PSM identified treatment by RFA (hazard ratio (HR), 2.934; P=0.006), size ≥30mm (HR, 3.130; P=0.007) and vascular contact (HR, 3.372; P=0.005) as risk factors for local progression. Factors associated with distant progression were a main tumor size ≥30mm (HR, 1.94; P=0.013), an alpha-fetoprotein (AFP) level above 100 ng/mL (HR, 2.56; p=0.002), and hepatitis B (HR, 0.51; p=0.047).

Conclusion: The rate of local HCC progression was lower after MWA when compared to monopolar expandable RFA, regardless of tumor size and vascular contact. Ablation technique did not influence the risk of distant progression.

SS 15.8

Predicting the response of colorectal cancer liver metastases to preoperative chemotherapy using gadoxetic acid-enhanced MRI

N.V. Costa[1], N. Bastati[2], S. Pötter-Lang[2], Z. Guengoern[2], Y. Bican[2], A. Ba-Ssalamah[2]; [1]Lisbon/PT, [2]Vienna/AT

Purpose: The aim of the study was to create a scoring system based upon gadoxetic acid-enhanced MRI (^{ga}MRI) features to predict the treatment response (TR) to chemotherapy.

Material and methods: This was a retrospective study of 30 consecutive patients (65.2±11.2years) with colorectal cancer liver metastases (CRCLM), who underwent gaMRI after chemotherapy and before hepatic resection. Metastases were classified according to a suggested scoring system (0-6 points) in three groups of response: optimal (≤2 points); partial (2-4 points); and no-response (≥4 points). The scoring system comprised three features: overall homogeneity (homogeneous=0, mixed=1, heterogeneous=2); tumor liver interface (sharp=0, mixed=1, ill-defined=2); and peripheral rim enhancement (≤2 mm=0, 2-4 mm=1, ≥4 mm=2). Apparent diffusion coefficient (ADC) values were measured. The primary outcome was residual vital tumor (RVT). The scoring system, response groups, and ADC values were calculated and compared with the RVT percentage. Demographic, laboratory, and imaging findings were included in a multivariate statistical analysis. The three groups of response were correlated with patient survival and the log-rank test was used to compare two survival distributions (optimal/partial responses vs no-response groups).

Results: Forty-one CRCLM showed good inter-observer agreement (κ=0.86). Multiple regression demonstrated an association between RVT (32.9±11.2) and the scoring system (p<0.001), the response group (p<0.001), and the ADC values (p<0.021). The survival distributions between optimal/partial response and no-response showed a trend to be different (p=0.066).

Conclusion: ^{ga}MRI correlated well with our scoring system, different response groups, and ADC values in patients with CRCLM treated with chemotherapy, and may be used to assess the RVT percentage.

SS 15.9

Early prediction of response to transarterial chemoembolization using CT perfusion in primary liver tumors

D. Tamandl, F. Waneck, A. Ba-Ssalamah, C. Loewe; Vienna/AT

Purpose: Assessment of CT perfusion (CTP) in the prediction of response early after transarterial chemoembolization (TACE) in patients with HCC and cholangiocarcinoma (CCC).

Material and methods: This prospective study was approved by the institutional review board and written informed consent was obtained from all patients. We performed CTP one day before and after (interquartile range [IQR]: 1-2 days) TACE in 18 patients. 46 lesions (41 HCC and 5 hypervascular CCC) were amenable for analysis. Various perfusion-related parameters were measured. In a lesion-based analysis, absolute and relative changes were compared to the clinical response on biphasic CT using modified response evaluation criteria in solid tumors (mRECIST) criteria 6 weeks after the procedure. Optimal cutoff values for detecting response were calculated using area under the ROC curves (AUROC). Follow-up analysis included assessment of overall survival (OS), local recurrence-free survival (LRFS) and local progression-free survival (LPFS), using Kaplan-Meier estimates.

Results: The clinical response was: complete response (CR, n=22, 48%), partial response (PR, n=9, 20%) and no response (14 stable, 1 progression) 6 weeks after TACE. CTP parameters were all reduced after TACE in responding patients (PR, CR) while no difference was observed in non-responders. Arterial liver perfusion (ALP_{post}) was superior in prediction of CR compared to blood flow (BF_{post}) and blood volume (BV_{post}) ($AUROC_{ALP}$ 0.953 vs. $AUROC_{BF}$ 0.859 and $AUROC_{BV}$ 0.831, p<0.001) with a sensitivity, specificity, positive predictive value, negative predictive value and accuracy of 91%, 92%, 91%, 92% and 91%. Only 4/22 lesions with CR recurred with a median local recurrence-free survival of 22.7 months.

Conclusion: Early response assessment after transarterial chemoembolization can reliably be performed with CT perfusion.

SS 15.10

Early recurrence of HCC predicted by whole-lesion radiomics on preoperative gadoxetic acid-enhanced MRI

Z. Zhang, J. Chen, H. Jiang, L. Cao, T. Duan, Z. Ye, B. Song; Chengdu/CN

Purpose: To investigate the role of gadoxetic acid (Gd-EOB-DTPA)-enhanced MRI-derived texture features in predicting early recurrence (≤6 months) of HCC.

Material and methods: 29 consecutive patients with preoperative Gd-EOB-DTPA-enhanced MRI were included. Early recurrence was determined within 6 months. 3D texture features on individual sequence were derived using an in-house software (Analysis Kit, GE Healthcare). LASSO logistic regression model was adopted for feature selection. Identified texture features were compared between patients with and without early recurrence. Receiver-operating characteristic (ROC) analysis of predicting early recurrence was performed for each texture feature.

Results: 17 early recurrences were confirmed with imaging follow-up. The skewness, sumEntropy, ShortRunHighGreyLevelEmphasis_AllDirection_offset7_SD, and LongRunLowGreyLevelEmphasis_AllDirection_offset7_SD of HCC on arterial-phase, the ShortRunHighGreyLevelEmphasis_AllDirection_offset4_SD and LongRunHighGreyLevelEmphasis_angle90_offset7 on portal venous-phase (PVP), and uniformity and LongRunLowGreyLevelEmphasis_AllDirection_offset7_SD on hepatobiliary phase (HBP) were found to be statistically different between patients with and without recurrence ($P < 0.05$). The areas under the ROC curves (AUCs) were 0.966 (CI[0.82, 0.99]), 0.725 (CI[0.53, 0.87]), 0.760 (CI[0.57, 0.89]) and 0.833 (CI[0.65, 0.95]) for the skewness, sumEntropy, ShortRunHighGreyLevelEmphasis_AllDirection_offset7_SD, and LongRunLowGreyLevelEmphasis_AllDirection_offset7_SD on AP, 0.789 (CI[0.59, 0.92]) and 0.814 (CI[0.63, 0.93]) for the ShortRunHighGreyLevelEmphasis_AllDirection_offset4_SD and LongRunHighGreyLevelEmphasis_angle90_offset7 on PVP, and 0.843 (CI[0.66, 0.99]) and 0.760 (CI[0.63, 0.93]) for the uniformity and LongRunLowGreyLevelEmphasis_AllDirection_offset7_SD on HBP, respectively, in predicting early recurrence of HCC. The highest sensitivity and specificity were shown on arterial-phase images (skewness) of 91.7% (CI[61.5%,99.8%]) and 94.1% (CI[71.3%,99.9%]).

Conclusion: Whole-lesion texture features based on Gd-EOB-DTPA-enhanced-MRI held promise for predicting early recurrence of HCC after hepatectomy, especially the skewness on arterial-phase images.


European Society
ESGAR
Gastrointestinal and Abdominal Radiology

K

L

M

N